DR 8.6: Proceedings of the TRADR Summer School Yr2 – Autonomous Micro Aerial Vehicles 2015

Sven Behnke, Hartmut Surmann, Rainer Worst*

**Fraunhofer IAIS, Sankt Augustin*
⟨sven.behnke@iais.fraunhofer.de⟩

Project, project Id:	EU FP7 TRADR / ICT-60963
Project start date:	Nov 1 2013 (50 months)
Due date of deliverable:	December 2015
Actual submission date:	February 2016
Lead partner:	Fraunhofer
Revision:	Final
Dissemination level:	PU

This deliverable describes the second year TRADR summer school, which was organized by Fraunhofer IAIS. The topic of the school was Autonomous Micro Aerial Vehicles. The school took place August 24th-28th 2015 at Schloss Birlinghoven, Sankt Augustin, Germany. Eight invited speakers delivered 90 minutes lectures. The program also featured hands-on exercises, an excursion, and social events.

Executive Summary

This deliverable describes the second TRADR summer school. As topic for the school *Autonomous Micro Aerial Vehicles* was chosen, as micro aerial vehicles are one important element of the TRADR system to provide situational awareness to the rescue team, and autonomy is necessary to assist MAV operators, e.g. by obstacle avoidance, and make MAVs usable for unskilled pilots like fire fighters. The school was organized by Fraunhofer IAIS and took place in Schloss Birlinghoven, Sankt Augustin, Germany, from August 24th to August 28th, 2015. Eight invited speakers were lecturing. Participants had to apply for the school and only a fraction of the applicants could be accepted. More than 50 participants from 14 countries were present, around one quarter of them were from the TRADR consortium. The summer school inspired vivid discussions and lead to new collaborations. The impact was deepened by a TRADR integration meeting that directly followed the school.

Role of the Summer School in TRADR

The general role of the yearly TRADR summer schools is to gain new knowledge and disseminate experience. In this second instance, there was a balance between gaining new knowledge on micro aerial vehicles and disseminating experiences and results obtained within the TRADR project.

Contribution to the TRADR SOTA and Prototypes

The Year 2 TRADR summer school focused on the topic *Autonomous Micro Aerial Vehicles*.

Micro aerial vehicles (MAV) such as multicopters have become a popular research tool in recent years and are used in an increasing number of application domains such as aerial photography and inspection tasks [2, 4, 1, 3]. They are also becoming increasingly relevant for the search and rescue domain that TRADR addresses. The objective of the school was to give researchers and students deep insights into the currently leading approaches to essential subproblems, such as 3D environment perception, mapping, navigation planning, and control of autonomous MAVs.

1 Tasks, objectives, results

1.1 Planned work

The project proposal plans summer schools organized yearly. For the Year 2 it was decided that Fraunhofer IAIS organizes it in Schloss Birlinghoven, Sankt Augustin, Germany.

1.2 Actual work performed

1.2.1 Advertisement and participant selection

A call for participation was sent to several mailing lists, published on the website, and advertised in social media like Facebook, Google+, and Twitter. A total of 77 applications were submitted through EasyChair, many of them from international applicants. Applications were reviewed by the organizers and 55 applicants were accepted. Accepted applicants had to provide a billing address for the registration fees and 40 bills were issued for non-TRADR participants. 17 of these came from Germany, six from Italy, 15 from eight other European countries, one from China, and one from Russia. 11 participants from the TRADR project registered free of charge. At the summer school, also the eight speakers and the four organizers participated. Four PhD and Master students from the Autonomous Intelligent Systems group of University of Bonn prepared a MAV demonstration and attended parts of the lectures.

1.2.2 Dissemination

Before the start of the school, a press release was issued by Fraunhofer IAIS[1], which increased the visibility of the school and led to interviews with journalists, e.g. of the speaker Angela Schoellig by Deutschlandradio.

1.2.3 Event organization

The event took place in Schloss Birlinghoven, Sankt Augustin, Germany from Monday, August 24th to Friday August 28th, 2015. Fig. 1 gives some impressions. The venue featured a highly decorated main hall for the lectures, which was equipped with tables, electric power, and wireless network (Fig. 1a). Coffee and cakes were served twice a day in the hall next to the main lecture hall. Smaller rooms were available for storing and preparing equipment. Lunch was catered at the cafeteria of the Fraunhofer Campus Birlinghoven, in close vicinity of the castle. Participants could also use the large terrace of the castle and its park. A total of 67 persons attended the school at least partially. Fig. 1f shows a group photo.

[1] Press release of Fraunhofer IAIS on TRADR Summer School on Autonomous Micro Aerial Vehicles `https://idw-online.de/de/event51127`

1.2.4 Scientific program

The summer school was opened with a presentation from the organizers, which also introduced the participants to the TRADR project. Eight invited speakers were teaching, see `http://www.iais.fraunhofer.de/6257.html` and Sec. 2.2 for the schedule. Each speaker delivered a 90 minute lecture. Table 1 summarizes the topics. The abstracts of the lectures are listed in Sec. 2.1. All lectures, except for the last one, were followed by a 90 minute exercise, where the students solved tasks with provided software or had the opportunity to try MAVs provided by AscTec (Fig. 1c,d). In addition, participants were encouraged to bring own micro aerial vehicles and had the possibility to exhibit and demonstrate them (Fig. 1e). Furthermore, participants had the opportunity to present their research in posters and to advertise these with poster teasers. About 15 posters were presented (Fig. 1b).

All lecture slides are available on the web, `http://www.iais.fraunhofer.de/6257.html`. The slides are also included in the Annex of this deliverable.

Speaker(s)	**Topic**
Rainer Worst, Hartmut Surmann, Sven Behnke, Fraunhofer IAIS	Welcome, Project TRADR Long-Term Human-Robot Teaming for Robot-Assisted Disaster Response
Michael Achtelik, Ascending Technologies, Germany	MAVs - Daily Operations and Practical Applications
Sebastian Scherer, Carnegie Mellon University, USA	Motion Planning for Aerial Robots
Cyrill Stachniss, University of Bonn, Germany	Graph-based Simultaneous Localization and Mapping
Angela Schoellig, University of Toronto, Canada	Controls for Multi-Rotor Vehicles: From Model-Based to Learning-Enabled Approaches
Igor Gilitschenski, ETH Zurich, Switzerland	Advances in Nonlinear Dynamic State Estimation
Guido de Croon, TU Delft, Netherlands	Vision for Autonomous Flight of Light-weight Micro Air Vehicles
Daniel Cremers, TU Munich, Germany	Direct and Dense 3D Reconstruction from Autonomous Quadrotors
Anibal Ollero, University of Sevilla, Spain	Aerial Robotic Manipulation: Control, Perception and Planning Functionalities

Table 1: List of invited speakers and the lectured topics.

Figure 1: Impressions from the 2015 TRADR Summer School. a) Lecture hall in Schloss Birlinghoven. b) Discussion during poster session. c) Practical exercise with AscTec copter. d) AscTec copter. e) Discussing an exhibit. f) Group photo in front of Schloss Birlinghoven. g) Excursion to Drachenfels. h) Group photo on top of Drachenfels.

1.2.5 Social program

The social program consisted of

- a welcome reception on Monday evening,
- a visit of the Museum for German History in Bonn, followed by a guided tour though the UN campus and dinner in the park restaurant Rheinaue on Tuesday evening,
- an excursion to Königwinter by boat on the river Rhine (Fig. 1g) and a hike to the top of the Drachenfels (Fig. 1h), followed by a dinner in Königswinter on Wednesday afternoon and evening, and
- a guided tour through the historic city center of Bonn, followed by a dinner at a brewery in the city center on Thursday evening.

1.2.6 Results

The 2015 TRADR summer school was a big success. Only one registered participant dropped out due to illness. The program was run according to the announced schedule. All speakers delivered their lectures and the participants gave very positive feedback on the quality of the presentations and the usefulness of the exercises.

The poster sessions, exhibits, coffee breaks, and lunches gave many opportunities for in-depth discussions on the many issues related to autonomous micro aerial vehicles. Not the least, the social program facilitated that participants got to know each other better, established new friendships and collaborations, some of which will certainly be beneficial for the remaining work in TRADR. Another positive outcome was the high visibility of the TRADR project in the autonomous MAV community.

2 Annexes

2.1 Programme

This annex lists the talk abstracts provided by the speakers. The photos were recorded during the summer school.

Opening Presentation and TRADR Overview

Rainer Worst, Fraunhofer IAIS, Germany
The talk introduces the European FP7 integrated research project TRADR - Long-Term Human-Robot Teaming for Robot-Assisted Disaster Response, which organizes and sponsors the 2015 Summer School on Autonomous Micro Aerial Vehicles.

Lecture 1: MAVs Daily Operation and Practical Applications

Michael Achtelik, Ascending Technologies, Germany
Based on real applications, we will show what is already possible with MAVs and how they are used by professional customers. Showing sample applications, we will point out the key requirements for todays and future applications. Furthermore the use of MAVs in the TRADR project will be shown and key requirements derived. We will show state of the art flight control systems and onboard sensing capabilities. In the second part, the attendees will have the opportunity to gather hands-on experience on new and existing MAVs.

Lecture 2: Motion Planning for Aerial Robots

Sebastian Scherer, Carnegie Mellon University, USA
The goal of this lecture is to convey the problem and fundamental techniques that are required for fast and safe motion planning of autonomous aerial vehicles. This includes state of the art results for motion planning and fundamentals of the motion planning problem and approach for flying robots. The talk will present the problem representation, how these representations influence the approach, and examples of different representative approaches such as optimization, sampling-based, and graph-search algorithms. The lecture will be followed by a tutorial where the students can explore the ideas presented in a Matlab planning toolbox.

Lecture 3: Graph-based Simultaneous Localization and Mapping

Cyrill Stachniss, University of Bonn, Germany
Being able to build a map of the environment and to simultaneously localize within this map is an essential skill for flying as well as wheeled robots

navigating in unknown environments. This so-called simultaneous localization and mapping or SLAM problem has been investigated in robotics over the last two decades and efficient approaches have been proposed. One intuitive way of formulating SLAM is to use a graph whose nodes correspond to the poses of the robot at different points in time and whose edges represent constraints between the poses. The latter are obtained from observations of the environment or from movements. Once such a graph is constructed, the map can be computed by finding the spatial configuration of the nodes that is mostly consistent with the measurements modeled by the edges. In this tutorial, we provide an introductory description to the graph-based SLAM problem. We discuss a state-of-the-art solutions that is based on least-squares error minimization and exploits the structure of the SLAM problems during optimization. The goal of this tutorial is to enable the reader to implement the proposed methods from scratch.

Lecture 4: Controls for Multi-Rotor Vehicles: From Model-Based to Learning-Enabled Approaches

Angela Schoellig, University of Toronto, Canada

In my lecture, I will provide the fundamentals of model-based controls for multi-rotor vehicles. I will highlight how non-idealities such as time delays and modeling errors affect the flight performance. Finally, I will introduce some recent learning-based controls approaches, which achieve high performance despite modeling errors.

Lecture 5: Advances in Nonlinear Dynamic State Estimation

Igor Gilitschenski, ETH Zurich, Switzerland

Since the development of the Kalman Filter, it has become one of the most famous and widely used sensor fusion algorithms. However, the underlying assumption of linear dynamics is not satisfied by most real-world systems. Thus, in this talk, we will revisit classical nonlinear filtering approaches and provide an introduction to some more-recent filtering techniques.

Typically, linearization of system and measurement models is performed in order to make consideration of nonlinear systems possible which is known as the extended Kalman filter (EKF). The last two decades have witnessed a rapid development of novel nonlinear filtering techniques that are inherently better suitable for consideration of nonlinear systems. These techniques improve state estimation by better considering nonlinear system models and nonlinear underlying domains.

First, consideration of nonlinear system and measurement models is improved, e.g., by making use of deterministic sampling based nonlinear filtering techniques that do not require the computation of derivatives (thus, they are sometimes referred to as derivative-free filters). Second, a sound consideration of nonlinear underlying state spaces is possible by making use of probability distributions that are defined on these state spaces rather than assuming Gaussians. This is made possible by making use of directional statistics, which is a subfield of statistics that considers directional quantities such as angles or orientations. Both classes of approaches will be addressed by describing their functionality and enabling the participants to apply them in dynamic state estimation problems.

Lecture 6: Vision for Autonomous Flight of Light-weight Micro Air Vehicles

Guido C. H. E. de Croon, TU Delft, Netherlands

The fundamental challenge for achieving autonomous flight with light-weight (< 50 gram) Micro Air Vehicles derives from the severe limitations in the onboard energy, sensors and processing. This argues for a minimal sensor suite and efficient algorithms for vision and control. In this lecture, I will mostly focus on a bio-inspired approach, in which optical flow cues such as time-to-contact and ventral flow are used directly for control. Furthermore, I will highlight how optical flow can be complemented with different, visual appearance cues. I will place the discussed methods in the context of the DelFly Explorer, a fully autonomous 20-gram flapping wing MAV.

Lecture 7: Direct and Dense 3D Reconstruction from Autonomous Quadrotors

Daniel Cremers, TU Munich, Germany

The reconstruction of the 3D world from images is among the central challenges in computer vision. Starting in the 2000s, researchers have pioneered algorithms which can reconstruct camera motion and sparse feature-points in real-time. In my talk, I will show that one can autonomously fly quadrotors and reconstruct their environment using onboard color or RGB-D cameras. In particular, I will introduce spatially dense methods for camera tracking and reconstruction which do not require feature point estimation, which exploit all available input data and which recover dense geometry rather than sparse point clouds. This is joint work with Jakob Engel, Vladyslav Usenko, Jan Sthmer, Martin R. Oswald, Frank Steinbrcker, Christian Kerl, Erik Bylow, Jrgen Sturm and Jrg Stckler.

Lecture 8: Aerial Robotic Manipulation: Control, Perception and Planning Functionalities

Anibal Ollero, University of Sevilla, Spain

The presentation will start with a general view of aerial robots physically interacting with the environments and with other aerial robots. This will include load transportation and deployment. Then aerial robots with manipulation capabilities in the FP7 ARCAS project will be presented by including both multirotor systems and helicopters equipped multi-joint (6 or 7 Degrees of Freedom) arms. The control systems of the aerial robots with the arms will be described. Moreover, both perception and planning functionalities of the aerial robots will be summarized. The presentation will also introduce the aerial cooperative assembly functionalities in the ARCAS project. The last part of the presentation will be devoted to introduce the AEROARMS H2020 project devoted to aerial robots with multiple arms for inspection and maintenance applications, with particular attention devoted to the application in oil and gas industries and other new aerial robotic manipulation projects at the University of Seville and CATEC.

TRADR Summer School
Autonomous Micro Aerial Vehicles

Castle Birlinghoven, Sankt Augustin, Germany, August 24th-28th 2015, Hosted by the Fraunhofer Institute for Intelligent Analysis and Information Systems IAIS.
Co-financed by the EU Project TRADR (FP7-ICT-609763).

Speakers

Angela Schoellig,
University of Toronto, Canada

Aníbal Ollero,
University of Sevilla, Spain

Cyrill Stachniss,
University of Bonn, Germany

Daniel Cremers,
TU Munich, Germany

Guido C. H. E. de Croon,
TU Delft, Netherlands

Igor Gilitschenski,
ETH Zurich, Switzerland

Michael Achtelik,
Ascending Technologies, Germany

Sebastian Scherer,
Carnegie Mellon University, USA

Sven Behnke,
University of Bonn, Germany

Rainer Worst
Fraunhofer IAIS, Germany

References

[1] David Droeschel, Matthias Nieuwenhuisen, Marius Beul, Dirk Holz, Jörg Stückler, and Sven Behnke. Multi-layered mapping and navigation for autonomous micro aerial vehicles. *Journal of Field Robotics*, 2015.

[2] Vijay Kumar and Nathan Michael. Opportunities and challenges with autonomous micro aerial vehicles. *The International Journal of Robotics Research*, 31(11):1279–1291, 2012.

[3] Matthias Nieuwenhuisen, David Droeschel, Marius Beul, and Sven Behnke. Autonomous navigation for micro aerial vehicles in complex GNSS-denied environments. *Journal of Intelligent and Robotic Systems*, 2015.

[4] Kenzo Nonami, Farid Kendoul, Satoshi Suzuki, Wei Wang, and Daisuke Nakazawa. *Autonomous Flying Robots: Unmanned Aerial Vehicles and Micro Aerial Vehicles*. Springer Science & Business Media, 2010.

2.2 Summer School Main Webpage

This annex includes the main web page of the summer school `http://www.iais.fraunhofer.de/6257.html`.

Fraunhofer
IAIS

TRADR Summer School on Autonomous Micro Aerial Vehicles

Fraunhofer-Institut für Intelligente Analyse- und Informationssysteme IAIS

August 24th-28th 2015, Schloss Birlinghoven

Micro aerial vehicles (MAV) such as multicopters have become a popular research tool in recent years and are used in an increasing number of application domains such as aerial photography and inspection tasks. Most MAVs are remotely controlled or follow GNSS waypoints in obstacle-free heights. Many tasks require navigation in complex 3D environments, close to obstacles, however. Hence, the degree of autonomy of the MAVs must be increased.

The objective of the school is to give students deep insights into the currently leading approaches to 3D environment perception, mapping, navigation planning, and control of autonomous MAVs. Lectures by internationally leading experts will provide the necessary theoretical background for hands-on exercises with MAVs.

Program

The program is based on three pillars:

- **Theory**: Ranging from state estimation based on multimodal sensors and environment mapping by cameras and laser scanners over control of dynamic flight, obstacle avoidance, navigation planning, and exploration to contact with the environment and aerial manipulation.
- **Case studies**: Leading micro aerial systems for research on autonomy such as Ascending Technologies Firefly, the “Mapping on Demand” and InventAIRy copters of University of Bonn, the multirotors developed at CMU, the aerial manipulators of University of Seville, and the DelFly flapping wing MAVs of TU Delft will be presented.
- **Practical exercises**: Students will apply the theory in hands-on tutorials. Ascending Technologies will provide sensor equipped Firefly copters for these. Participants are encouraged to also bring their own micro aerial vehicles. Space for indoor and outdoor experiments with autonomous micro aerial vehicles will be available.

Venue

Fraunhofer Institute Center Schloss Birlinghoven
53757 Sankt Augustin
Germany

Travel directions

Map link

Schedule

Monday, 24.8.2015

11:00	Registration opens
11:30	Lunch opens
13:00 - 14:00	Rainer Worst, Hartmut Surmann, Sven Behnke: Welcome, Project TRADR Long-Term Human-Robot Teaming for Robot-Assisted Disaster Response
14:00 - 15:30	Lecture Michael Achtelik: MAVs - Daily Operations and Practical Applications
15:30	Coffee break
16:00 - 17:30	Excercise Michael Achtelik
17:30 - 18:00	Poster teaser (Participants are welcome to display their research in a poster and advertise it with a three-slides three minutes teaser presentation)
18:00 -	Welcome reception

Tuesday, 25.8.2015

9:00 - 10:30	Lecture Sebastian Scherer: Motion Planning for Aerial Robots
10:30	Coffee break
11:00 - 12:30	Exercise Sebastian Scherer
12:30	Lunch
14:00 - 15:30	Lecture Cyrill Stachniss: Graph-based Simultaneous Localization and Mapping
15:30	Coffee break
16:00 - 17:30	Exercise Cyrill Stachniss
18:00 -	Evening program and dinner

Wednesday, 26.8.2015

9:00 - 10:30	Lecture Angela Schoellig: Controls for Multi-Rotor Vehicles: From Model-Based to Learning-Enabled Approaches
10:30	Coffee break
11:00 - 12:30	Exercise Angela Schoellig
12:30	Lunch
14:00 -	Excursion and dinner

Thursday, 27.8.2015

9:00 - 10:30	Lecture Igor Gilitschenski: Advances in Nonlinear Dynamic State Estimation
10:30	Coffee break
11:00 - 12:30	Exercise Igor Gilitschenski
12:30	Lunch
14:00 - 15:30	Lecture Guido de Croon: Vision for Autonomous Flight of Light-weight Micro Air Vehicles
15:30	Coffee break

16:00 - 17:30	Exercise Guido de Croon
18:00 -	Evening program and dinner

Friday, 28.8.2015

9:00 - 10:30	Lecture Daniel Cremers: Direct and Dense 3D Reconstruction from Autonomous Quadrotors
10:30	Coffee break
11:00 - 12:30	Lecture Anibal Ollero: Aerial Robotic Manipulation: Control, Perception and Planning Functionalities
12:30	Lunch
14:00 - 15:30	Exercise Daniel Cremers
15:30 -	Farewell coffee

Speakers

- Michael Achtelik, Ascending Technologies, Germany
- Daniel Cremers, TU Munich, Germany
- Guido C. H. E. de Croon, TU Delft, Netherlands
- Igor Gilitschenski, ETH Zurich, Switzerland
- Aníbal Ollero, University of Sevilla, Spain
- Sebastian Scherer, Carnegie Mellon University, USA
- Angela Schoellig, University of Toronto, Canada
- Cyrill Stachniss, University of Bonn, Germany

Application Procedure for Participants

The number of participants is limited.
Interested students and researchers needed to apply for participation prior to the application deadline through EasyChair.

Registration Fees

- Regular: 500 €
- PhD students and students: 300 €
- Registration information will be sent to accepted applicants.

Accomodation

- Easy to reach by bus is Hotel Hangelar
- Easy to reach by car is Waldcafe Hotel, Holzlar
- Many hotels are available in Bonn, about 30 minutes by public transport.
    - New and directly at the main train station is InterCityHotel Bonn (85€/night single room, including breakfast code AMAV2015 until July 27th).
    - Close to the S66 city train is Hotel Aigner 81€/night single rom including breakfast with code AMAV2015.
    - For low-budget participants, the Ibis Hotel Bonn** is recommended.
- In Siegburg, Hotel Herting is located next to the train station (S66 connection), 79€/night including breakfast with code AMAV2015.

Important Dates

- Application for participation: June 20th, 2015 (closed)
- Acceptance decision: June 30th, 2015 (sent)
- Registration deadline: July 31st, 2015
- Summer school: August 24th-August 28th, 2015

Organizers

- Sven Behnke, University of Bonn / Fraunhofer IAIS
- Hartmut Surmann, Westfälische Hochschule Gelsenkirchen / Fraunhofer IAIS
- Rainer Worst, Fraunhofer IAIS
- Birgit Dorn (local arrangements), Fraunhofer IAIS

Acknowledgement

The school is supported by the EU FP7 ICT project TRADR "Long-term Human-Robot Teaming for Robot Assisted Disaster Response", grant agreement no. 60963.

2.3 Lecture materials

This annex includes all the lecture materials.

Long-Term Human-Robot Teaming
for Robot Assisted Disaster Response

TRADR Overview

Ivana Kruijff-Korbayová (DFKI)
Rainer Worst (Fraunhofer)

TRADR is funded by the EU FP7 Programme
ICT Cognitive Systems, Interaction, Robotics, Project #609763.
www.tradr-project.eu

Motivation

- Robot-assisted disaster response
  - Robots can save lives
- Human-robot teamwork
  - From robots as tools to robots as interdependent team-members
- Long-term: disaster response takes time
  - NIFTi project deployment in Mirandola 2012: 1 week
  - Fukushima: more than a year
  - Human-robot team performs multiple sorties and missions
  - Situation changes
- Core challenge is to create persistent situation awareness
  - Persistent models of perception and action
  - Persistent multi-robot action models
  - Persistent models for human-robot teaming

  objectives
- Industrial accident scenario

Real life scenario

Phase 1 | Phase 2 (hours) | Phase 3 (hours -days) | Phase 4 (days)

Disaster onset — 7-10 days later

Disaster response

High degree of structural dynamics → Low degree of structural dynamics

Global-scale threat dynamics → Localized, static threats

Roadmap

Phase 1 | Phase 2 (hours) | Phase 3 (hours -days) | Phase 4 (days)

Disaster onset — 7-10 days later

Disaster response

Year 1

Year 2

Year 3

Year 4

Roadmap: complexity scaling

Yr1 Yr2 Yr3 Yr4

Space — Scaling in #Actors, #Time

Basis, Benchmarking — Task — Scaling in #Actors, #Time

Basis, Benchmarking — Team

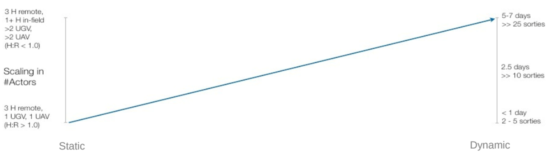

User-centric methodology

- use cases definition
- user-centric requirements analysis
- user-centric experimental evaluation
- user domain studies
- data gathering
- user-centric integrated design
- system-level testing
- component technology development
- concept-level technology integration
- system-level technology integration
- component-level tests&evaluation

Yearly cycles

TRADR Work Package Structure

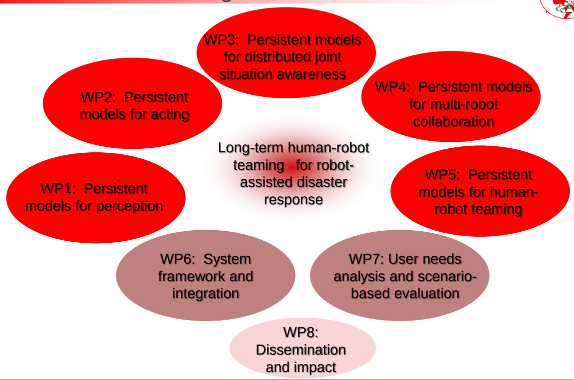

TRADR Year 1

Multiple asynchronous sorties (1 UGV, 1 UAV) to assess a large-scale static disaster

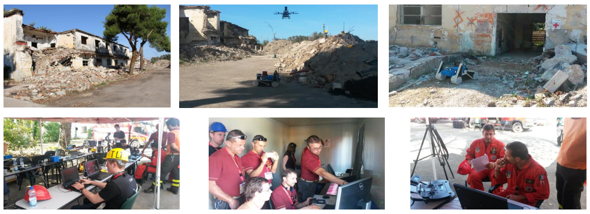

TRADR Joint Exercise, September 2014

WP1: Persistent Models for Perception

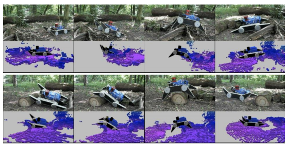

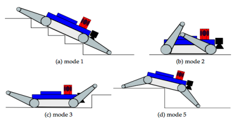

- Adaptive traversability (implicit terrain classification)
- New approach to 3D localization and mapping
- Fusing data with different rates and error characteristics

WP2: Persistent Models for Action

- UGV
  - Standard teleoperation of UGV and Arm
  - Tensor based voting and D*-Lite based path planning combined with Adaptive Traversability Flipper Control

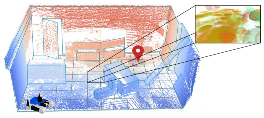

- UAV
  - Work towards near obstacle UAV operation

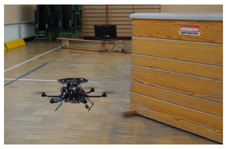

WP3: Persistent Models for Situation Awareness

- Evaluating and modeling national command structures
- Assessment and evaluation of TREX and identification of requirements towards development of new TRADR Display System (TDS)
- Design and prototypical implementation of OCU (Operator Control Unit)
- Framework for the development of a flexible speech-enabled multimodal interface

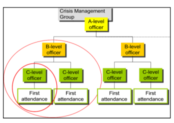

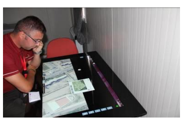

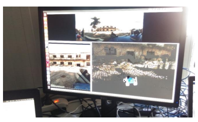

WP4: Multi-Robot Collaboration

- Multi-robot task allocation
- Task switching in robot cognitive control
- Processing necessary to enable higher level planning
- Augmented Reality Environment for mobile robots

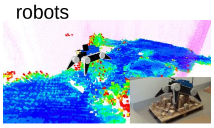

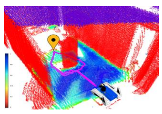

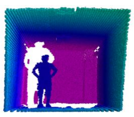

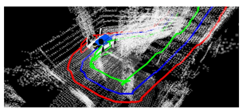

WP5: Human-Robot Teaming

- Cognitive task load modeling and dynamic task allocation
- Better understanding of human-robot teamwork
  - Formal task modeling and investigation of coordination requirements
- Agent-based modeling
  - Ontology for teamwork in search & rescue
  - Agent-based framework design
- Tools for modeling and experiments
- Natural language reporting

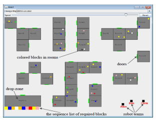

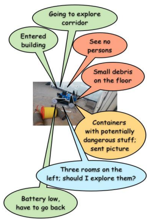

WP6: Framework and Integration

- Migration from NIFTi to TRADR incl. software updates

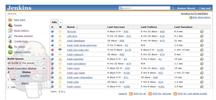

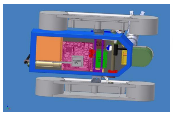

- Re-design of UGV platform and introduction of new UAVs
- Integration of an operable system for TJEx 2014

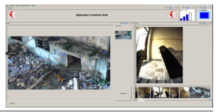

WP7: User Needs and Evaluation

- Specification of the socio-technical design rationale
(use cases, requirements, scenarios)

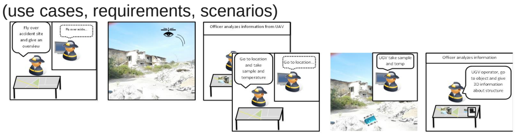

- T-JEx: system evaluation & end-user studies
+ related end-user studies (value assessment workshop, gaze machine)

Outcomes T-JEx:
• systems evaluation and qualitative user studies; identification of positive and negative aspects of the system
• identification of stakeholders, their values and value tensions
• assessment of gaze machine in USAR environment

WP8: Dissemination and Impact

- Summer school 2014 in Prague
- Raising awareness among first responders
- Robot-assisted disaster response guidelines

TRADR Team at TJEx 2014 and…

… one particular team member at TJEx 2015

ASCENDING TECHNOLOGIES

Amazing Technology!

UAVs – Daily Operation and Practical Applications

/// Michael Achtelik and André Ryll

Amazing Technology!

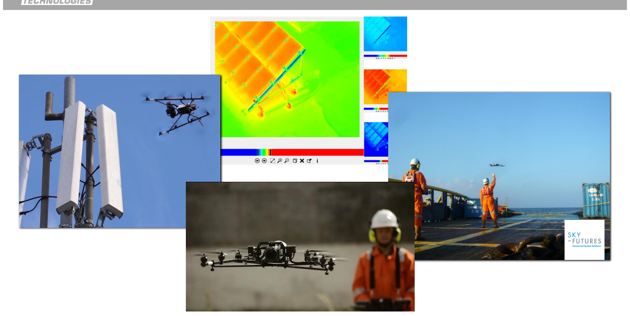

About Ascending Technologies

/// From X-UFO to Volocopter VC200.

Amazing Technology!

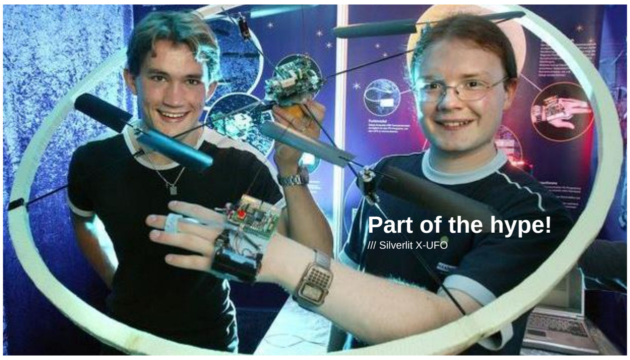

About Ascending Technologies

/// Facts & figures

- Founders have been working successfully on unmanned multi-rotor & autopilot technology since 2002.
- Based in Krailling (Munich), Germany.
- Founded in January 2007.
- About 60 employees.
- Owner-managed.
- 2015: Intel first external investor & minority shareholder.
- Production depth / manufacturing: In-house development & production.

AscTec Research Line

/// Research platforms for …

- Target: Flying robot researchers.
- Flight dynamics
- CV & SLAM
- Swarming

References: US Air Force, NASA, SIEMENS, MIT, TUM, ETHZ, Intel, Google

AscTec Professional Line

Professional aerial sensing platform.

- Target: Professionals, commercial users.
- Inspection
- Survey
- HD imaging

References: AAIR, Cyberhawk, HUVR, Orbiton, Resource Group & Sky-Futures

UAV Applications

/// Proven & tested in a magnitude of over 100,000 professional flying hours.

Amazing Technology!

ASCENDING TECHNOLOGIES

UAV inspection & monitoring.

/// The AscTec Falcon 8 for efficient professional aerial industrial inspection.

/// The quick flight check.

- Check your engines or faulty equipment more efficient.
- Safety by precision – even at tight spots.

Amazing Technology!

ASCENDING TECHNOLOGIES

UAV inspection.

/// The AscTec Falcon 8 for efficient professional aerial industrial inspection.

/// Key Features & Benefits

- AscTec Falcon 8 saves budget and time: e.g. Live flare oil/gas inspection: up to -90 %.
- Conventional methods are risky and expensive.
- Minimizing downtime.
- More quality and details due to aerial HD imaging. Thermal & RGB stills/videos.
- Precise structure analysis & quick damage detection.
- Low-noise & emission-free operations.

https://youtu.be/xAPZvp6C8P4

0:49-1:34

ASCENDING TECHNOLOGIES

UAV inspection.

/// The AscTec Falcon 8 for efficient professional aerial industrial inspection.

ASCENDING TECHNOLOGIES

AscTec Trinity – Short version

https://www.youtube.com/watch?v=fsNGwSjSZd4

Amazing Technology!

ASCENDING TECHNOLOGIES

Inspection

/// Key Features & Benefits

- Quick initialization: No waiting, but prompt starting after switching on.
- Enhanced efficiency in every operation: Faster takeoff, rising, flying, descending and landing possible.
- Perfectly predictable flight behaviour & exactly reproducible waypoint navigation.
- Wind load balancing: Up to 15 m/s (GPS Mode: 12 m/s)
- Robust against electromagnetic fields.

ASCENDING TECHNOLOGIES

https://vimeo.com/116945708

UAV surveying & mapping.

/// The AscTec Falcon 8 for efficient professional aerial industrial inspection.

/// High accuracy & resolution.

- 36 Megapixel camera.
- Perfect for volume calculation.

Amazing Technology!

Land survey.

/// Key Features & Benefits:

- AscTec Falcon 8 is closing the gap between fixed- and rotary-wing UAV.
- Ease of use of a multi-rotor, but much more efficient.
- Complex flight planning & Quick Survey (PC-less) based on waypoint navigation.
- High area output. High resolution.
- Precise position hold.

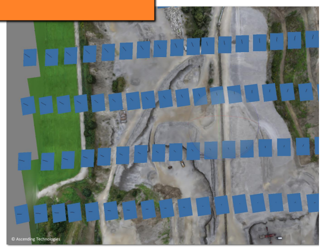

Structural analysis

/// Key Features & Benefits

- AscTec Falcon 8 for monument & heritage protection, topography & archaeology.
- Reduction of budget and time.
- E.g. retaining wall inspection: 12.000 sqm, 1.6 mm resolution in 24 min. (Based on test without AscTec Trinity)
- Accurate positioning with GPS. (Height or Manual Mode possible)
- Robust against external influences.

https://youtu.be/aNq-9xyzXhE

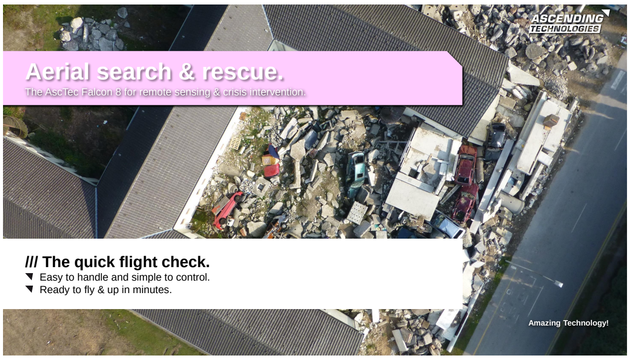

Aerial search & rescue.

The AscTec Falcon 8 for remote sensing & crisis intervention.

/// The quick flight check.

- Easy to handle and simple to control.
- Ready to fly & up in minutes.

Amazing Technology!

Aerial search & rescue.

/// Exploration in active zone.

- Quick overview & mapping.
- Transportable fully assembled.
- Easy deployment

/// Remote sensing solution:

- High-Performance GPS for weak signals in tight spots.
- Various payloads

Aerial search & rescue.
/// Case Study: Fire Department of Dortmund

images deleted because of copy right problems

Aerial search & rescue.
/// Case Study: Fire Department of Dortmund

/// Hot Spot Detection

- Thermal camera + Raw data processing
- Inside the hall (right)
- Synchronous use of thermal and daylight camera
- Outside overview (bottom)

images deleted because of copy right problems

Aerial search & rescue.
/// Case Study: Fire Department of Dortmund

images deleted because of copy right problems

/// Comparison between natural and thermal image
/// Colors indicate relative temperature range spread over the lowest and highest measured temperature.

Aerial search & rescue.
/// Case Study: Fire Department of Dortmund

/// Conclusion

“A fast taken foto as an overview of the scenario delivers application-tactical information. In case of fire fighting, hot spots can be detected or the spread out of fire can be watched and prognosticated. It is important to provide the information as quickly as possible to the person who needs it for its tactical as well as operative approach. E.g. the fire fighter on the ladder. This can be fulfilled by small scaled UAVs, so called „out of the box“ solutions like the Falcon 8.”

UAVs & the TRADR Project

/// Providing a new perspective

Amazing Technology!

https://youtu.be/4z86nUlgEqc

1:05 – 2:01

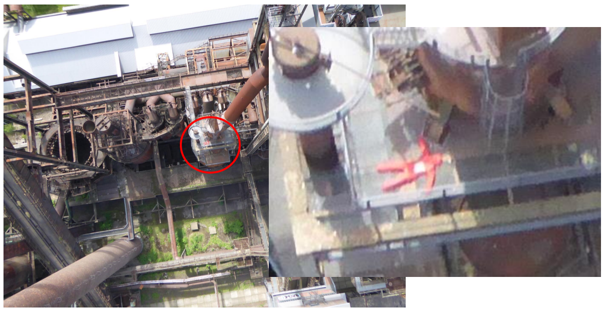

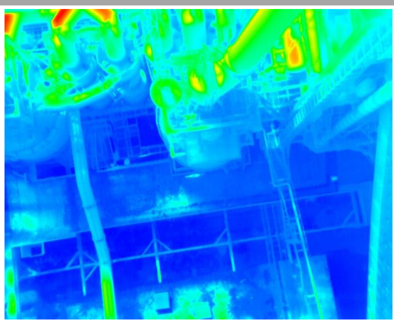

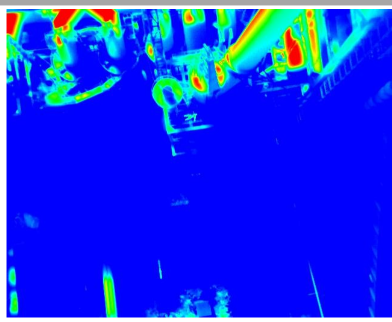

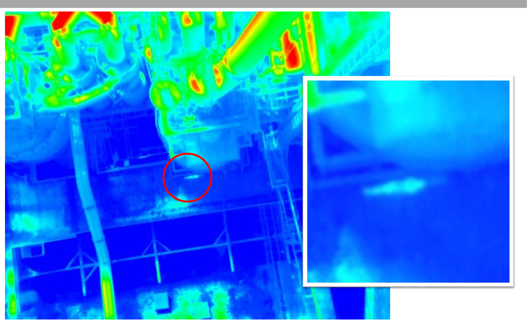

Moving Indoors & Close to Structures

/// Detecting and Avoiding Obstacles

Amazing Technology!

Intel keynote @ CES

https://youtu.be/Us0BqJvsF9k

3:15 - end

Amazing Technology!

Research Platforms and Projects

/// Stable and Robust Obstacle Avoidance:
The Holy Grail in UAV Technology?

Amazing Technology!

TRADR

Long-Term Human-Robot Teaming
for Robot Assisted Disaster Response

European Robotics Challenge (EuRoC)

https://youtu.be/8z8FAF2qJDA

- 3 industry-relevant challenges
- Challenge 3:
  Plant servicing and inspection
- 3 Stages of increasing complexity:

Simulation Contest
- Qualification (34 teams registered from Europe)
- Team up with Industrial Partner and his use-case

Realistic Labs
- Experiments with real platforms in realistic lab environment
- Tasks based on submitted use-cases

Field Tests
- Demonstrate pilot experiments on end-user site
- → EuRoC Winner

EuRoC Qualification impressions

- Sorry, video not on youtube

The new UAV platform for cutting edge research:

- New Platform for EuRoC and TRADR
- Configurations:
  - Quad
  - Hex
  - 9" propellers
  - 11" propellers
- AscTec Trinity flight controller
- Available summer 2016
- Beta Series for TRADR and EuRoC 2015

AscTec Neo – Key Features

- Payloads up to 1.5kg
- Total weight below 4kg
- Flight Time: >20mins
- Folding propellers
- Highly efficient motor controllers
- Detachable motor booms
- Redundant flight controllers
- Redundant smart batteries
- User-Programmable AscTec Trinity
- Standardized mechanical interface

AscTec Neo – Dimensions and Flight Time

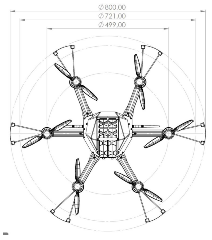

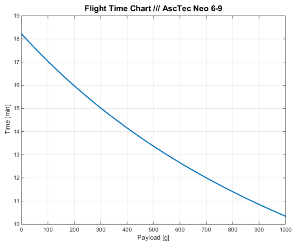

AscTec Neo – Key Features

AscTec Neo – Flight controller comparison

AscTec AutoPilot

- Dual processor approach
- Safe evaluation of custom algorithms
- Fallback to single processor (LLP) always possible (in flight)
- 2x ARM7 processor @ 58MHz
- One processor (almost) freely programmable by end-user (HLP)

AscTec Trinity

- 3x fully equipped processors + all sensors
- Redundant flight control at all times
- Two AscTec Trinity used as „LLP"
- Fallback to redundant LLP
- 3x Cortex-M4 + FPU @ 180MHz
- One AscTec Trinity fully user-programmable (HLP)

AscTec Neo - Interfaces

Mechanical

- Standardized 80x80mm mount on all payloads
- Connection struts are side-accessible
  - Remove one payload without dismounting all payloads above it

Power Outlets

- Battery voltage (14 – 16.8V)
- 12V, 2A
- 5V, 2A

AscTec Neo - Interfaces

Electrical

- UART: up to 2
- I2C: up to 2
- SPI: 1
- CAN: 1
- PWM: 2
- USB: 1 (host or client)

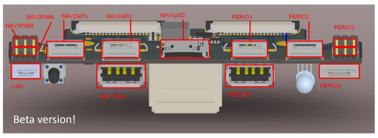

AscTec Neo – Planned Payloads

- Intel NUC with Core i7
- 360° Intel RealSense Sensor-Ring
- Atomboard
- Laser Scanner
- Various camera mount options
- Optical Flow Sensor
- Propeller Protection

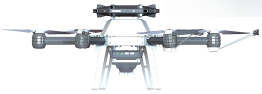

AscTec Neo - SDK

- Only uses free tools
  - Eclipse
  - GCC 4.9
  - OpenOCD
- STM32F4 microcontroller
- Recommended RTOS: ChibiOS (v3)
- Bare Metal programming possible
- Embedded Debugging
  - with Thread awareness
- Access to all sensors on the user-programmable Trinity
  - Accelerometer
  - 2x Gyroscope
  - Barometer
  - Compass
- Access to raw and fusioned data from the other Trinitys
- Various control options

/// Your flight plan:

/// New career?

Amazing Technology!

Job Opportunities

- Mitarbeiter UAV Entwickler / In Für Robotik
  – Mit Schwerpunkt Sensordatenverarbeitung / Regelungstechnik
- Mitarbeiter UAV Hardware Entwickler / In – Embedded Software Entwickler / In
- Mitarbeiter UAV Entwicklungsingenieur / In Hochfrequenztechnik / Embedded Elektronik
- Mitarbeiter UAV Softwareentwickler / In
- Softwareentwickler Für Anwendersoftware
- Entwicklungsingenieur Embedded Elektronik
- Application Engineer
- Mitarbeiter UAV Produktion
- Produktionshelfer Im Bereich Bestückung
- Werkstudent Entwicklung

/// Address for applications
Mrs Natalie Achtelik
Ascending Technologies GmbH
Konrad-Zuse-Bogen 4
82152 Krailling Germany
Please direct your application to:
jobs@asctec.de

Let‘s go out and Fly

/// Try the AscTec Neo and Falcon yourself

Amazing Technology!

Outline

- **Introduction**
- Problem
- Abstraction and Approach
- Results
- Summary
- Exercise

Why autonomy?
Increase Efficiency of Operations

Drone Cockpit, Brian William Jones ,http://goo.gl/G73vhs

Increase Safety

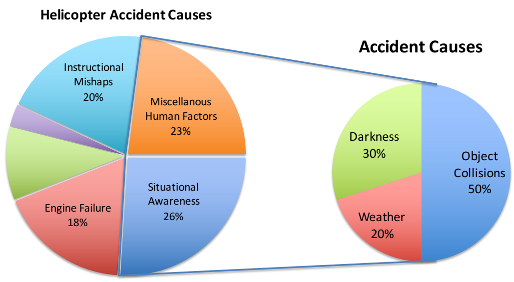

(United States Industry study by Honeywell 2010, http://goo.gl/R06naI)

Improve Applications
such as Cargo Delivery

Drone Delivery, Netflix, http://youtu.be/ucz3JpvDQjk

Improve Applications
such as Cargo Delivery

AACUS Demonstration, Office of Naval Research, http://goo.gl/JtMkNm

Enable New Applications

Water Drop by Helicopter at Fukushima, NHK World TV, approx. 10am JST 03/16/2011, http://goo.gl/NHlGek

Enable New Vehicle Designs

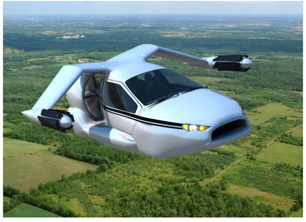

Flying Car, Terrafugia, http://goo.gl/Aiyd5R

ARES, DARPA, http://goo.gl/O2CDCL

Why is Autonomy Difficult?

Why is Autonomy Difficult?

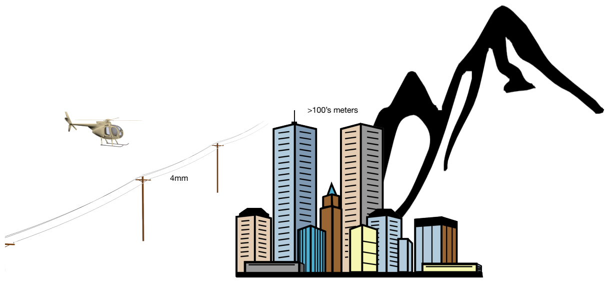

Why is Autonomy Difficult?

Goal

Make a robotic pilot that is safer and more efficient than human pilots or birds.

(Manual Flight)

Research Areas

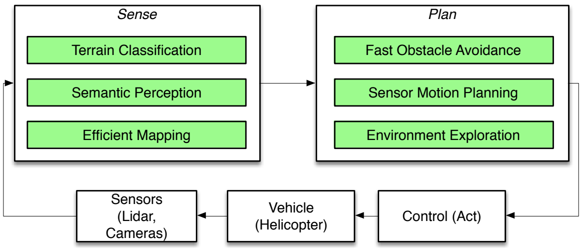

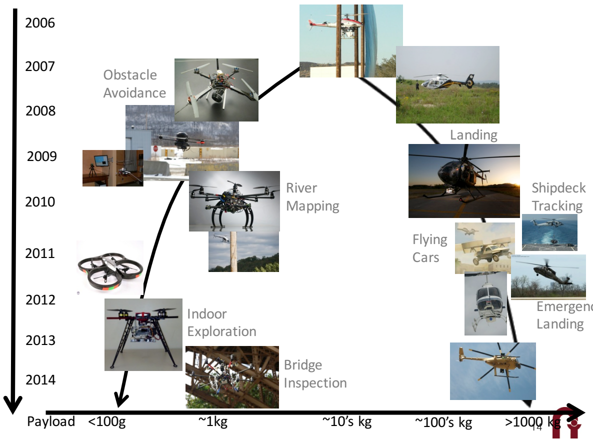

Small: Autonomous Flight inside Smoke-Filled Ship

Fang and Scherer, ICRA 2015, Fang et al. FSR 2015, Holtz and Scherer FSR 2015

Medium:Autonomous Self-Guided River Exploration

Nuske et al. , JFR 2015

Bridge Inspection with Micro Aerial Vehicles

Yoder and Scherer FSR 2015

Large: Autonomous Approach and Landing

Choudhury et al. AHS Forum 2014, and other work

Each System Operates in Different Environments and Has a Different Motion Planning Approach

- Why don't we have an ultimate motion planning system that works well for all applications?
- What is common and what is different between applications?
- What are potential approaches?

Outline

- Introduction
- **Problem**
- Abstraction and Approach
- Results
- Summary
- Exercise

Motion Planning Problem

React in real-time to previously unknown obstacles, avoid no-fly-zones, and land.

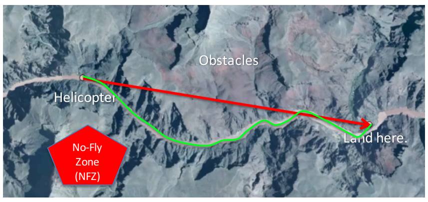

Assumptions

Here:
- Little uncertainty
- No exploration actions necessary

<u>Variations on the problem</u>
System uncertainties:
- Position
- Sensing
- Action

Need to gather data about the world:
- Maximize information gain
- No explicit goal state
- Viewpoint planning or active exploration

The Trajectory Planning Problem

find	$\sigma(t) = \{x(t), y(t), z(t), \psi(t), t_f\}$	Time parameterized trajectory
minimize :	$J = \int_0^{t_f} c(\sigma(t))dt + c(\sigma(t_f))$	Cost function
constraints :	$\sigma(0) = \sigma_0$ $\sigma(t_f) = \sigma_f$	Boundary value constraints
	$h(\sigma(t), \dot{\sigma}(t), \ddot{\sigma}(t), \dots) = 0$	Non-holonomic constraints
	$g(\sigma(t), \dot{\sigma}(t), \ddot{\sigma}(t), \dots) \leq 0$	System limitations
	$J < \infty$	Cost function constraints

Variant of the optimal control problem constrained to a trajectory

Note that typically *J* is partially known and discovered on the fly.

Example

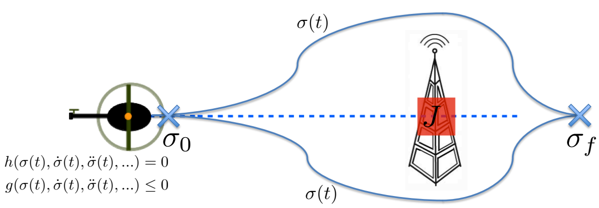

Planning Problem: Cost Functions

$$J_{total} = \sum_i w_i J_i$$

1. Time to Mission Completion

$$J_1 = t_f$$

2. No Fly Zone

$$J_2 = \begin{cases} \infty & \sigma(t) \in X_{NFZ} \\ 0 & otherwise \end{cases}$$

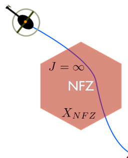

Planning Problem: Cost Functions

3. Time to Collision

- Representation of collision risk
- Scales with velocity
- Based on reachability volume
- Approximated by a pyramid

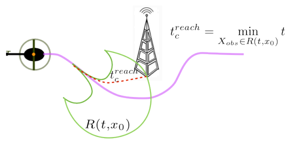

(Reachability)

$$t_c^{reach} = \min_{X_{obs} \in R(t,x_0)} t$$

$$J_3 = \begin{cases} (t_{max} - t_c^{reach})^2 & \\ \infty & d_{obs} < d_{critical} \end{cases}$$

Obstacle Representation

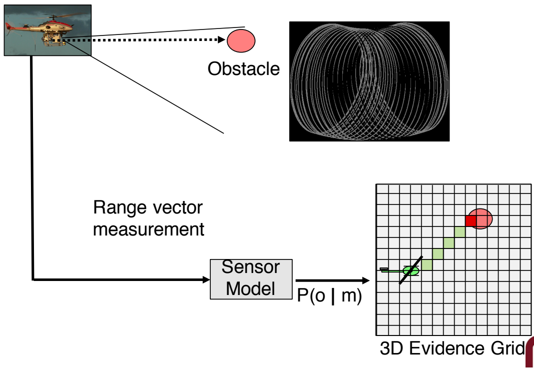

Updating an Evidence Grid Cell

- Each cell is assumed to be independent and contains the belief of occupancy of the volume
- The belief can be updated as follows (assuming the prior *P(m)=0.5*):

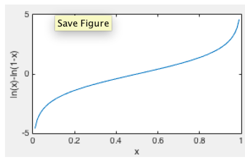

$$b'(m) = 1 - \left(1 + \frac{P(m|o)}{1-P(m|o)} \cdot \frac{b(m)}{1-b(m)}\right)^{-1}$$

- However usually a log-odds representation is used:

$$\bar{b}'(m) = \bar{b}(m) + \ln P(m \mid o) - \ln(1 - P(m \mid o))$$

Foessel02

A typical Sense, Plan, and Act Cycle (Comparison between Ground and Air Robots)

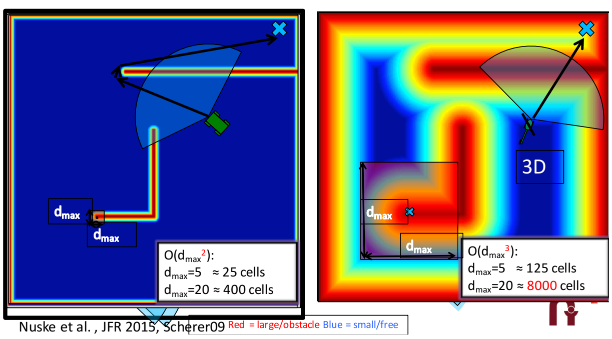

Nuske et al. , JFR 2015, Scherer09

A Completely Incremental Framework for Planning

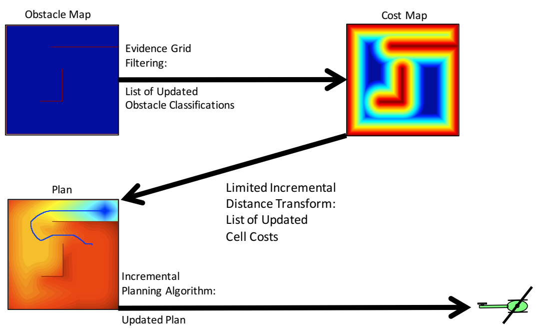

Nuske et al. , JFR 2015, Scherer09

How does one handle large environments and speeds?

- Full-scale helicopter at 60 m/s. Mission lengths ~ 400km.
- Scrolling buffer grids:

$$i = rx \mod n$$
$$j = ry \mod n$$
$$k = r_z z \mod m$$

- *r*, r_z = resolution, *n*,*m* = map size,
- *x*,*y*,*z* = coordinates, *I*,*j*,*k* = map indices

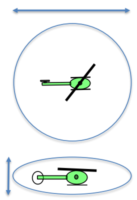

Nuske et al. , JFR 2015

Questions

- What are some of the pros/cons of this type of approach for filtering?
- What are alternative approaches to represent the world what are their advantages and disadvantages?

Planning Problem: Constraints

1. Dynamics

Coordinated vehicle motion with no sideslip (above 20 knots)

$$\psi = \tan^{-1}\frac{\dot{y}}{\dot{x}}$$
$$\phi = \tan^{-1}\frac{v\dot{\psi}}{g}$$

ψ heading
ϕ roll

2. Actuator Limits

$$\phi \le \phi_{max}, \dot{\phi} \le \dot{\phi}_{max}, \dot{v} \le a_{max}, \dot{\psi} \le \psi_{max}, v \le v_{max}, v_h \le v_{h,max}$$

(3. Wind)

~~Related motion in airmass to ground track – constrains the minimum radius of curvature.~~

$$\cancel{\dot{x}_g = V_a \cos(\psi(t)) + V_{w,x}}$$
$$\cancel{\dot{y}_g = V_a \sin(\psi(t)) + V_{w,y}}$$

Coordinated Turn Equations

Turning Radius
$$R = \frac{V_a^2}{g \tan\phi}$$

Center of Turn
$$c_n = p_n + R\cos(\psi - s\frac{\pi}{2})$$
$$c_e = p_e + R\sin(\psi - s\frac{\pi}{2})$$

Change in Angle
$$\Delta\phi = \frac{V_a}{R}\Delta t$$

New Position
$$p_n' = c_n + R\cos(\psi + s\frac{\pi}{2} - \Delta\phi)$$
$$p_e' = c_e + R\sin(\psi + s\frac{\pi}{2} - \Delta\phi)$$

V_a = Forward speed
R = Turning radius
ϕ = Roll angle
ψ = Heading angle
p_n, p_e = North, east position
c_n, c_e = Center of turn

Outline

- Introduction
- Problem
- **Abstraction and Approach**
- Results
- Summary
- Exercise

The Trajectory Planning Problem

find	$\sigma(t) = \{x(t), y(t), z(t), \psi(t), t_f\}$	Time parameterized trajectory
minimize :	$J = \int_0^{t_f} c(\sigma(t))dt + c(\sigma(t_f))$	Cost function
constraints :	$\sigma(0) = \sigma_0$ $\sigma(t_f) = \sigma_f$	Boundary value constraints
	$h(\sigma(t), \dot{\sigma}(t), \ddot{\sigma}(t), \ldots) = 0$	Non-holonomic constraints
	$g(\sigma(t), \dot{\sigma}(t), \ddot{\sigma}(t), \ldots) \le 0$	System limitations
	$J < \infty$	Cost function constraints

What are potential approaches to solve this problem?

How do we discretize the problem?

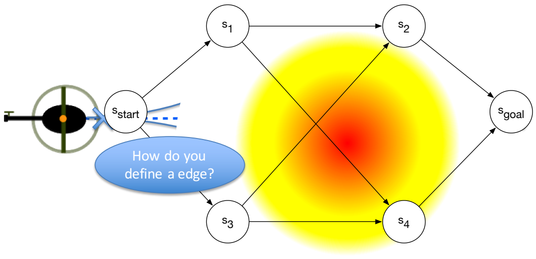

(Not always explicitly constructed)

How do we find the best path through the graph?

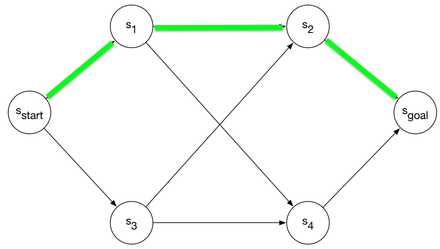

Edge Costs

- Cost between two nodes. (Can also have vertex costs but typically only edge.)
- Cost *c(s,s')* depends on the cost of the objective *J* of the trajectory segment of the edge *s->s'*
- Calculating *c(s,s')* can be expensive (collision checking)

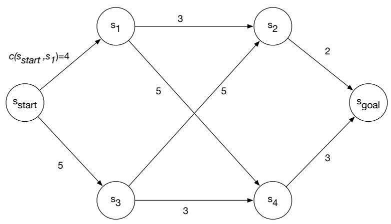

Calculating the least-cost path

g(s) cost of the least-cost path. Optimal *g* satisfies: $g(s) = \min_{s' \in pred(s)} g(s') + c(s', s)$

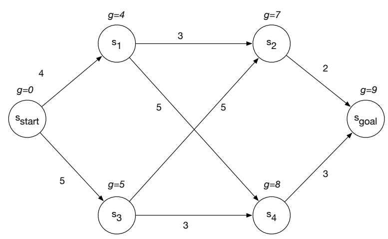

Finding the Least-Cost Path: Backtracking

- Start at the goal and greedily backtrack to start: $s'' = argmin_{s' \in pred(s)}(g(s') + c(s', s)$

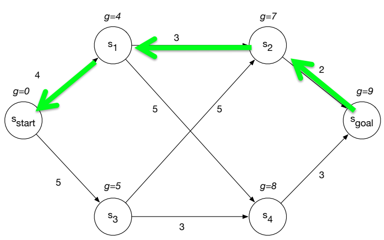

What are the main questions?

Fixed time/memory budget (real-time planning):

1. What vertices to create?
2. Where to search?

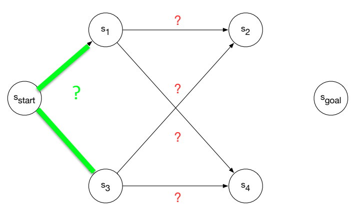

3 Representative approaches:

- Regular graph search: A*-grid search
- Sampling-based: RRT*
- Trajectory optimization: CHOMP

A*

Compute optimal *g* and heuristic *h*

1. What vertices to create?
   Based on heuristic and cost *g+h*
2. Where to search?
   Look at priority queue

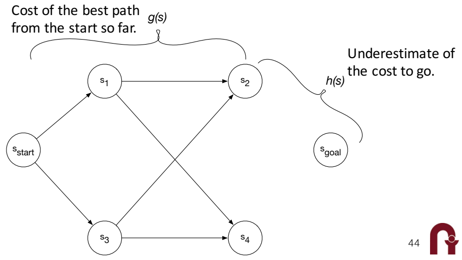

Admissible Heuristic Function *h*

- Popular function: Euclidean distance

h(s):

- Admissible: $h(s) \leqq c(s, s_{goal})$
- Consistent (satisfies triangle inequality):
  - $h(s_{goal}, s_{goal}) = 0$ and for all other states:
  - $h(s) \leqq c(s, succ(s)) + h(succ(s))$

A* Search

Update *g* based on the smallest g+h cost:
A:*

$g(s_{start})=0$; $g(s \neq s_{start})=\infty$; OPEN=$\{s_{start}\}$

while($s_{goal} \neq s$)
  remove *s* with the smallest *g(s)+h(s)* from *OPEN*
  expand *s*

A* Properties

- Resolution-complete and optimal
- Minimum number of state expansions

Questions

- What graph should you create?
- What resolution to pick?
- How do you expand it?
- Performance depends on
  - Graph: Branching factor/Abstraction of the system
  - Quality of the heuristic for the system and environment
  - Match of the graph abstraction to the environment

Going Deeper

- How do you incorporate dynamics into your graph?
  – State lattice: [Pivtoraika09]
  – Maneuver Automaton: [Frazzoli02]
- What are more interesting heuristics for dynamical systems?
  – Precompute heuristics [Knepper06]
  – Dubin's heuristic [Dubins57]
- How do we repair rather than redo the search for the changing graph?
  – D* Lite [Koenig02]
  – Anytime D* [Likhachev05]
  – Anytime Search [Hansen07]

Sampling Based Planning

- Where should you put your graph?
- What resolution to pick?

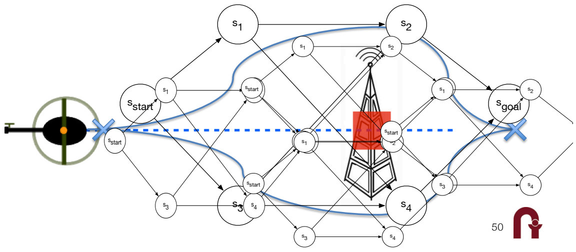

Sample the Environment (in an Increasingly Denser Fashion) and Connect the Samples to Construct a Tree to Find a Path to the Goal (RRT*)

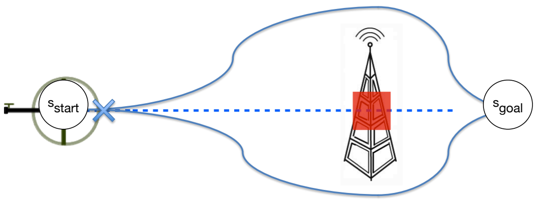

Sample a Potential Location to Expand To

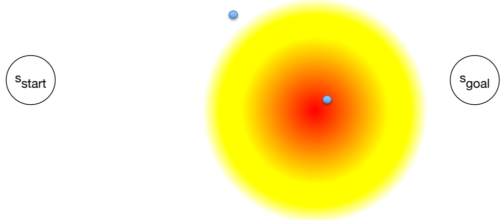

Add Edge to Connect to Graph

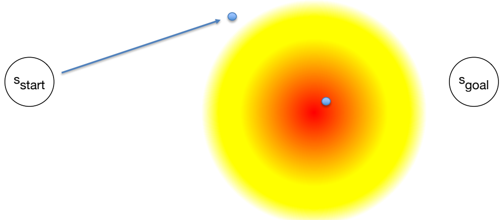

Add Edge to Connect to Graph

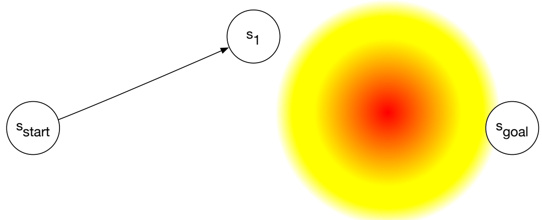

Add Edge to Connect to Graph and Repeat

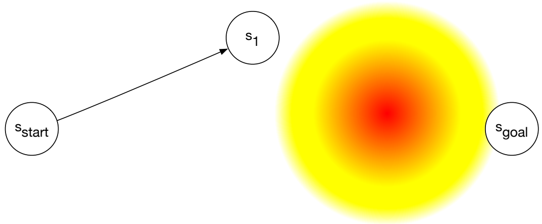

Some Iterations Later…

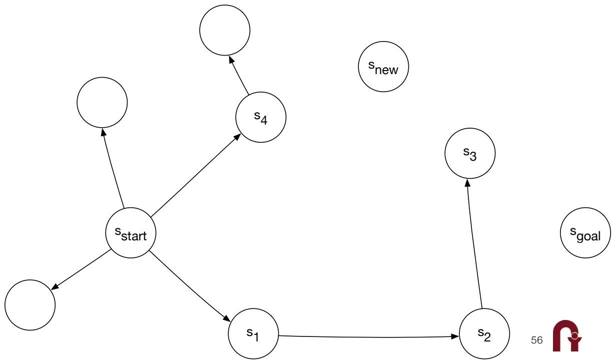

Look at the neighbors within *r*

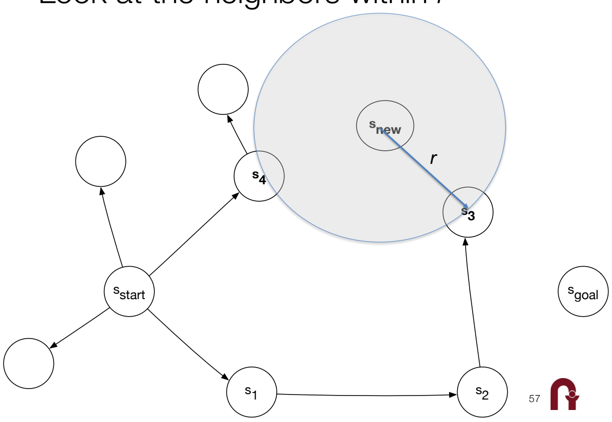

Connect

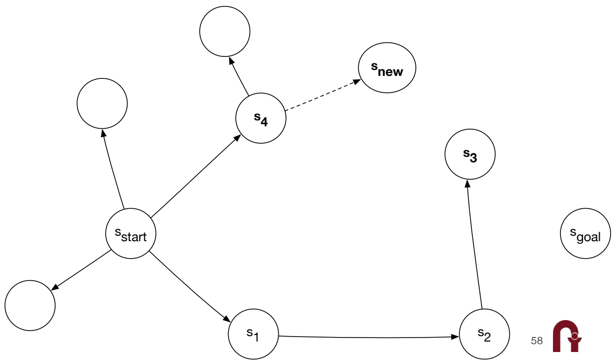

Check outgoing edges for lower costs (Rewiring)

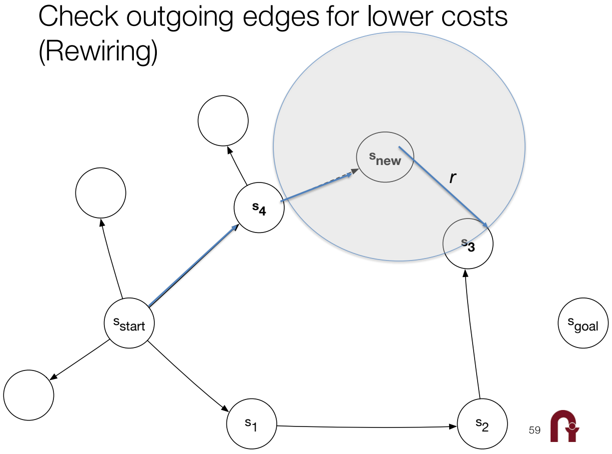

Change the Parent and Fix Tree

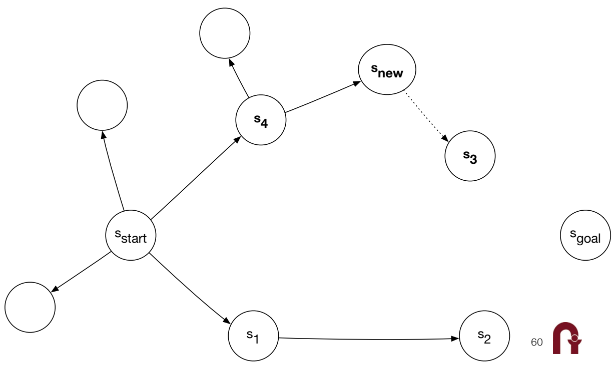

Change the Parent and Fix Tree

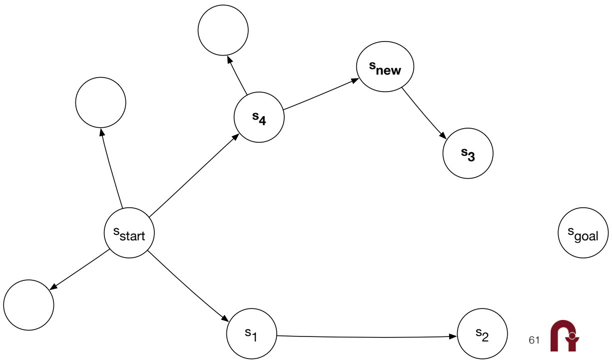

RRT* Algorithm (Concept)

$V = s_{start}$; $E=\{\}$

for i=1…n

s_{new} = getNewValidRandomSample()

S_{near} = getVerticesWithin($r(i)$)

(s_{min}, J_{min}) = getLowestCostNeighbor(S_{near})

$E = E \cup (s_{min}, s_{new})$, $S = S \cup s_{new}$

E = rewireTree(E, S_{near})

Radius

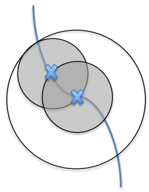

card(V)= number of vertices, *d* = number of dimensions

$\mu(X_{free})/\zeta_d$ Ratio of the volume to the volume of the unit sphere.

$$r = \gamma_{RRT^*}\left(\frac{\log(card(V))}{card(V)}\right)^{1/d}$$

$$\gamma_{RRT^*} = 2\left(1+\frac{1}{d}\right)^{1/d}(\mu(X_{free})/\zeta_d)^{1/d}$$

Why rewire the tree?

- Remove unnecessary detours
- Optimize for the minimum cost rather than committing to connections to early.

Questions

- What is expensive in this algorithm?
- What about *r* if our robot is motion constrained?
- How can one incorporate heuristics?
- In what environments will this algorithm perform well?

Going Deeper

- Why does this particular choice of *r* lead to optimum plans? [Karaman11]
- What if we consider a batch of samples to expand and keep a heuristic? [Gammell15]
- What if we one to have alternative routes instead of just the best route? [Choudhury13]

Trajectory Optimization (CHOMP)

- Exploit the first order information available about the trajectory
- Perturb an initial guess to minimize the cost function
- Example on left:
  - Straight line initial guess
  - Several optimization steps

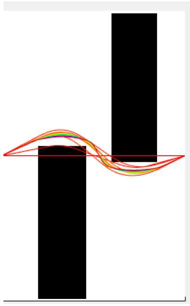

Zucker13

Going Back To Our Graph Example:

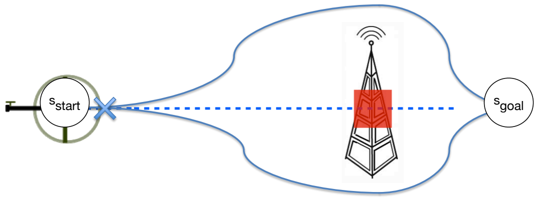

Add Vertices based on the Gradient

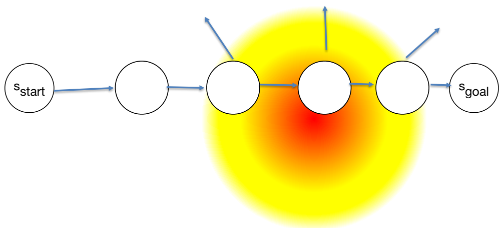

Add Vertices based on the Gradient

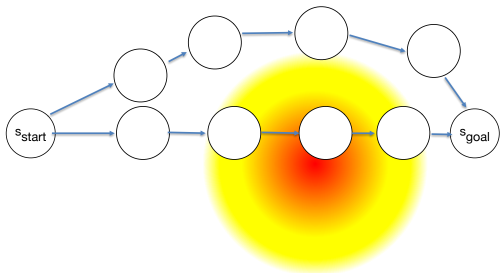

Cost Function

- Want the trajectory to be smooth to be executable by the robot and reach the goal

$$\mathcal{F}_{smooth}[\xi] = \frac{1}{2}\|K\xi + e\|^2 = \frac{1}{2}\xi^{\mathsf{T}}A\xi + \xi^{\mathsf{T}}b + c$$

- Avoid obstacles

$$\mathcal{U}[\xi] = \mathcal{F}_{obs}[\xi] + \lambda\mathcal{F}_{smooth}[\xi]$$

Key Idea

- Minimize the update to the trajectory with a smooth perturbation of the trajectory
- For example minimize the amount of velocity or acceleration added

=> Perform steepest descent in trajectory space

$$\xi_{k+1} = \xi_k - \frac{1}{\lambda}M^{-1}g_k$$

Measuring the Difference in Trajectory Space

Depends on your representation.

Example *M* for waypoints:

Finite difference between waypoints

M

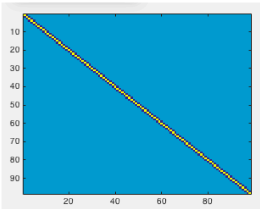

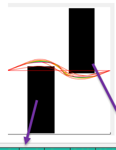

g_k

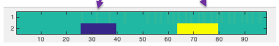

M^{-1}

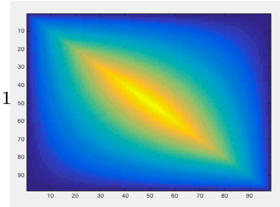

$\frac{1}{\lambda} M^{-1} g_k$

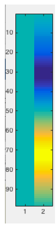

$$\xi_{k+1} = \xi_k - \frac{1}{\lambda} M^{-1} g_k$$

Questions?

- Is it complete and optimal?
- How could include dynamic constraints in the trajectories (other than projection)?
- Why is it an effective method for air vehicles?
- How could you include other planning approaches in the optimization?

Going Deeper

- Enforcing constraints on the trajectory? Project back along same space
- More challenging or larger environments? [He2013]
- Other trajectory optimization approaches? [Kolter09]

Planner Ensemble Idea

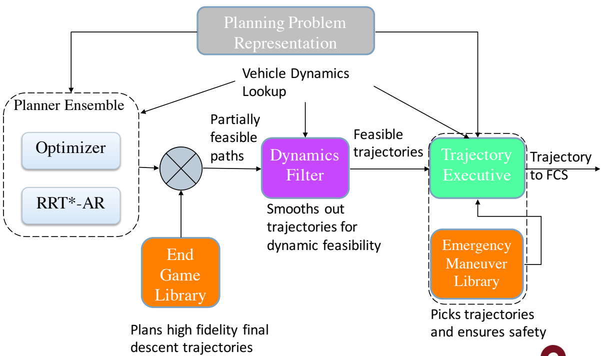

Choudhury et al. AHS Forum 2014

Conceptual Illustration of Trajectory Planner

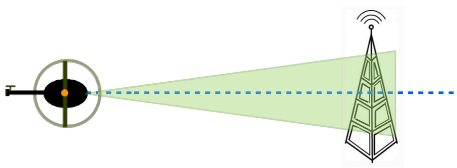

Obstacle enters sensor range

Conceptual Illustration of Trajectory Planner

Obstacle mapping updates occupancy grid

Conceptual Illustration of Trajectory Planner

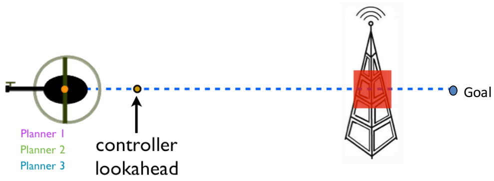

Planners receive start pose (lookahead) and goal pose

Conceptual Illustration of Trajectory Planner

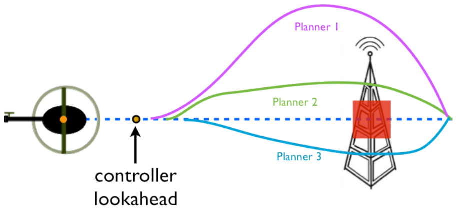

Each planners computes a trajectory and gives it to the executive

Conceptual Illustration of Trajectory Planner

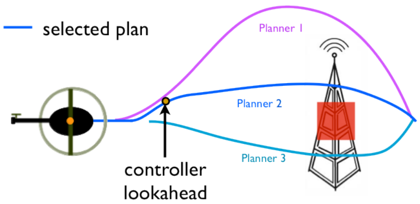

Executive selects planner 2 trajectory as optimal path

Conceptual Illustration of Trajectory Planner

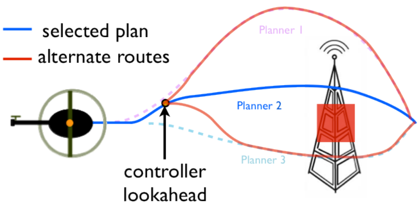

Executive retains other paths as alternate routes

Ensemble/Executive result

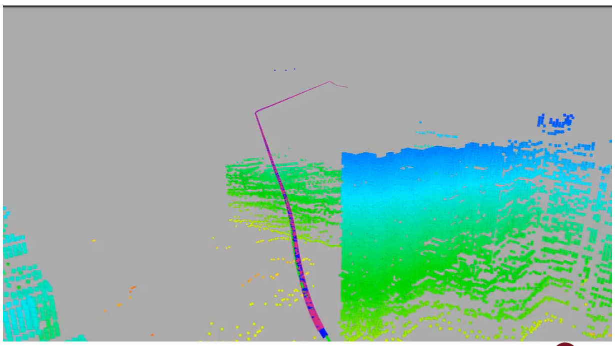

Dynamics Filter – Producing feasible paths

Dynamic's Filter

- Accepts a partially feasible trajectory and filters it to be fully dynamically feasible.
- Dynamics have non-linear constraints – no analytical solution exists
- Thus planners plan dubin's curve (analytic) which is filtered to be within a funnel around the original path.

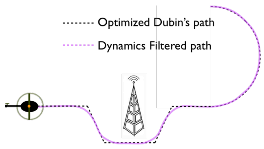

Choudhury and Scherer, ICRA 2015

Outline

- Introduction
- Problem
- Abstraction and Approach
- **Results**
- Summary
- Exercise

Avoiding a Mountain in the Flight Path

Planning Result for Optimizer.

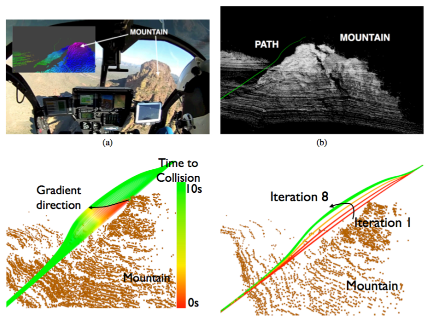

(a) (b) (c) (d)

The optimizer can smoothly avoid the mountain and is selected because the cost optimal

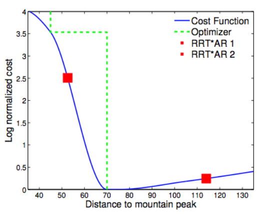

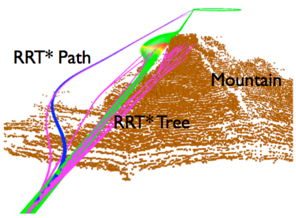

Obstacle Avoidance with a No-Fly-Zone: Comparison between RRT* and Optimizer

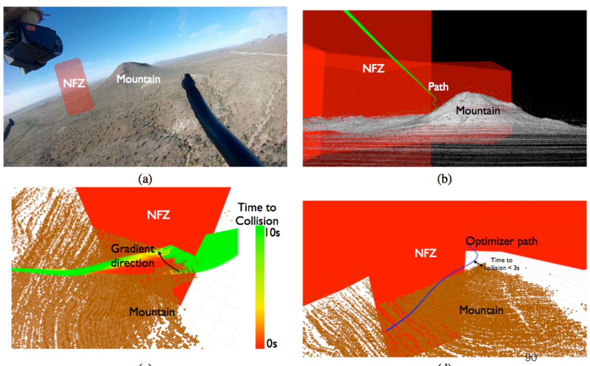

(a) (b) (c) (d)

RRT*-AR Path is Picked Because the Optimizer Gets Stuck in a Local Minimum

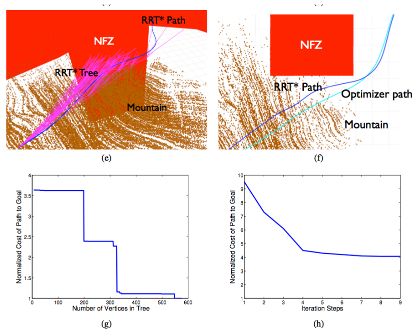

91

Trajectory Planner Design

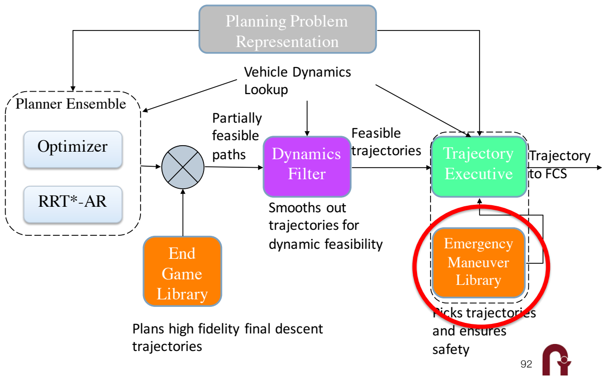

92

Emergency Maneuver Library – Defining Safety

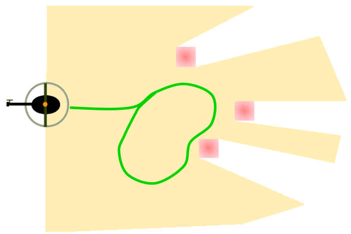

Known Volume — Safe Trajectory

Known Obstacles

93

Emergency Maneuver Problem

$$
\begin{aligned}
&\mathit{find} && \sigma(t) = \{x(t), y(t), z(t), \phi(t), \psi(t), \theta(t)\}\\
&\mathit{constraints} && \forall t, \sigma(t) \in K_t / O_t \quad \text{Safety Constraint}\\
& && \sigma(0) = \sigma_0\\
& && h(\sigma(t), \dot{\sigma}(t), \ddot{\sigma}(t), \ldots) = 0\\
& && g(\sigma(t), \dot{\sigma}(t), \ddot{\sigma}(t), \ldots) \le 0
\end{aligned}
$$

$\sigma(t)$	Time parameterized trajectory
K_t	Known Volume at time t
O_t	Known Obstacles at time t
$\sigma(0)$	Boundary value constraints
$h(\ldots)$	Non-holonomic equality constraints
$g(\ldots)$	Inequality bounds specifying system limitations

94

Example Use Case

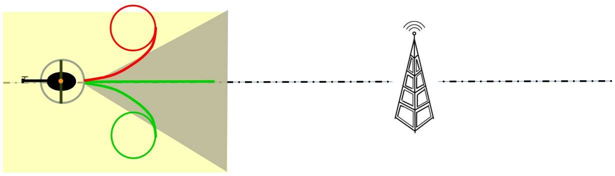

Planned Trajectory — Safe Emergency Maneuver

Known Space — Unsafe Emergency Maneuver

Current Laser Coverage

95

Example Use Case

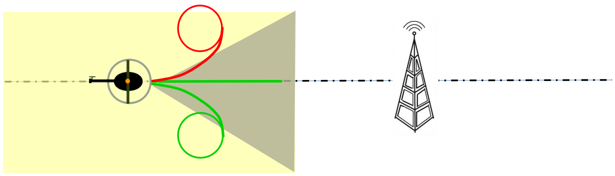

Planned Trajectory — Safe Emergency Maneuver

Known Space — Unsafe Emergency Maneuver

Current Laser Coverage

96

Example Use Case

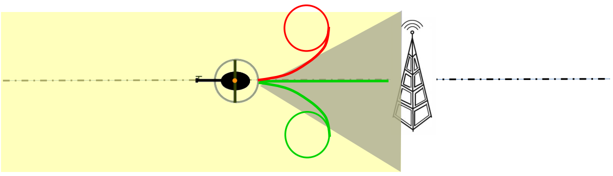

- Planned Trajectory
- Known Space
- Current Laser Coverage
- Safe Emergency Maneuver
- Unsafe Emergency Maneuver

Example Use Case

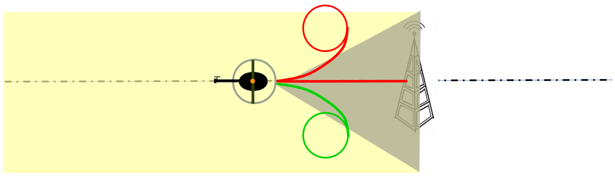

- Planned Trajectory
- Known Space
- Current Laser Coverage
- Safe Emergency Maneuver
- Unsafe Emergency Maneuver

Approach: Emergency Library is Computed Offline to Enable Verification

$$\Upsilon_d = argmax_{\Upsilon} P_u(\Upsilon)$$

$constraints$

$$|\Upsilon| \leq n$$

Υ	Set of dynamically feasible control invariant trajectories
n	Number of trajectories allowed in the set
$P_u(.)$	Probability of at least one trajectory in the set being unoccupied

The Emergency Maneuver Set can be Found Greedily

The general optimization problem is NP hard

We greedily generate a set, while proving a sub-optimality bound on the greedy optimization

$$\Upsilon_d = argmax_{\Upsilon} P_u(\Upsilon)$$

$constraints$

$$|\Upsilon| \leq n$$

Υ	Set of dynamically feasible control invariant trajectories
n	Number of trajectories allowed in the set
$P_u(.)$	Probability of at least one trajectory in the set being unoccupied

Arora et al., AHS 2014

Example Emergency Maneuver Library

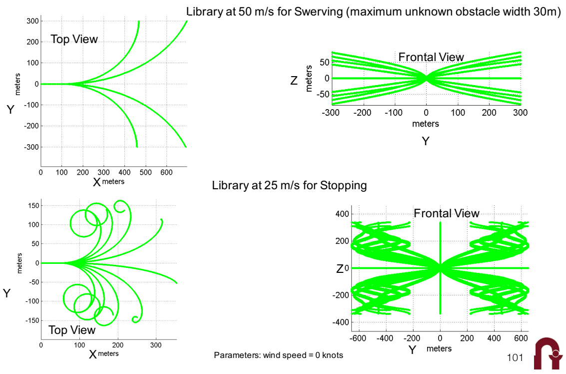

Example Simulation Result

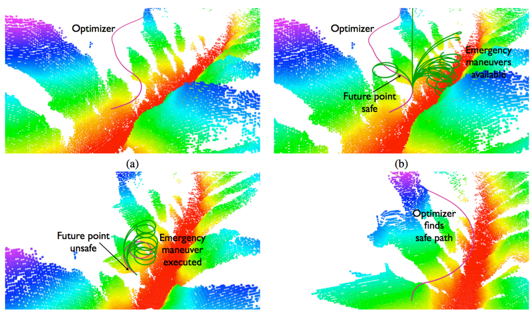

Flight Test Result

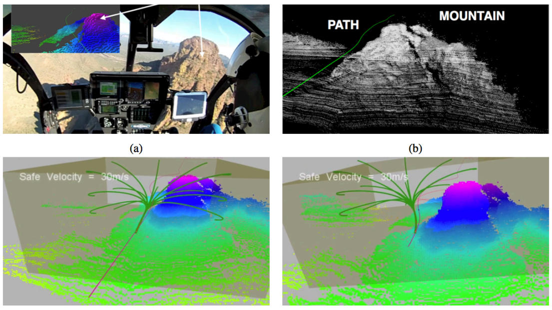

Outline

- Introduction
- Problem
- Abstraction and Approach
- Results
- **Summary**
- Exercise

Are we done?

- Fragile (e.g. ignoring position, execution and sensor uncertainties)
  ➔ *Robust*
- Static (e.g. ignoring wind, changing capability of robot)
  ➔ *Adaptive*
- Myopic (e.g. limited sensor range, overly simplified inference about the world)
  ➔ *Deliberate*

Robust: Safety in Partially-Known Environments Depends on the Sensor Capability

- Safety assessment restricted by limited sensor capabilities
- Obstacle detection range and size is proportional to range
- How can we still show safety if small obstacles can appear close to the robot?

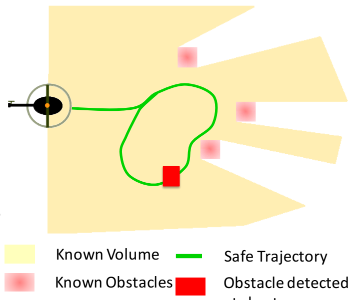

Althoff and Scherer, ICRA 2015

Adaptive: Adapting to Changing Abilities of the Robot

- Ignoring the changing capabilities of the system reduces robustness
- Need to adapt to changes in robot capability (wind, obscurants, localization) to enable long-term autonomy
- How can the behavior of the system adapt to unmodelled changes?

Compute Reachable Sets of the Emergency Trajectories to Guarantee Safety with Execution Uncertainties

- Online: Compute reachable set of nominal trajectory (<5s trajectory time)
- Offline: Compute reachable set of emergency trajectory (<70s)
- Concatenate the nominal and emergency trajectory to form a Robust Control Invariant Set.

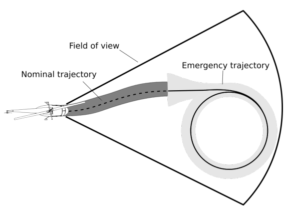

Althoff, Althoff, Scherer IROS 2015

Performance of planning algorithm depends on the environment

- Can we learn the best ensemble?
  - Learn the best planner
  - Learn the second planner with the highest marginal gains …
- Can we build a combined trajectory optimization/search-based planner that adapts?
- Can we extend the ensemble idea to other applications? (For example odometry)

Choudhury, Arora, Scherer ICRA 2015, Holtz and Scherer FSR 2015

Learnt planner ensemble

Choudhury, Arora, Scherer ICRA 2015

Deliberate: Incorporating Semantic Information in Decision Making

- Behavior of vehicle is limited by the information available to the planning algorithms
- Semantic information can improve the performance and autonomy of the system
- How do we incorporate semantic information effectively?

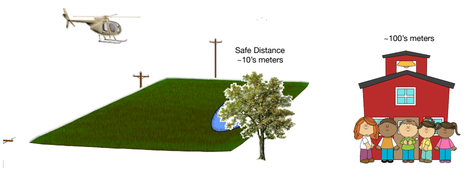

Dense Semantic Classification
Fully Connected Deep Networks

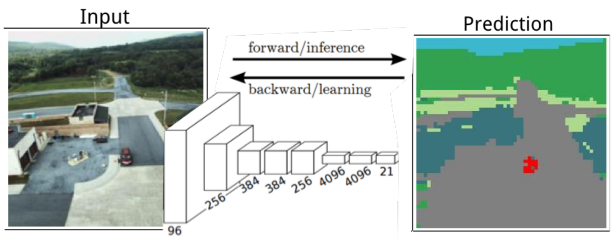

Long, Shelhamer and Darrell, CVPR 2015

Real-time Semantic Classification for Scouting using Deep Learning

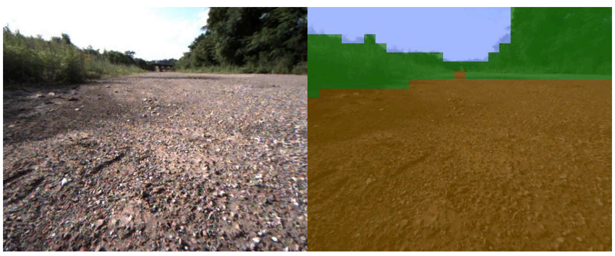

Semantics at Close Range -VoxNet

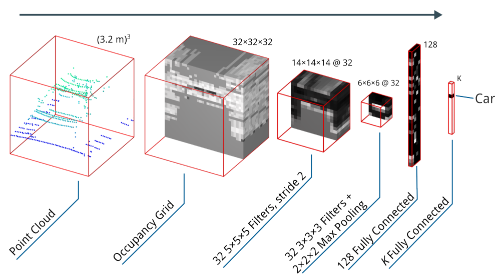

[1] Maturana and Scherer, ICRA 2015
[2] Maturana and Scherer, IROS 2015

Landing Zone Detection with 3D LIDAR

Volumetric Convolutional Neural Networks for Landing Zone Detection in vegetated terrain from LiDAR

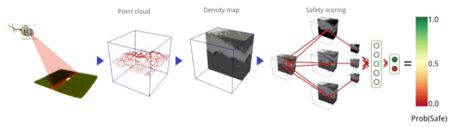

Daniel Maturana and Sebastian Scherer

Submission #2850

theairlab.org

Carnegie Mellon University

Summary

- Reviewed the planning problem for autonomous flying robots
- Considered several algorithms and the idea of planning ensembles
- Which approaches are successful is highly dependent on your environment and dynamical system

Toolbox Setup

1. Install MATLAB (no toolboxes necessary)
2. Download MATLAB toolbox. In a command line execute:

```
git clone
https://bitbucket.org/castacks/matlab_planning_toolbox.git
```

(Supported platforms: Mac, Linux, and
Windows, for Windows you also need Visual C++)

3. Go to
https://bitbucket.org/castacks/matlab_planning_toolbox
and follow the directions.

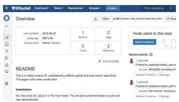

Outline

- Introduction
- Problem
- Abstraction and Approach
- Results
- Summary
- **Exercise**

Goals

1. Setup the toolbox (10 min)
2. Get familiar with the different planning algorithms from the lecture (20 min)
3. Explore the concept of environment dependence for planning algorithms (20 min)
4. Planning Challenge (40 min)

1. Toolbox Setup

1. Install MATLAB
2. Download MATLAB toolbox. In a command line execute:

```
git clone git@bitbucket.org:castacks/matlab_planning_toolbox.git
```

(Supported platforms: Mac, Linux, and
Windows, for Windows you also need Visual C++)

3. Go to
https://bitbucket.org/castacks/matlab_planning_toolbox
and follow the directions.

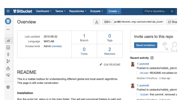

1. Matlab Toolbox Overview

- Run `init_setup.m` to setup paths and compile mex files
- Folders
  - `global_search`: Sampling and grid planners
  - `local_search`: Trajectory optimization
  - `cost_functions`: Tools to setup and evaluate cost functions
  - `environment_generation`: Tools to generate environments
  - `saved_environments`: Different maps

2. Get familiar with the different planning algorithms

Different examples are located here:
`planning_experiments/detailed_examples/`

1. `example_astar.m`
2. `example_chomp.m`
3. `example_rrtstar.m`

2. Questions

- How do the different algorithms behave?
- What happens if you vary the parameters?
- What happens if you inflate the heuristic? (Turn A* into Weighted-A*)
- How do you turn RRT* into RRT?

3. Run Algorithms on this Matrix

	CHOMP	A*	RRT*
Env 1			
Env 2			
Env 3			

Where do the algorithms work?

Fill out the matrix.

3. Assumptions so Far:

- No dynamics
- Start
- Goal
- **No changing environment**
- **No time budget/real-time**

4. Planning Challenge

Use this file:
`planning_experiments/planning_challenge/run_planner_challenge.m`

Prize: **Fame and a large pack of gummy bears!**

You can use at most 2 planning algorithms

- Develop your own planning approach on the training set.
- The test set will be released in the last ten minutes. Please write your score on the white board and we will announce the winner after lunch.

4. Test Dataset

Please download this file und place the environments in the saved environments folder:

http://bit.ly/1Lu8BlD

Please report the lowest number.
First initials and day.

References 1

[Nuske15] Stephen T. Nuske, Sanjiban Choudhury, Sezal Jain, Andrew D. Chambers, Luke Yoder, Sebastian Scherer, Lyle J. Chamberlain, Hugh Cover, and Sanjiv Singh, "Autonomous Exploration and Motion Planning for an Unmanned Aerial Vehicle Navigating Rivers," Journal of Field Robotics, June, 2015.

[Arora15a] Sankalp Arora, Sanjiban Choudhury, Daniel Althoff, and Sebastian Scherer, "Emergency Maneuver Library – Ensuring Safe Navigation in Partially Known Environments," 2015 IEEE International Conference on Robotics and Automation, May, 2015.

[Arora15b] Sankalp Arora and Sebastian Scherer, "PASP: Policy Based Approach for Sensor Planning," 2015 IEEE International Conference on Robotics and Automation, May, 2015.

[Choudhury15a] Sanjiban Choudhury and Sebastian Scherer, "The Dynamics Projection Filter (DPF) - Real-Time Nonlinear Trajectory Optimization Using Projection Operators," IEEE International Conference on Robotics and Automation, May, 2015.

[Choudhury15b] Sanjiban Choudhury, Sankalp Arora, and Sebastian Scherer, "The Planner Ensemble: Motion Planning by Executing Diverse Algorithms," IEEE Conference on Robotics and Automation, May, 2015.

[Maturana15] Daniel Maturana and Sebastian Scherer, "3D Convolutional Neural Networks for Landing Zone Detection from LiDAR," International Conference on Robotics and Automation, March, 2015.

[Althoff15] Daniel Althoff and Sebastian Scherer, "Connected Invariant Sets for High-Speed Motion Planning in Partially-Known Environments," 2015 IEEE International Conference on Robotics and Automation, March, 2015.

[Arora14] Sankalp Arora, Sanjiban Choudhury, Sebastian Scherer, and Daniel Althoff, "A Principled Approach to Enable Safe and High Performance Maneuvers for Autonomous Rotorcraft," AHS 70th Annual Forum, Montre´al, Que´bec, Canada, May 20–22, May, 2014.

[Choudhury14] Sanjiban Choudhury, Sankalp Arora, and Sebastian Scherer, "The Planner Ensemble and Trajectory Executive: A High Performance Motion Planning System with Guaranteed Safety," AHS 70th Annual Forum, Montre´al, Que´bec, Canada, May, 2014.

[Foessel02] A. Foessel, "Scene Modeling from Motion-Free Radar Sensing," The Robotics Institute, CMU, Pittsburgh, PA, 2002.

[Scherer09] S. Scherer, D. Ferguson, and S. Singh, "Efficient C-space and cost function updates in 3D for unmanned aerial vehicles," presented at the Robotics and Automation, 2009. ICRA '09. IEEE International Conference on, 2009, pp. 2049–2054.

[Gammell15] Gammell, J.D.; Srinivasa, S.S.; Barfoot, T.D., "Batch Informed Trees (BIT*): Sampling-based optimal planning via the heuristically guided search of implicit random geometric graphs," *Robotics and Automation (ICRA), 2015 IEEE International Conference on* , vol., no., pp.3067,3074, 26-30 May 2015

References 2

[Koenig02] S. Koenig and M. Likhachev, "D* Lite." In Proceedings of the AAAI Conference on Artificial Intelligence (AAAI), pages 476-483, 2002.

[Knepper06] R. Knepper and A. Kelly, "High Performance State Lattice Planning Using Heuristic Look-Up Tables." Proceedings of the 2006 IEEE/RSJ International Conference on Intelligent Robots and Systems, October, 2006, pp. 3375-3380.

[LaValle06] S. LaValle, "Planning Algorithms". Cambridge: Cambridge University Press. ISBN 0521862051.

[Hansen07] E.A. Hansen and R. Zhou, "Anytime Heuristic Search". Journal of Aritifical Intelligence Research 28 (2007) pages 267-297.

[Likhachev04] Maxim Likhachev, Geoff Gordon and Sebastian Thrun, "ARA*: Anytime A* with Provable Bounds on Sub-Optimality, " Advances in Neural Information Processing Systems 16 (NIPS), MIT Press, Cambridge, MA, 2004.

[Dubins57] L.E. Dubins. "On Curves of Minimum Length with a Constraint on Average Curvature and with Prescribed Initial and Terminal Positions and Tangents," American Journal of Mathematics, 79: (1957) pages 497-516, 1957.

[Pivtoraiko09] M. Pivtoraiko, R. A. Knepper, and A. Kelly, "Differentially constrained mobile robot motion planning in state lattices," *Journal of Field Robotics*, vol. 26, no. 3, pp. 308–333, Mar. 2009.

[Frazzoli02] E. Frazzoli, M. Dahleh, and E. Feron, "Real-time motion planning for agile autonomous vehicles," *AIAA Journal of Guidance Control and Dynamics*, vol. 25, no. 1, pp. 116–129, 2002.

[He13] Keliang He '13, Elizabeth Martin '13, and Matt Zucker. "Multigrid CHOMP with local smoothing" *Proc. IEEE-RAS Int'l Conf. on Humanoid Robotics*, 2013.

[Kolter09] Z. Kolter, and A. Ng "Task-Space Trajectories via Cubic Spline Optimization," ICRA 2009

[Fang15a] Zheng Fang, Shichao Yang , Sezal Jain, Geetesh Dubey, Silvio Mano Maeta, Stephan Roth, Sebastian Scherer, Yu Zhang, and Stephen T. Nuske, "Robust Autonomous Flight in Constrained and Visually Degraded Environments," Field and Service Robotics, June, 2015.

[Holtz15] Kristen Holtz, Daniel Maturana, and Sebastian Scherer, "Learning a Context-Dependent Switching Strategy for Robust Visual Odometry," Field and Service Robotics, June, 2015.

[Fang15b] Zheng Fang and Sebastian Scherer, "Real-time Onboard 6DoF Localization of an Indoor MAV in Degraded Visual Environments Using a RGB-D Camera," 2015 IEEE International Conference on Robotics and Automation, May, 2015.

Graph-Based SLAM

Cyrill Stachniss

universitätbonn

Graph-Based SLAM ??

Graph-Based SLAM ??

SLAM = simultaneous localization and mapping

Graph-Based SLAM ??

SLAM = simultaneous localization and mapping

graph = representation of a set of objects where pairs of objects are connected by links encoding relations between the objects

Is this relevant?

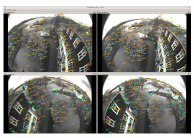


Yes, it is!


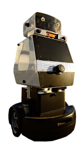


What is my goal for today?

Graph-Based SLAM

- Nodes represent poses or locations
- Constraints connect the poses of the robot while it is moving
- Constraints are inherently uncertain

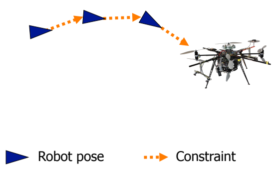

Graph-Based SLAM

- Observing previously seen areas generates constraints between non-successive poses

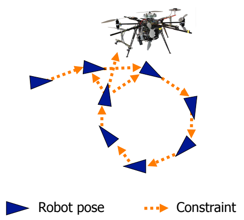

Idea of Graph-Based SLAM

- Use a **graph** to represent the problem
- Every **node** in the graph corresponds to a pose of the robot during mapping
- Every **edge** between two nodes corresponds to a spatial constraint between them
- **Graph-Based SLAM:** Build the graph and find a node configuration that minimize the error introduced by the constraints

Graph-SLAM and Least Squares

- The nodes represent the **state**
- Given a state, we can compute what we **expect** to perceive
- We have **real observations** relating the nodes with each other

Graph-SLAM and Least Squares

- The nodes represent the **state**
- Given a state, we can compute what we **expect** to perceive
- We have **real observations** relating the nodes with each other

Find a configuration of the nodes so that the real and predicted observations are as similar as possible

Graphical Explanation

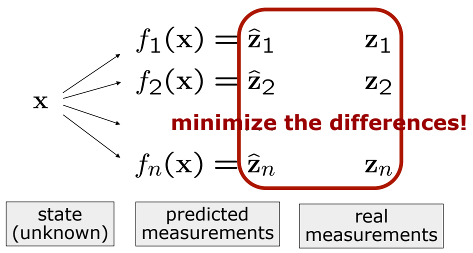

Error Function

- Error $\mathbf{e}_i$ is typically the **difference** between the **predicted and actual** measurement

$$\mathbf{e}_i(\mathbf{x}) = \mathbf{z}_i - f_i(\mathbf{x})$$

- We assume that the measurement error has **zero mean** and is **normally distributed**
- Gaussian error with information matrix $\mathbf{\Omega}_i$
- The squared error of a measurement depends only on the state and is a scalar

$$e_i(\mathbf{x}) = \mathbf{e}_i(\mathbf{x})^T \mathbf{\Omega}_i \mathbf{e}_i(\mathbf{x})$$

Goal: Find the Minimum

- Find the state $\mathbf{x}^*$ which minimizes the error given all measurements

$$\begin{aligned}
\mathbf{x}^* &= \operatorname*{argmin}_{\mathbf{x}} F(\mathbf{x}) \longleftarrow \boxed{\text{global error (scalar)}} \\
&= \operatorname*{argmin}_{\mathbf{x}} \sum_i e_i(\mathbf{x}) \longleftarrow \boxed{\text{squared error terms (scalar)}} \\
&= \operatorname*{argmin}_{\mathbf{x}} \sum_i \mathbf{e}_i^T(\mathbf{x}) \mathbf{\Omega}_i \underbrace{\mathbf{e}_i(\mathbf{x})}_{\boxed{\text{error terms (vector)}}}
\end{aligned}$$

Goal: Find the Minimum

- Find the state $\mathbf{x}^*$ which minimizes the error given all measurements

$$\mathbf{x}^* = \operatorname*{argmin}_{\mathbf{x}} \sum_i \mathbf{e}_i^T(\mathbf{x}) \mathbf{\Omega}_i \mathbf{e}_i(\mathbf{x})$$

- A general solution is to derive the global error function and find its nulls
- In general no closed form solution

Assumptions

- A good **initial guess** is available
- The error functions are "smooth" in the neighborhood of the (hopefully global) minima
- Then, we can solve the problem by **iterative linearizations**

Solve Via Iterative Linearizations

- Linearize the error terms around the current solution/initial guess
- Compute the first derivative of the squared error function
- Set it to zero and solve linear system
- Obtain the new state (that is hopefully closer to the minimum)
- Iterate

Linearizing the Error Function

- Approximate the error functions around an initial guess $\mathbf{x}$ via Taylor expansion

$$\mathbf{e}_i(\mathbf{x}+\Delta\mathbf{x}) \simeq \underbrace{\mathbf{e}_i(\mathbf{x})}_{\mathbf{e}_i} + \mathbf{J}_i(\mathbf{x})\Delta\mathbf{x}$$

- Reminder: Jacobian

$$\mathbf{J}_f(x) = \begin{pmatrix} \frac{\partial f_1(x)}{\partial x_1} & \frac{\partial f_1(x)}{\partial x_2} & \cdots & \frac{\partial f_1(x)}{\partial x_n} \\ \frac{\partial f_2(x)}{\partial x_1} & \frac{\partial f_2(x)}{\partial x_2} & \cdots & \frac{\partial f_2(x)}{\partial x_n} \\ \cdots & \cdots & \cdots & \cdots \\ \frac{\partial f_m(x)}{\partial x_1} & \frac{\partial f_m(x)}{\partial x_2} & \cdots & \frac{\partial f_m(x)}{\partial x_n} \end{pmatrix}$$

Squared Error

- With this linearization, we can fix $\mathbf{x}$ and carry out the minimization in the increments $\Delta\mathbf{x}$
- We replace the Taylor expansion in the squared error terms:

$$e_i(\mathbf{x}+\Delta\mathbf{x}) = \ldots$$

Squared Error

- With this linearization, we can fix $\mathbf{x}$ and carry out the minimization in the increments $\Delta\mathbf{x}$
- We replace the Taylor expansion in the squared error terms:

$$\begin{aligned} e_i(\mathbf{x}+\Delta\mathbf{x}) &= \mathbf{e}_i^T(\mathbf{x}+\Delta\mathbf{x})\Omega_i\mathbf{e}_i(\mathbf{x}+\Delta\mathbf{x}) \\ &\simeq (\mathbf{e}_i+\mathbf{J}_i\Delta\mathbf{x})^T\Omega_i(\mathbf{e}_i+\mathbf{J}_i\Delta\mathbf{x}) \end{aligned}$$

Squared Error

- With this linearization, we can fix $\mathbf{x}$ and carry out the minimization in the increments $\Delta\mathbf{x}$
- We replace the Taylor expansion in the squared error terms:

$$\begin{aligned} e_i(\mathbf{x}+\Delta\mathbf{x}) &= \mathbf{e}_i^T(\mathbf{x}+\Delta\mathbf{x})\Omega_i\mathbf{e}_i(\mathbf{x}+\Delta\mathbf{x}) \\ &\simeq (\mathbf{e}_i+\mathbf{J}_i\Delta\mathbf{x})^T\Omega_i(\mathbf{e}_i+\mathbf{J}_i\Delta\mathbf{x}) \\ &= \mathbf{e}_i^T\Omega_i\mathbf{e}_i + \\ &\quad \mathbf{e}_i^T\Omega_i\mathbf{J}_i\Delta\mathbf{x} + \Delta\mathbf{x}^T\mathbf{J}_i^T\Omega_i\mathbf{e}_i + \\ &\quad \Delta\mathbf{x}^T\mathbf{J}_i^T\Omega_i\mathbf{J}_i\Delta\mathbf{x} \end{aligned}$$

Squared Error (cont.)

- By grouping similar terms, we obtain:

$$\begin{aligned} & e_i(\mathbf{x}+\Delta\mathbf{x}) \\ &\simeq \underbrace{\mathbf{e}_i^T\Omega_i\mathbf{e}_i}_{c_i} + 2\underbrace{\mathbf{e}_i^T\Omega_i\mathbf{J}_i}_{\mathbf{b}_i^T}\Delta\mathbf{x} + \Delta\mathbf{x}^T\underbrace{\mathbf{J}_i^T\Omega_i\mathbf{J}_i}_{\mathbf{H}_i}\Delta\mathbf{x} \\ &= c_i + 2\mathbf{b}_i^T\Delta\mathbf{x} + \Delta\mathbf{x}^T\mathbf{H}_i\Delta\mathbf{x} \end{aligned}$$

Global Error

- The global error is the sum of the squared errors terms corresponding to the individual measurements

$$\begin{aligned} F(\mathbf{x}+\Delta\mathbf{x}) &\simeq \sum_i \left(c_i + \mathbf{b}_i^T\Delta\mathbf{x} + \Delta\mathbf{x}^T\mathbf{H}_i\Delta\mathbf{x}\right) \\ &= \sum_i c_i + 2\left(\sum_i \mathbf{b}_i^T\right)\Delta\mathbf{x} + \Delta\mathbf{x}^T\left(\sum_i \mathbf{H}_i\right)\Delta\mathbf{x} \end{aligned}$$

Global Error

- The global error is the sum of the squared errors terms corresponding to the individual measurements

$$F(\mathbf{x}+\Delta\mathbf{x}) \simeq \sum_i \left(c_i + \mathbf{b}_i^T \Delta\mathbf{x} + \Delta\mathbf{x}^T \mathbf{H}_i \Delta\mathbf{x}\right)$$
$$= \underbrace{\sum_i c_i}_{c} + 2\underbrace{(\sum_i \mathbf{b}_i^T)}_{\mathbf{b}^T} \Delta\mathbf{x} + \Delta\mathbf{x}^T \underbrace{(\sum_i \mathbf{H}_i)}_{\mathbf{H}} \Delta\mathbf{x}$$

Global Error

- The global error is the sum of the squared errors terms corresponding to the individual measurements

$$F(\mathbf{x}+\Delta\mathbf{x}) \simeq \sum_i \left(c_i + \mathbf{b}_i^T \Delta\mathbf{x} + \Delta\mathbf{x}^T \mathbf{H}_i \Delta\mathbf{x}\right)$$
$$= \underbrace{\sum_i c_i}_{c} + 2\underbrace{(\sum_i \mathbf{b}_i^T)}_{\mathbf{b}^T} \Delta\mathbf{x} + \Delta\mathbf{x}^T \underbrace{(\sum_i \mathbf{H}_i)}_{\mathbf{H}} \Delta\mathbf{x}$$
$$\boxed{= c + 2\mathbf{b}^T \Delta\mathbf{x} + \Delta\mathbf{x}^T \mathbf{H} \Delta\mathbf{x}}$$

$$\mathbf{b}^T = \sum_i \mathbf{e}_i^T \Omega_i \mathbf{J}_i \qquad \mathbf{H} = \sum_i \mathbf{J}_i^T \Omega \mathbf{J}_i$$

Quadratic Form

- We can write the global error terms as a quadratic form in $\Delta\mathbf{x}$

$$\boxed{F(\mathbf{x}+\Delta\mathbf{x}) \simeq c + 2\mathbf{b}^T \Delta\mathbf{x} + \Delta\mathbf{x}^T \mathbf{H} \Delta\mathbf{x}}$$

- Our goal is to **minimize** this function
- We need to compute the derivative of $F(\mathbf{x}+\Delta\mathbf{x})$ w.r.t. $\Delta\mathbf{x}$

Deriving a Quadratic Form

- Given a quadratic form

$$f(\Delta\mathbf{x}) = \Delta\mathbf{x}^T \mathbf{H} \Delta\mathbf{x} + \mathbf{b}^T \mathbf{x}$$

- its first derivative is

$$\frac{\partial f}{\partial \Delta\mathbf{x}} = (\mathbf{H} + \mathbf{H}^T)\Delta\mathbf{x} + \mathbf{b}$$

See: The Matrix Cookbook, Section 2.2.4

Quadratic Form

- We can write the linearized global error terms as a quadratic form in $\Delta\mathbf{x}$

$$F(\mathbf{x}+\Delta\mathbf{x}) \simeq c + 2\mathbf{b}^T \Delta\mathbf{x} + \Delta\mathbf{x}^T \mathbf{H} \Delta\mathbf{x}$$

- The derivative of $F(\mathbf{x}+\Delta\mathbf{x})$ w.r.t. $\Delta\mathbf{x}$ is then:

$$\frac{\partial F(\mathbf{x}+\Delta\mathbf{x})}{\partial \Delta\mathbf{x}} \simeq 2\mathbf{b} + 2\mathbf{H}\Delta\mathbf{x}$$

Minimizing the Quadratic Form

- Derivative $\frac{\partial F(\mathbf{x}+\Delta\mathbf{x})}{\partial \Delta\mathbf{x}} \simeq 2\mathbf{b} + 2\mathbf{H}\Delta\mathbf{x}$
- Setting it to zero leads to

$$0 = 2\mathbf{b} + 2\mathbf{H}\Delta\mathbf{x}$$

- Which leads to the linear system

$$\mathbf{H}\Delta\mathbf{x} = -\mathbf{b}$$

- The solution for the increment $\Delta\mathbf{x}^*$ is

$$\Delta\mathbf{x}^* = -\mathbf{H}^{-1}\mathbf{b}$$

Procedure on a Single Slide

Iterate the following steps:

- Linearize around $\mathbf{x}$ and compute for each measurement
  $$\mathbf{e}_i(\mathbf{x} + \Delta\mathbf{x}) \simeq \mathbf{e}_i(\mathbf{x}) + \mathbf{J}_i \Delta\mathbf{x}$$
- Compute the terms for the linear system $\mathbf{b}^T = \sum_i \mathbf{e}_i^T \boldsymbol{\Omega}_i \mathbf{J}_i \qquad \mathbf{H} = \sum_i \mathbf{J}_i^T \boldsymbol{\Omega}_i \mathbf{J}_i$
- Solve the linear system
  $$\Delta\mathbf{x}^* \;=\; -\mathbf{H}^{-1}\mathbf{b}$$
- Updating state $\mathbf{x} \leftarrow \mathbf{x} + \Delta\mathbf{x}^*$

Let’s use that for SLAM

Pose-Graph-Based SLAM

- Nodes represent poses or locations
- Constraints connect the poses of the robot while it is moving
- Constraints are inherently uncertain

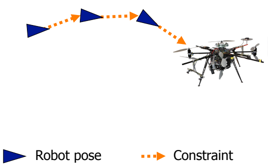

Pose-Graph-Based SLAM

- Observing previously seen areas generates constraints between non-successive poses

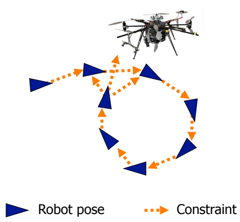

The Pose-Graph

- It consists of n nodes $\mathbf{x} = \mathbf{x}_{1:n}$
- Each $\mathbf{x}_i$ is a 2D or 3D **pose** (position and orientation of the robot at time t_i)
- A constraint/edge exists between the nodes $\mathbf{x}_i$ and $\mathbf{x}_j$ if…

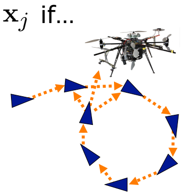

Create an Edge If… (1)

- …the robot moves from $\mathbf{x}_i$ to $\mathbf{x}_{i+1}$
- Edge corresponds to odometry

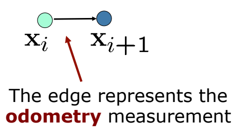

Create an Edge If… (2)

- …the robot observes the same part of the environment from $\mathbf{x}_i$ and from $\mathbf{x}_j$

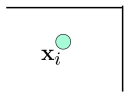

Measurement from $\mathbf{x}_i$

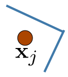

Measurement from $\mathbf{x}_j$

Create an Edge If… (2)

- …the robot observes the same part of the environment from $\mathbf{x}_i$ and from $\mathbf{x}_j$
- Construct a **virtual measurement** about the position of $\mathbf{x}_j$ seen from $\mathbf{x}_i$

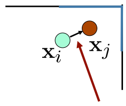

Edge represents the position of $\mathbf{x}_j$ seen from $\mathbf{x}_i$ based on the **observation**

Transformations

- **How to express $\mathbf{x}_i$ relative to $\mathbf{x}_j$?**
- Express this through transformations
- Let X_i be transformation of the origin into $\mathbf{x}_i$
- Let X_i^{-1} be the inverse transformation
- We can express relative transformation $\mathrm{X}_i^{-1}\mathrm{X}_j$

Transformations

- **How to express $\mathbf{x}_i$ relative to $\mathbf{x}_j$?**
- Express this through transformations
- Let X_i be transformation of the origin into $\mathbf{x}_i$
- Let X_i^{-1} be the inverse transformation
- We can express relative transformation $\mathrm{X}_i^{-1}\mathrm{X}_j$
- Transformations can be expressed using **homogenous coordinates**

Homogenous Coordinates

- N-dim space expressed in N+1 dim
- 4 dim. for modeling the 3D space
- To HC: $(x, y, z)^T \rightarrow (x, y, z, 1)^T = (a, b, c, d)^T$
- Backwards: $(a, b, c, d)^T \rightarrow \left(\frac{a}{d}, \frac{b}{d}, \frac{c}{d}\right)^T = (x, y, z)^T$

$$\mathrm{T} = \begin{pmatrix} 1 & 0 & 0 & t_x \\ 0 & 1 & 0 & t_y \\ 0 & 0 & 1 & t_z \\ 0 & 0 & 0 & 1 \end{pmatrix} \qquad \mathrm{R} = \begin{pmatrix} \mathrm{R}^{3D} & 0 \\ 0 & 1 \end{pmatrix} \qquad \mathrm{X} = \begin{pmatrix} \mathrm{R}^{3D} & \mathrm{t} \\ 0 & 1 \end{pmatrix}$$

translation rotation rigid-body

Transformations

- Transformations can be expressed using **homogenous coordinates**
- Odometry-Based edge

$$(\mathrm{X}_i^{-1}\mathrm{X}_{i+1})$$

- Observation-Based edge

$$(\mathrm{X}_i^{-1}\mathrm{X}_j)$$

describes "how node i sees node j"

The Edge Information Matrices

- Observations are affected by noise
- Information matrix $\mathbf{\Omega}_{ij}$ for each edge to encode its uncertainty
- The "bigger" $\mathbf{\Omega}_{ij}$, the more the edge "matters" in the optimization

Question

- What should these matrices look like when moving in a long, featureless corridor?

Pose-Graph

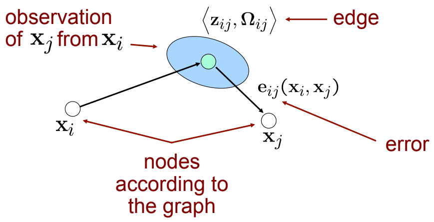

Pose-Graph

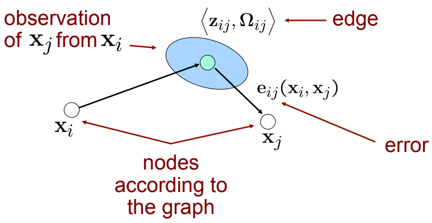

Goal: $\mathbf{x}^* = \underset{\mathbf{x}}{\operatorname{argmin}} \sum_{ij} \mathbf{e}_{ij}^T \mathbf{\Omega}_{ij} \mathbf{e}_{ij}$

The Error Function

- Error function for a single constraint

$$\mathbf{e}_{ij}(\mathbf{x}_i, \mathbf{x}_j) = \text{t2v}(\underbrace{\mathbf{Z}_{ij}^{-1}}_{\text{measurement}}(\underbrace{\mathbf{X}_i^{-1}\mathbf{X}_j}_{\mathbf{x}_j \text{ referenced w.r.t. } \mathbf{x}_i}))$$

- Error as a function of the whole state vector

$$\mathbf{e}_{ij}(\mathbf{x}) = \text{t2v}(\mathbf{Z}_{ij}^{-1}(\mathbf{X}_i^{-1}\mathbf{X}_j))$$

- Error takes a value of zero if

$$\mathbf{Z}_{ij} = (\mathbf{X}_i^{-1}\mathbf{X}_j)$$

Error Minimization Procedure

- Define the error function
- Linearize the error function
- Compute its derivative
- Set the derivative to zero
- Solve the linear system
- Iterate this procedure until convergence

Linearizing the Error Function

- We can approximate the error functions around an initial guess $\mathbf{x}$ via Taylor expansion

$$\mathbf{e}_{ij}(\mathbf{x} + \mathbf{\Delta x}) \simeq \mathbf{e}_{ij}(\mathbf{x}) + \mathbf{J}_{ij}\mathbf{\Delta x}$$

$$\text{with} \quad \mathbf{J}_{ij} = \frac{\partial \mathbf{e}_{ij}(\mathbf{x})}{\partial \mathbf{x}}$$

Derivative of the Error Function

- Does one error term $\mathbf{e}_{ij}(\mathbf{x})$ depend on all state variables?

Derivative of the Error Function

- Does one error term $\mathbf{e}_{ij}(\mathbf{x})$ depend on all state variables?
  - ➡ No, only on $\mathbf{x}_i$ and $\mathbf{x}_j$

Derivative of the Error Function

- Does one error term $\mathbf{e}_{ij}(\mathbf{x})$ depend on all state variables?
  - ➡ No, only on $\mathbf{x}_i$ and $\mathbf{x}_j$
- Is there any consequence on the **structure** of the Jacobian?

Derivative of the Error Function

- Does one error term $\mathbf{e}_{ij}(\mathbf{x})$ depend on all state variables?
  - ➡ No, only on $\mathbf{x}_i$ and $\mathbf{x}_j$
- Is there any consequence on the **structure** of the Jacobian?
  - ➡ Yes, it will be non-zero only in the rows corresponding to $\mathbf{x}_i$ and $\mathbf{x}_j$

$$
\begin{aligned}
\frac{\partial \mathbf{e}_{ij}(\mathbf{x})}{\partial \mathbf{x}} &= \left(\mathbf{0} \cdots \frac{\partial \mathbf{e}_{ij}(\mathbf{x}_i)}{\partial \mathbf{x}_i} \cdots \frac{\partial \mathbf{e}_{ij}(\mathbf{x}_j)}{\partial \mathbf{x}_j} \cdots \mathbf{0} \right) \\
\mathbf{J}_{ij} &= \left(\mathbf{0} \cdots \mathbf{A}_{ij} \cdots \mathbf{B}_{ij} \cdots \mathbf{0} \right)
\end{aligned}
$$

Jacobians and Sparsity

- Error $\mathbf{e}_{ij}(\mathbf{x})$ depends only on the two parameter blocks $\mathbf{x}_i$ and $\mathbf{x}_j$

$$\mathbf{e}_{ij}(\mathbf{x}) = \mathbf{e}_{ij}(\mathbf{x}_i, \mathbf{x}_j)$$

- The Jacobian will be zero everywhere except in the columns of $\mathbf{x}_i$ and $\mathbf{x}_j$

$$\mathbf{J}_{ij} = \left(\mathbf{0} \cdots \mathbf{0} \quad \underbrace{\frac{\partial \mathbf{e}(\mathbf{x}_i)}{\partial \mathbf{x}_i}}_{\mathbf{A}_{ij}} \quad \mathbf{0} \cdots \mathbf{0} \quad \underbrace{\frac{\partial \mathbf{e}(\mathbf{x}_j)}{\partial \mathbf{x}_j}}_{\mathbf{B}_{ij}} \quad \mathbf{0} \cdots \mathbf{0} \right)$$

Consequences of the Sparsity

- We need to compute the coefficient vector $\mathbf{b}$ and matrix $\mathbf{H}$:

$$
\begin{aligned}
\mathbf{b}^T &= \sum_{ij} \mathbf{b}_{ij}^T = \sum_{ij} \mathbf{e}_{ij}^T \boldsymbol{\Omega}_{ij} \mathbf{J}_{ij} \\
\mathbf{H} &= \sum_{ij} \mathbf{H}_{ij} = \sum_{ij} \mathbf{J}_{ij}^T \boldsymbol{\Omega}_{ij} \mathbf{J}_{ij}
\end{aligned}
$$

- The sparse structure of $\mathbf{J}_{ij}$ will result in a sparse structure of $\mathbf{H}$
- This structure reflects the adjacency matrix of the graph

Illustration of the Structure

$\mathbf{b}_{ij} = \mathbf{J}_{ij}^T \boldsymbol{\Omega}_{ij} \mathbf{e}_{ij}$

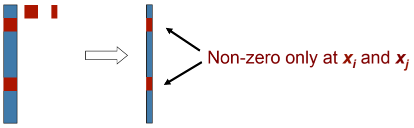

Illustration of the Structure

$\mathbf{b}_{ij} = \mathbf{J}_{ij}^T \boldsymbol{\Omega}_{ij} \mathbf{e}_{ij}$

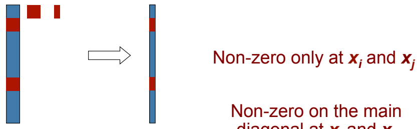

$\mathbf{H}_{ij} = \mathbf{J}_{ij}^T \boldsymbol{\Omega}_{ij} \mathbf{J}_{ij}$

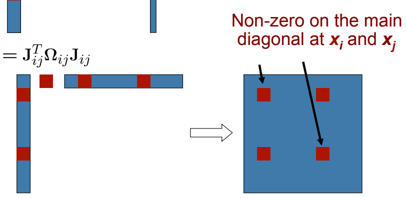

Illustration of the Structure

$\mathbf{b}_{ij} = \mathbf{J}_{ij}^T \boldsymbol{\Omega}_{ij} \mathbf{e}_{ij}$

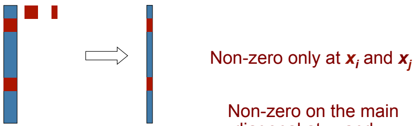

$\mathbf{H}_{ij} = \mathbf{J}_{ij}^T \boldsymbol{\Omega}_{ij} \mathbf{J}_{ij}$

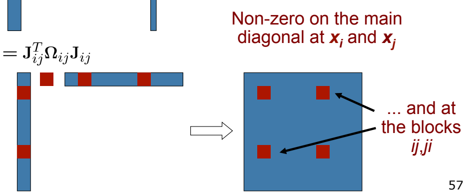

Illustration of the Structure

$\mathbf{b} = \sum_{ij} \mathbf{b}_{ij}$

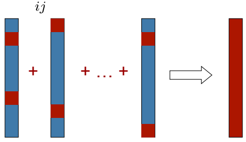

$\mathbf{H} = \sum_{ij} \mathbf{H}_{ij}$

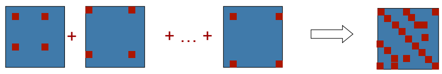

Sparsity Effect on b

- An edge contributes to the linear system via $\mathbf{b}_{ij}$ and $\mathbf{H}_{ij}$
- The coefficient vector is:

$$\begin{aligned}
\mathbf{b}_{ij}^T &= \mathbf{e}_{ij}^T \boldsymbol{\Omega}_{ij} \mathbf{J}_{ij} \\
&= \mathbf{e}_{ij}^T \boldsymbol{\Omega}_{ij} \begin{pmatrix} 0 \cdots \mathbf{A}_{ij} \cdots \mathbf{B}_{ij} \cdots 0 \end{pmatrix} \\
&= \begin{pmatrix} 0 \cdots \mathbf{e}_{ij}^T \boldsymbol{\Omega}_{ij} \mathbf{A}_{ij} \cdots \mathbf{e}_{ij}^T \boldsymbol{\Omega}_{ij} \mathbf{B}_{ij} \cdots 0 \end{pmatrix}
\end{aligned}$$

- It is non-zero only at the indices corresponding to $\mathbf{x}_i$ and $\mathbf{x}_j$

Sparsity Effect on H

- The coefficient matrix of an edge is:

$$\begin{aligned}
\mathbf{H}_{ij} &= \mathbf{J}_{ij}^T \boldsymbol{\Omega}_{ij} \mathbf{J}_{ij} \\
&= \begin{pmatrix} \vdots \\ \mathbf{A}_{ij}^T \\ \vdots \\ \mathbf{B}_{ij}^T \\ \vdots \end{pmatrix} \boldsymbol{\Omega}_{ij} \begin{pmatrix} \cdots \mathbf{A}_{ij} \cdots \mathbf{B}_{ij} \cdots \end{pmatrix} \\
&= \begin{pmatrix} \mathbf{A}_{ij}^T \boldsymbol{\Omega}_{ij} \mathbf{A}_{ij} & \mathbf{A}_{ij}^T \boldsymbol{\Omega}_{ij} \mathbf{B}_{ij} \\ \mathbf{B}_{ij}^T \boldsymbol{\Omega}_{ij} \mathbf{A}_{ij} & \mathbf{B}_{ij}^T \boldsymbol{\Omega}_{ij} \mathbf{B}_{ij} \end{pmatrix}
\end{aligned}$$

- Non-zero only in the blocks relating i,j

Sparsity Summary

- An edge ij contributes only to the
  - i[th] and the j[th] block of $\mathbf{b}_{ij}$
  - to the blocks ii, jj, ij and ji of $\mathbf{H}_{ij}$
- Resulting system is sparse
- System can be computed by summing up the contribution of each edge
- Efficient solvers can be used
  - Sparse Cholesky decomposition
  - Conjugate gradients
  - … many others

All We Need…

- Vector of the states increments:

$$\Delta\mathbf{x}^T = \begin{pmatrix} \Delta\mathbf{x}_1^T & \Delta\mathbf{x}_2^T & \cdots & \Delta\mathbf{x}_n^T \end{pmatrix}$$

- Coefficient vector:

$$\mathbf{b}^T = \begin{pmatrix} \bar{\mathbf{b}}_1^T & \bar{\mathbf{b}}_2^T & \cdots & \bar{\mathbf{b}}_n^T \end{pmatrix}$$

- System matrix:

$$\mathbf{H} = \begin{pmatrix} \bar{\mathbf{H}}^{11} & \bar{\mathbf{H}}^{12} & \cdots & \bar{\mathbf{H}}^{1n} \\ \bar{\mathbf{H}}^{21} & \bar{\mathbf{H}}^{22} & \cdots & \bar{\mathbf{H}}^{2n} \\ \vdots & & \ddots & \vdots \\ \bar{\mathbf{H}}^{n1} & \bar{\mathbf{H}}^{n2} & \cdots & \bar{\mathbf{H}}^{nn} \end{pmatrix}$$

… for the Linear System

For each constraint:

- Compute error $\mathbf{e}_{ij} = \text{t2v}(\mathbf{Z}_{ij}^{-1}(\mathbf{X}_i^{-1}\mathbf{X}_j))$
- Compute the blocks of the Jacobian:

$$\mathbf{A}_{ij} = \frac{\partial \mathbf{e}(\mathbf{x}_i, \mathbf{x}_j)}{\partial \mathbf{x}_i} \qquad \mathbf{B}_{ij} = \frac{\partial \mathbf{e}(\mathbf{x}_i, \mathbf{x}_j)}{\partial \mathbf{x}_j}$$

- Update the coefficient vector:

$$\bar{\mathbf{b}}_i^T += \mathbf{e}_{ij}^T \Omega_{ij} \mathbf{A}_{ij} \qquad \bar{\mathbf{b}}_j^T += \mathbf{e}_{ij}^T \Omega_{ij} \mathbf{B}_{ij}$$

- Update the system matrix:

$$\bar{\mathbf{H}}^{ii} += \mathbf{A}_{ij}^T \Omega_{ij} \mathbf{A}_{ij} \qquad \bar{\mathbf{H}}^{ij} += \mathbf{A}_{ij}^T \Omega_{ij} \mathbf{B}_{ij}$$
$$\bar{\mathbf{H}}^{ji} += \mathbf{B}_{ij}^T \Omega_{ij} \mathbf{A}_{ij} \qquad \bar{\mathbf{H}}^{jj} += \mathbf{B}_{ij}^T \Omega_{ij} \mathbf{B}_{ij}$$

Algorithm

optimize($\mathbf{x}$):

while (!*converged*)
  $(\mathbf{H}, \mathbf{b}) = \text{buildLinearSystem}(\mathbf{x})$
  $\mathbf{\Delta x} = \text{solveSparse}(\mathbf{H}\mathbf{\Delta x} = -\mathbf{b})$
  $\mathbf{x} = \mathbf{x} + \mathbf{\Delta x}$
end
return $\mathbf{x}$

Real World Examples

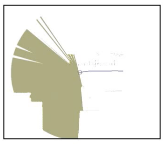

The Graph with Landmarks

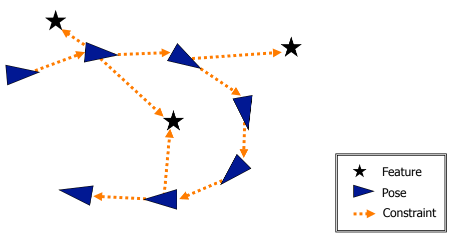

The Graph with Landmarks

- **Nodes** can represent:
  - Robot poses
  - Landmark locations
- **Edges** can represent:
  - Landmark observations
  - Odometry measurements
- The minimization optimizes the **landmark locations and robot poses**

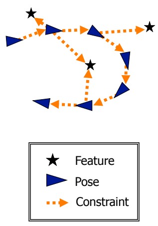

Landmarks Observation

- Expected observation (x-y sensor)

$$\hat{\mathbf{z}}_{il}(\underset{\substack{\uparrow\\ \text{robot}}}{\mathbf{x}_i}, \underset{\substack{\uparrow\\ \text{landmark}}}{\mathbf{x}_l}) = \mathbf{X}_i^{-1} \begin{pmatrix} \mathbf{x}_l \\ 1 \end{pmatrix}$$

Landmarks Observation

- Expected observation (x-y sensor)

$$\hat{\mathbf{z}}_{il}(\underset{\substack{\uparrow\\ \text{robot}}}{\mathbf{x}_i}, \underset{\substack{\uparrow\\ \text{landmark}}}{\mathbf{x}_l}) = \mathbf{X}_i^{-1} \begin{pmatrix} \mathbf{x}_l \\ 1 \end{pmatrix}$$

- Error function (in Euclidian space)

$$\mathbf{e}_{il}(\mathbf{x}_i, \mathbf{x}_l) = \hat{\mathbf{z}}_{il} - \mathbf{z}_{il}$$

Bearing Only Observations

- A landmark is still a 2D point
- The robot observe only the bearing towards the landmark
- 1D Observation function

$$\hat{\mathbf{z}}_{il}(\underset{\substack{\uparrow\\ \text{robot}}}{\mathbf{x}_i}, \underset{\substack{\uparrow\\ \text{landmark}}}{\mathbf{x}_l}) = \underset{\substack{\uparrow\\ \text{robot-landmark}\\ \text{angle}}}{\text{atan}\frac{(\mathbf{x}_l - \mathbf{t}_i).y}{(\mathbf{x}_l - \mathbf{t}_i).x}} - \underset{\substack{\uparrow\\ \text{robot}\\ \text{orientation}}}{\theta_i}$$

Bearing Only Observations

- Observation function

$$\hat{\mathbf{z}}_{il}(\underset{\substack{\uparrow\\ \text{robot}}}{\mathbf{x}_i}, \underset{\substack{\uparrow\\ \text{landmark}}}{\mathbf{x}_l}) = \underset{\substack{\uparrow\\ \text{robot-landmark}\\ \text{angle}}}{\text{atan}\frac{(\mathbf{x}_l - \mathbf{t}_i).y}{(\mathbf{x}_l - \mathbf{t}_i).x}} - \underset{\substack{\uparrow\\ \text{robot}\\ \text{orientation}}}{\theta_i}$$

- Error function

$$\mathbf{e}_{il}(\mathbf{x}_i, \mathbf{x}_l) = \text{atan}\frac{(\mathbf{x}_l - \mathbf{t}_i).y}{(\mathbf{x}_l - \mathbf{t}_i).x} - \theta_i - \mathbf{z}_{il}$$

The Rank of the Matrix H

- What is the rank of $\mathbf{H}_{ij}$ for a 2D landmark-pose constraint?

The Rank of the Matrix H

- What is the rank of $\mathbf{H}_{ij}$ for a 2D landmark-pose constraint?
  - The blocks of $\mathbf{J}_{ij}$ are a 2x3 matrices
  - $\mathbf{H}_{ij}$ cannot have more than rank 2

  $\mathrm{rank}(A^T A) = \mathrm{rank}(A^T) = \mathrm{rank}(A)$

The Rank of the Matrix H

- What is the rank of $\mathbf{H}_{ij}$ for a 2D landmark-pose constraint?
  - The blocks of $\mathbf{J}_{ij}$ are a 2x3 matrices
  - $\mathbf{H}_{ij}$ cannot have more than rank 2

  $\mathrm{rank}(A^T A) = \mathrm{rank}(A^T) = \mathrm{rank}(A)$

- What is the rank of $\mathbf{H}_{ij}$ for a bearing-only constraint?

The Rank of the Matrix H

- What is the rank of $\mathbf{H}_{ij}$ for a 2D landmark-pose constraint?
  - The blocks of $\mathbf{J}_{ij}$ are a 2x3 matrices
  - $\mathbf{H}_{ij}$ cannot more than rank 2

  $\mathrm{rank}(A^T A) = \mathrm{rank}(A^T) = \mathrm{rank}(A)$

- What is the rank of $\mathbf{H}_{ij}$ for a bearing-only constraint?
  - The blocks of $\mathbf{J}_{ij}$ are a 1x3 matrices
  - $\mathbf{H}_{ij}$ has rank 1

Where is the Robot?

- Robot observes one landmark (x,y)
- Where can the robot be relative to the landmark?

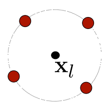

The robot can be somewhere on a circle around the landmark

It is a 1D solution space (constrained by the distance and the robot's orientation)

Where is the Robot?

- Robot observes one landmark (bearing-only)
- Where can the robot be relative to the landmark?

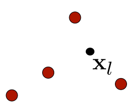

The robot can be anywhere in the x-y plane

It is a 2D solution space (constrained by the robot's orientation)

Rank

- In landmark-based SLAM, the system can be under-determined
- The rank of $\mathbf{H}$ is **less or equal** to the sum of the ranks of the constraints
- To determine a **unique solution**, the system must have **full rank**

Questions

- The rank of $\mathbf{H}$ is **less or equal** to the sum of the ranks of the constraints
- To determine a **unique solution**, the system must have **full rank**
- **Questions:**
  - How many 2D landmark observations are at least needed to obtain the robot pose?
  - How many bearing-only observations are at least needed to obtain the robot pose?

Under-Determined Systems

- No guarantee for a full rank system
  - Landmarks may be observed only once
  - Robot might have no odometry
- We can still deal with these situations by adding a "damping" factor to $\mathbf{H}$
- Instead of solving $\mathbf{H}\Delta\mathbf{x} \;=\; -\mathbf{b}$, we solve

$$(\mathbf{H} + \lambda\mathbf{I})\Delta\mathbf{x} \;=\; -\mathbf{b}$$

What is the effect of that?

Levenberg Marquardt Idea

- Damping factor for $\mathbf{H}$
- $(\mathbf{H} + \lambda\mathbf{I})\Delta\mathbf{x} \;=\; -\mathbf{b}$
- The damping factor $\lambda\mathbf{I}$ makes the system positive definite
- Weighted sum of Gauss Newton and Steepest Descent

Bundle Adjustment

- 3D reconstruction based on images taken at different viewpoints
- Minimizes the reprojection error
- Often uses Levenberg Marquardt
- Developed in photogrammetry during the 1950ies

UAV Example

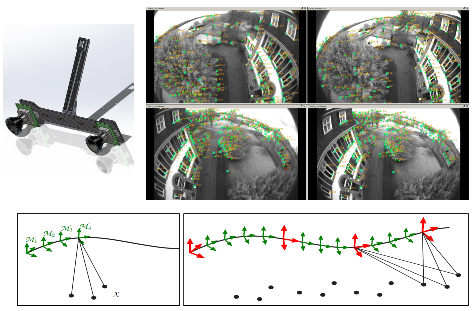

UAV Example

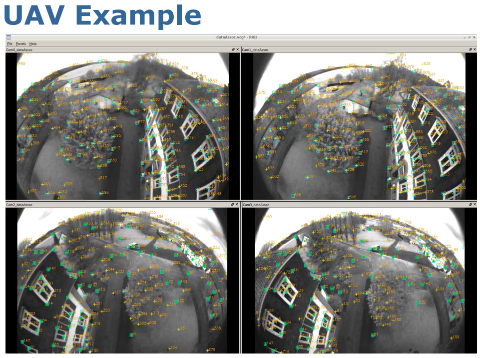

Summary

- The back-end part of the SLAM problem can be solved with GN or LM
- The $\mathbf{H}$ matrix is typically sparse
- This sparsity allows for efficiently solving the linear system
- There are several extensions (online, robust methods wrt outliers or initialization, hierarchical approaches, exploiting sparsity, multiple sensors)

Further Reading

Least Squares SLAM

- Grisetti, Kümmerle, Stachniss, Burgard: "A Tutorial on Graph-based SLAM", 2010
- Triggs et al. "Bundle Adjustment — A Modern Synthesis"

Thank you for your attention!

Slide Information

- These slides have been created by Cyrill Stachniss and Giorgio Grisetti evolving from different courses and tutorials we taught over the years between 2010 and 2015.
- I tried to acknowledge all people that contributed image or video material. In case I missed something, please let me know. If you adapt this course material, please make sure you keep the acknowledgements.
- Feel free to use and change the slides. If you use them, I would appreciate an acknowledgement as well. To satisfy my own curiosity, I appreciate a short email notice in case you use the material in your course.
- My video recordings of my lectures on robot mapping are available through YouTube: http://www.youtube.com/playlist?list=PLgnQpQtFTOGQrZ4O5QzbIHgl3b1JHimN_&feature=g-list

Cyrill Stachniss, 2015
cyrill.stachniss@igg.uni-bonn.de

Controls for Multi-Rotor Vehicles

… from Model-Based to Learning-Enabled Approaches

Prof. Angela Schoellig, University of Toronto

TRADR Summer School on Autonomous Micro Aerial Vehicles
August 25, 2015

Institute for Aerospace Studies
UNIVERSITY OF TORONTO

DYNAMIC
SYSTEMS LAB

What is Controls?

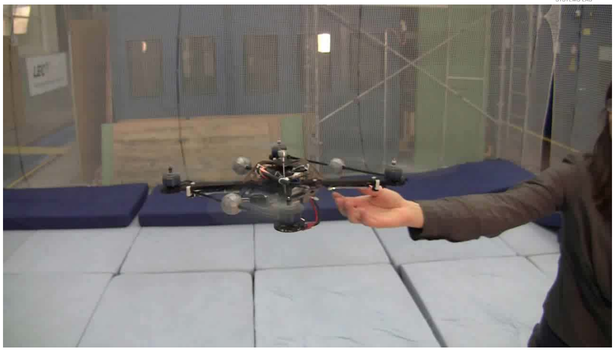

What is Controls?

It's MAGIC!

What is Controls?

Controls enables a machine to achieve a task without human interaction. Despite disturbances.

⇨ Self-regulating system.

How is this relevant for flying robots?

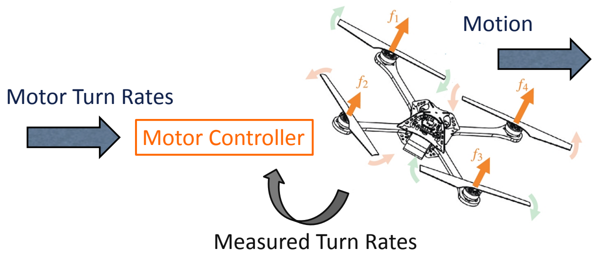

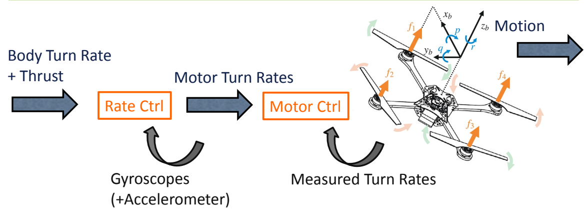

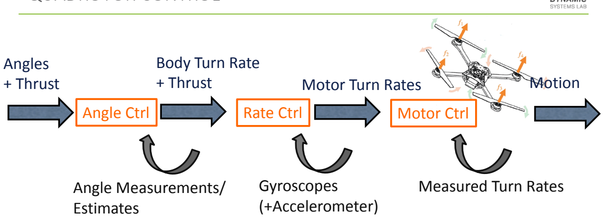

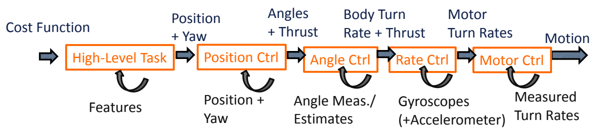

Allows us to focus on the high-level task.

How does it fit together?

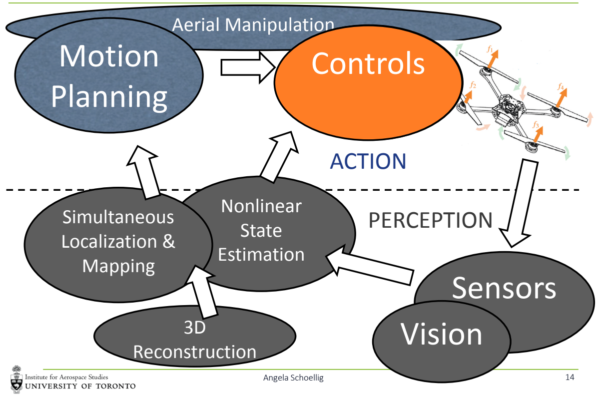

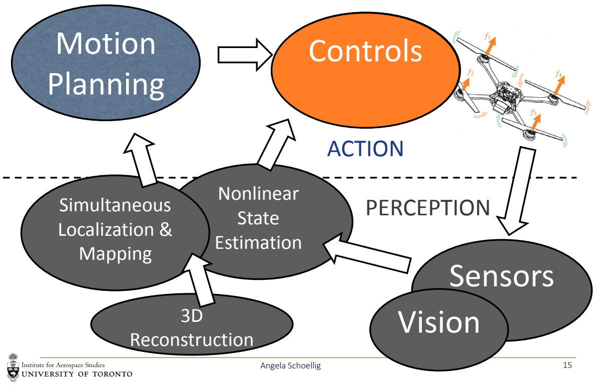

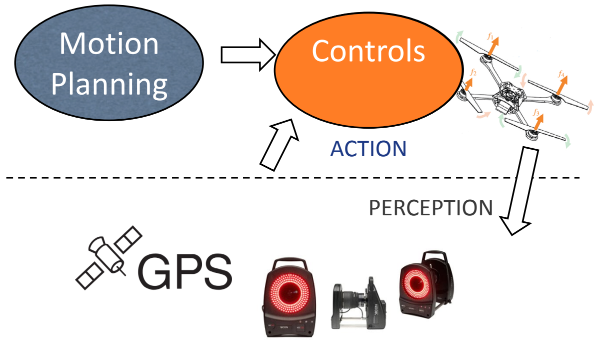

My goal for today!

Prepare you to design your own advanced controllers.

OUTLINE

BASICS

GOAL OF CONTROLS:
Want the error to go exponentially to zero as function of time.

$$e := x_d - x$$

Example:

$$\dot{e} + ke = 0 \quad \Rightarrow \quad e(t) = e_o \exp(-kt), \;\; k > 0.$$

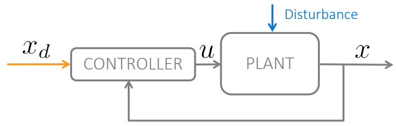

BASICS

GOAL OF CONTROLS:
Want the error to go exponentially to zero as function of time.

$$e := x_d - x$$

Example:

$$\dot{e} + ke = 0 \quad \Rightarrow \quad e(t) = e_o \exp(-kt), \;\; k > 0.$$

Can be higher-order,
but coefficients must be non-negative.

BASICS

Example:

$$\ddot{x} = u, \qquad u := k_p(x_d - x) + k_v(\dot{x}_d - \dot{x}) + \ddot{x}_d$$

Feed-forward term.

$$\Rightarrow \quad \ddot{e} + k_v\dot{e} + k_p e = 0$$

$$\Rightarrow \quad \boxed{\ddot{e} + 2\xi\omega_n\dot{e} + \omega_n^2 e = 0}$$

Intuitive parameterization:
- Damping ratio: $\xi \in [0.7..1]$
- Natural frequency, related to rise time (10-90%): $\omega_n \sim \frac{t_r}{1.8}$

MODEL-FREE VS. MODEL-BASED CONTROL

Plant: $m\ddot{x} + b\dot{x} + kx = u$

Model-free:

$$u = k_p e + k_v\dot{e} + \int e \, dt + \ddot{x}_d$$

Advantages? Disadvantages?
- No model needed.
- Performance depends on model parameters.
- Need to <u>tune</u> gains to maximize performance.

MODEL-FREE VS. MODEL-BASED CONTROL

Plant: $m\ddot{x} + b\dot{x} + kx = u$

Model-based:

$$u = m(\ddot{x}_d + k_p e + k_v\dot{e}) + b\dot{x} + kx$$

$$\Rightarrow \quad \boxed{\ddot{e} + 2\xi\omega_n\dot{e} + \omega_n^2 e = 0}$$

Advantages? Disadvantages?
- Model needed. Model parameter errors?
- Model-based part: cancels dynamics of the system.
- Model-independent part: design/tune independent of the model.

MODEL-FREE VS. MODEL-BASED CONTROL

Tracking error bounded…

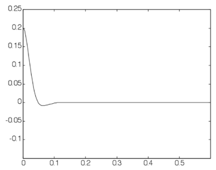

Perfect model

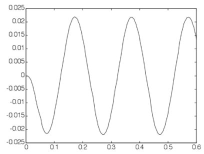

Imperfect model, 10% errors in parameters

SUMMARY

Model-free:

- No model needed.
- Performance depends on model parameters. Re-tune often…
- Need to tune gains to maximize performance.

Advantages? Disadvantages?

- Model needed. Model errors?
- Model-based part: cancels dynamics of the system.
- Model-independent part: design/tune independent of the model.

OUTLINE

I. Model-Based Control
- Model-Free Vs. Model-Based Control
- Quadrotor Model
- Position Control Approach
- Other Approaches
- What Can Go Wrong?

II. Learning-Enabled Control
- Task-Dependent Learning
- Task-Independent and Safe Learning

III. Summary

QUADROTOR BASICS

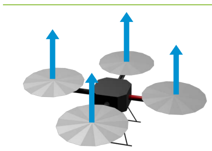

Hover

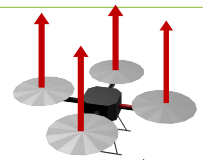

Ascend

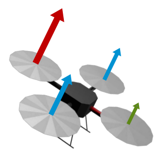

Pitch/Roll

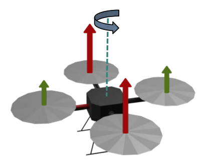

Yaw

MODEL

$$\begin{bmatrix} \ddot{x} \\ \ddot{y} \\ \ddot{z} \end{bmatrix} = \begin{bmatrix} 0 \\ 0 \\ -g \end{bmatrix} + \boldsymbol{R} \begin{bmatrix} 0 \\ 0 \\ c \end{bmatrix}$$

Maps from body to inertial frame.

$$c = (f_1 + f_2 + f_3 + f_4)/m$$

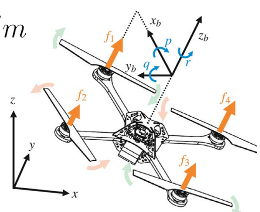

MODEL

$$\boldsymbol{J} \begin{bmatrix} \dot{p} \\ \dot{q} \\ \dot{r} \end{bmatrix} = \begin{bmatrix} l(f_2 - f_4) \\ l(f_3 - f_1) \\ \kappa(f_1 - f_2 + f_3 - f_4) \end{bmatrix} - \begin{bmatrix} p \\ q \\ r \end{bmatrix} \times \boldsymbol{J} \begin{bmatrix} p \\ q \\ r \end{bmatrix}$$

$$\dot{\boldsymbol{R}} = \boldsymbol{R} \begin{bmatrix} 0 & -r & q \\ r & 0 & -p \\ -q & p & 0 \end{bmatrix}$$

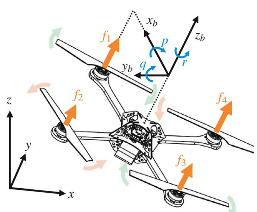

OUTLINE

I. Model-Based Control
- Model-Free Vs. Model-Based Control
- Quadrotor Model
- Position Control Approach
- Other Approaches
- What Can Go Wrong?

II. Learning-Enabled Control
- Task-Dependent Learning
- Task-Independent and Safe Learning

III. Summary

PART 1: VERTICAL CONTROL

$$\begin{bmatrix}\ddot{x}\\ \ddot{y}\\ \ddot{z}\end{bmatrix} = \begin{bmatrix}0\\0\\-g\end{bmatrix} + \boldsymbol{R}\begin{bmatrix}0\\0\\c\end{bmatrix}$$

$$c = (f_1 + f_2 + f_3 + f_4)/m$$

$$\boxed{c_d = \frac{1}{R_{33}}\Big(\underbrace{\omega_{n,z}^2(z_d - z) + 2\xi_z\omega_{n,z}(\dot{z}_d - \dot{z})}_{a_z} + \ddot{z}_d + g\Big)}$$

PART 1: LATERAL CONTROL

Define similarly for lateral direction:

$$a_x = \omega_{n,x}^2(x_d - x) + 2\xi_x\omega_{n,x}(\dot{x}_d - \dot{x}) + \ddot{x}_d$$
$$a_y = \dots$$

Transform into desired turn rates:

$$\begin{bmatrix}a_x\\a_y\end{bmatrix} = \begin{bmatrix}R_{13,d}\\R_{23,d}\end{bmatrix}c_d \qquad \begin{aligned}\dot{R}_{13,d} &= \tfrac{1}{\tau_{13}}(R_{13,d} - R_{13})\\ \dot{R}_{23,d} &= \tfrac{1}{\tau_{23}}(R_{23,d} - R_{23})\end{aligned}$$

$$\begin{bmatrix}p_d\\q_d\end{bmatrix} = \frac{1}{R_{33}}\begin{bmatrix}R_{21} & -R_{11}\\ R_{22} & -R_{12}\end{bmatrix}\begin{bmatrix}\dot{R}_{13,d}\\ \dot{R}_{23,d}\end{bmatrix}$$

OVERALL CONTROL

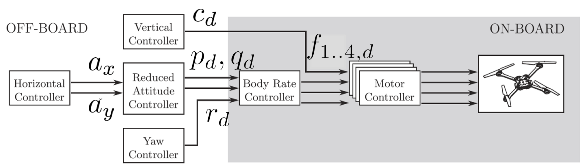

Body rate controller:

$$\boldsymbol{J}\begin{bmatrix}\frac{1}{\tau_p}(p_d - p)\\ \frac{1}{\tau_q}(q_d - q)\\ \frac{1}{\tau_r}(r_d - r)\end{bmatrix} + \begin{bmatrix}p\\q\\r\end{bmatrix} \times \boldsymbol{J}\begin{bmatrix}p\\q\\r\end{bmatrix} = \begin{bmatrix}l(f_{2,d} - f_{4,d})\\ l(f_{3,d} - f_{1,d})\\ \kappa(f_{1,d} - f_{2,d} + f_{3,d} - f_{4,d})\end{bmatrix}$$

$$(f_{1,d} + f_{2,d} + f_{3,d} + f_{4,d}) = mc_d$$

OUTLINE

I. Model-Based Control
- Model-Free Vs. Model-Based Control
- Quadrotor Model
- Position Control Approach
- Other Approaches
- What Can Go Wrong?

II. Learning-Enabled Control
- Task-Dependent Learning
- Task-Independent and Safe Learning

III. Summary

OTHER APPROACHES

- Linear controller based on linearized system [Gurdan, et al. 2007][Boubadallah, 2007][Hoffman et al., 2008]
- LQR
- Backstepping
- Exact linearization, differentially flat system [Mellinger]
- L1 adaptive control

OUTLINE

LIMITATIONS

Latency

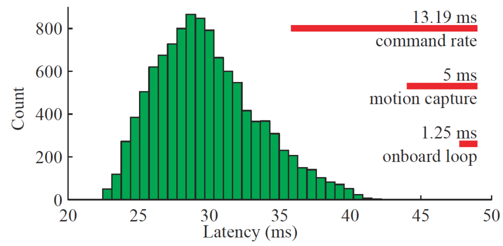

LIMITATIONS

Latency

Predict the vehicle position at the time the input arrives at the vehicle.

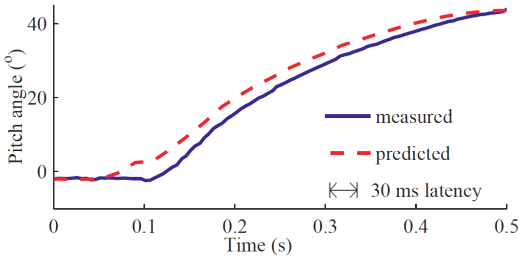

LIMITATIONS

Latency

Circle motion at 4 m/s.

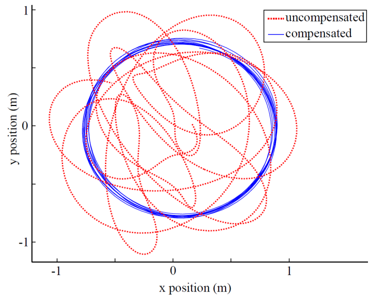

LIMITATIONS

Offsets

Calibrate during hover.

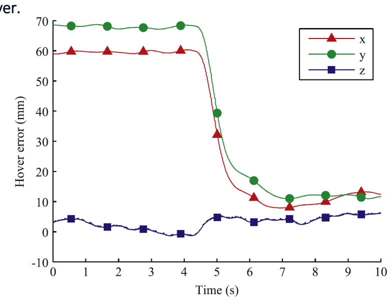

LIMITATIONS

Aggressive Maneuvers

1. Triple flip with a quadrotor.
2. Time-optimized slalom.
3. Fast path following with a ground vehicle.

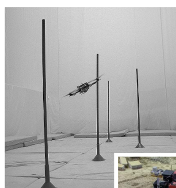

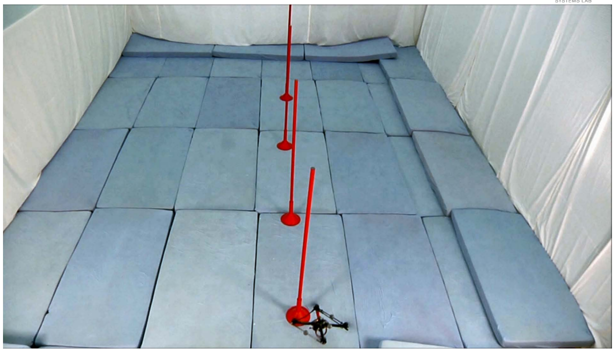

MOTIVATING EXAMPLE

EXPLANATION

- Unmodelled dynamics
- Unknown external disturbances (e.g., environment conditions such as surface material, topography or weather)

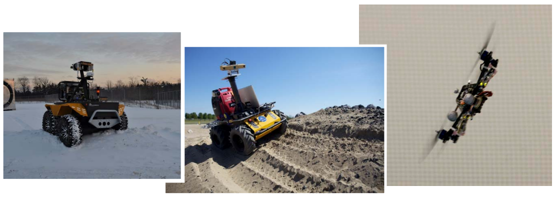

Model inaccuracies limit achievable performance!

CLAIM

Learning/adaptation enables safe, high-performance motions in uncontrolled, unknown or changing environments.

RESEARCH FOCUS

DYNAMICS → CONTROLS → MACHINE LEARNING → ROBOTICS

Prior information	+ Current sensor measurement	+ Past experiment data
– Which motions are feasible? – How to plan collision-free motions?	– How to guide the vehicle along a desired path?	– Can the performance be improved by leveraging past data?

Towards robotics applications.

FRAMEWORK

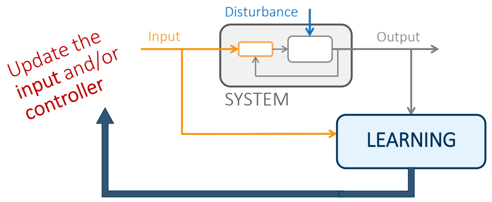

Improve the controls performance by learning from data.

OUTLINE

1 | TASK-DEPENDENT LEARNING

Task Executing a *given* motion.
Data Incorporation Adaptation of input parameters.

1. TRIPLE FLIPS

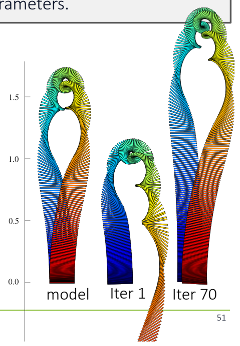

Lupashin, Schoellig, Sherback, D'Andrea, "A simple learning strategy for high-speed quadrocopter multi-flips," ICRA 2010.

APPROACH

A Priori Knowledge First-principles model, input constraints, parameterized input trajectory

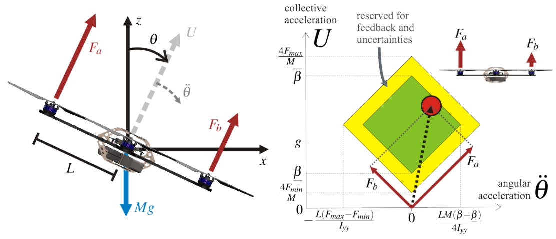

1 | APPROACH

A Priori Knowledge First-principles model, input constraints, parameterized input trajectory

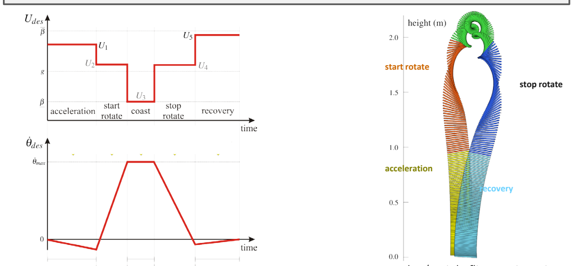

1600 deg/s triple flip – 70 iterations

1 | APPROACH

Algorithm Policy gradient method

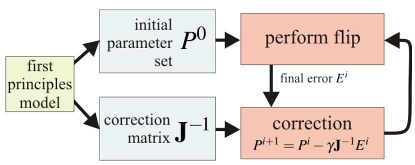

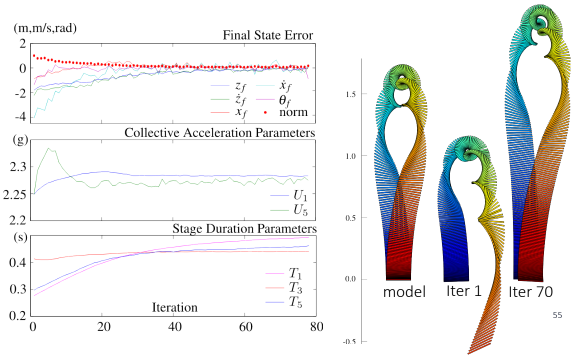

Task Executing a *given* motion.
Data Incorporation Adaptation of full discretized input trajectory.

2. FINITE-TIME TRAJECTORY

Slalom racing example.

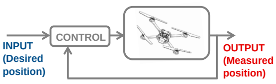

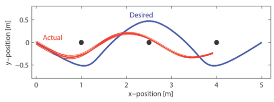

1. Extract system model from numeric simulation
2. Estimate model error/systematic offset along trajectory
3. Update input trajectory

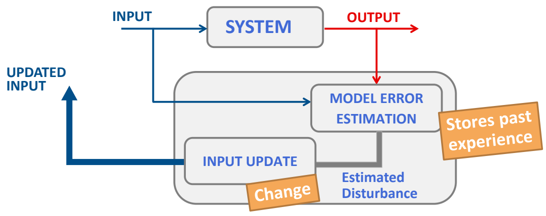

A Priori Knowledge First-principles model, input and state constraints, desired output trajectory

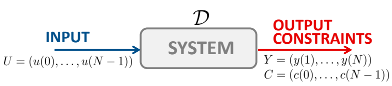

Prerequisites:

- Coarse model $\mathcal{D}: U \to (Y, C)$
- Desired output trajectory $(Y^*, C^*) = \mathcal{D}(U^*)$

Linear mapping from numeric simulation of coarse model:

$\mathrm{y} = F\,\mathrm{u}, \quad \mathrm{c} = L\,\mathrm{u} \qquad \mathrm{u} = U - U^*, \mathrm{y} = Y - Y^*, \quad \mathrm{c} = C - C^*$

Algorithm Optimization-based Iterative Learning

Iteration-Domain Model:

- For each trial $j,\ j \in \{1, 2, \dots\}$,

$$\mathrm{y}_j = F\,\mathrm{u}_j + \mathrm{d}_j + \mu_j$$
$$\mathrm{d}_{j+1} = \mathrm{d}_j + \omega_j$$

$d_j -$ unknown recurring disturbance

$\mu_j, \omega_j -$ trial-uncorrelated, zero-mean Gaussian noise

Disturbance estimate: Kalman filter in the iteration domain

- From jth execution get y_j and estimate $\hat{\mathrm{d}}_{j+1}$

Input update: minimize expected tracking error

$$\min_{\mathrm{u}_{j+1}} \left\| F\,\mathrm{u}_{j+1} + \hat{\mathrm{d}}_{j+1} \right\|_p$$
subject to
$$L\,\mathrm{u}_{j+1} \preceq \mathrm{c}_{\max}$$

Convex optimization

3| RESULT

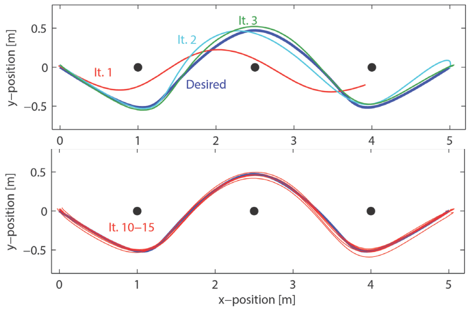

TASK-DEPENDENT LEARNING

Task Executing a *given* motion.
Data Incorporation Adaptation of input parameters.

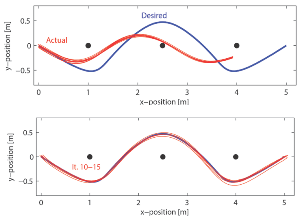

If task changes, learning is started from scratch!

OUTLINE

I. Model-Based Control
- Model-Free Vs. Model-Based Control
- Quadrotor Model
- Position Control Approach
- Other Approaches
- What Can Go Wrong?

II. Learning-Enabled Control
- Task-Dependent Learning
- Task-Independent and Safe Learning

III. Summary

TASK-INDEPENDENT LEARNING

Task Executing a *set of* motions.
Procedure *Continuous* operation.
Data Incorporation Adaptation of *system model* and *feedback controller.*

LEARNING-BASED MODEL PREDICTIVE CONTROL

Ostafew, Schoellig, Barfoot, "Learning-based nonlinear model predictive control to improve vision-based mobile robot path-tracking in challenging outdoor environments," ICRA 2014.


Prof. Tim Barfoot


Chris Ostafew

LEARNING-BASED MODEL PREDICTIVE CONTROL

State-space model with **state- and input-dependent disturbance model**:

$$\mathbf{x}_{k+1} = \overbrace{\mathbf{f}(\mathbf{x}_k, \mathbf{u}_k)}^{\text{a priori model}} + \overbrace{\mathbf{g}(\mathbf{a}_k)}^{\text{learned using GP}}$$

$$\mathbf{a}_k = (\mathbf{x}_k, \mathbf{v}_{k-1}, \mathbf{u}_k, \mathbf{u}_{k-1}),$$

Using a **Gaussian Process** to estimate the disturbance function.

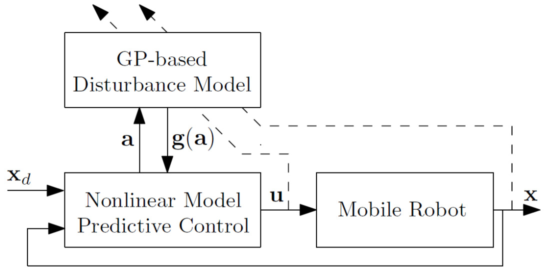

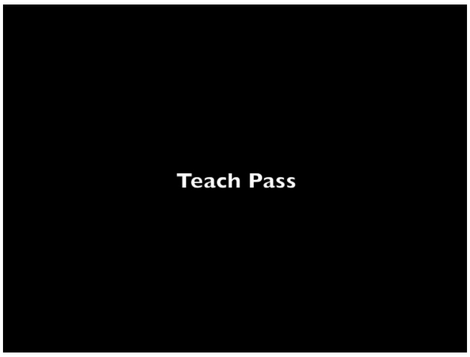

- Disturbance modelled as function of state and input using a Gaussian Process.
- Learning data can be transferred from one task to another.
- Uncertainty estimate is not considered, safety during learning not guaranteed.

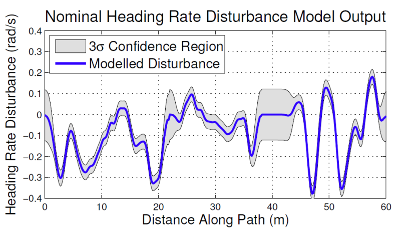

Procedure	*Continuous* operation.
Data Incorporation	Adaptation of *system model* and *feedback controller.*

ROBUST LEARNING CONTROL

- Guarantee stability while improving performance [1]

[1] Schaal, Atkeson, "Learning control in robotics," IEEE Robotics & Automation Magazine, 2010.

Berkenkamp, Schoellig, "Learning-based robust control: guaranteeing stability while improving performance," Machine Learning in Planning and Control of Robot Motion Workshop, IROS 2014.

Felix Berkenkamp

Robust control

- Specify prior uncertainty in model
- Guarantee stability and performance for all possible models

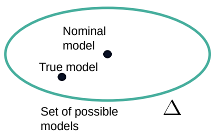

Online learning

- Learn from online data
- Improve the model

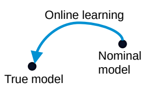

	Robust Control	Online learning
Models uncertainty	✓	✓
Guarantees stability	✓	✗
Improves online	✗	✓

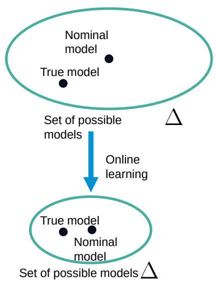

APPROACH

$$\mathbf{x}_{k+1} = \underbrace{\mathbf{f}(\mathbf{x}_k, \mathbf{u}_k)}_{a\ priori\ \text{model}} + \underbrace{\mathbf{g}(\mathbf{x}_k, \mathbf{u}_k)}_{\text{to be learned}}$$

$$\mathbf{y}_k = \mathbf{C}\mathbf{x}_k + \boldsymbol{\omega}_k,$$

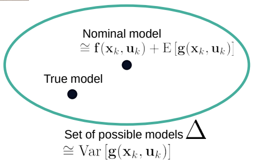

- **Gaussian Process:** Online learning
- **Robust Control:** Guaranteed stability / performance

SAFE, TASK-INDEPENDENT LEARNING

- **Combined** Gaussian Process **learning** with Linear **Robust Control**
- Enables **controller performance to improve online** while providing **stability guarantees**

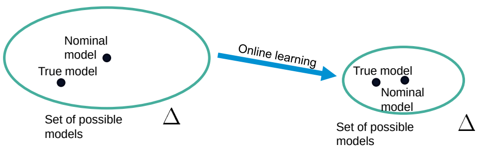

DEVELOPMENT

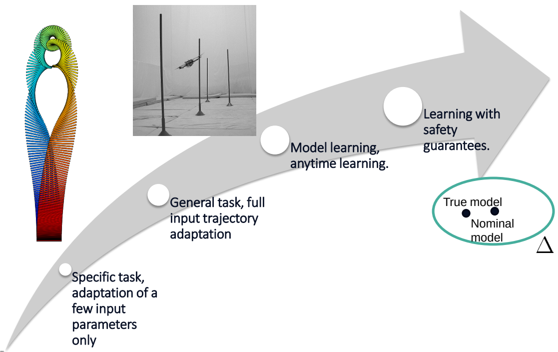

SAFE, TASK-INDEPENDENT LEARNING

… more to come!

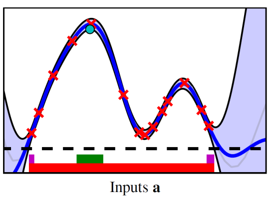

Follow us!

www.dynsyslab.org

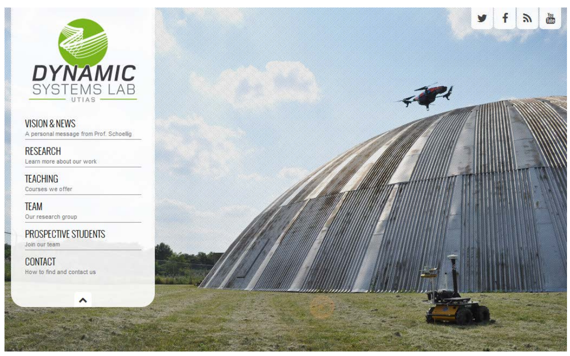

MY GROUP

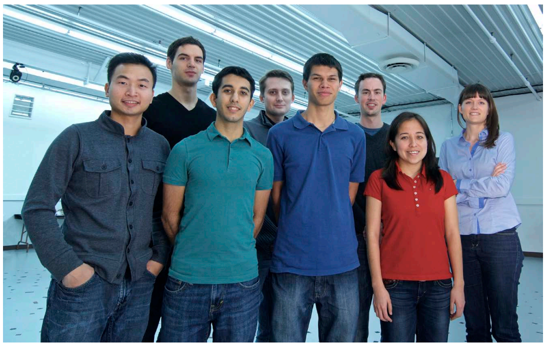

SUMMARY

LEARNING HELPS US TO ACHIEVE…

Excellence

Safety

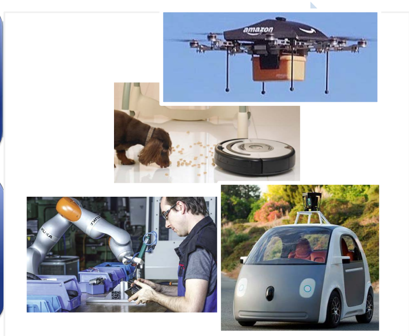

THANK YOU

For follow-up discussions, please contact me:

Angela P. Schoellig
web: www.schoellig.name
email: schoellig@utias.utoronto.ca

Follow us!

EXCERCISE

You get the task to fly the Parrot AR.Drone autonomously in an indoor motion capture system.

- Measurements:
  Full vehicle state
- Inputs to be computed:
  Roll, pitch (ZYX Euler angles), rate around body z-axis, z velocity

⇨Start with quadsim_user_interface.m

⇨Fill out DSLcontroller.m, desiredstate.m, parameters.m

⇨Do not change given parameters.

CHALLENGE

Fly a circle of 4m/s and 1m radius (e.g. sin(4t)).

- Calculate your tracking error

⇨Start with quadsim_user_interface.m

⇨Fill out DSLcontroller.m, desiredstate.m, parameters.m

⇨Do not change given parameters.

ETH zürich

Nonlinear Dynamic State Estimation

TRADR Summer School on Autonomous Micro Aerial Vehicles
Schloss Birlinghoven, 27.8.2015

Igor Gilitschenski (igilitschenski@ethz.ch)

Overview

Overview

ETH zürich

Motivation

Robotic Perception

Mixed and Augmented Reality

Autonomous MAVs



1809 Karl Friedrich Gauss
"Theoria Motus Corporum Celestium"

1823 Karl Friedrich Gauss
"Theoria Combinationis Observationum Erroribus Minimis Obnoxiae"

1960 Rudolf Kálmán
"A New Approach to Linear Filtering and Prediction Problems",
Journal of Basic Engineering

1962 Gerald Smith, Stanley Schmidt, Leonard McGee
"Application of Statistical Filter Theory to the Optimal Estimation of Position and Velocity on Board a Circumlunar Vehicle",
Technical Report, National Aeronautics and Space Administration (NASA)

Overview

- Introduction
- **Kalman Filter**
- Extended Kalman Filter
- Moment Matching
- Unscented Kalman Filter
- Directional Approaches
- Conclusions

ETH zürich

Dynamic State Estimation

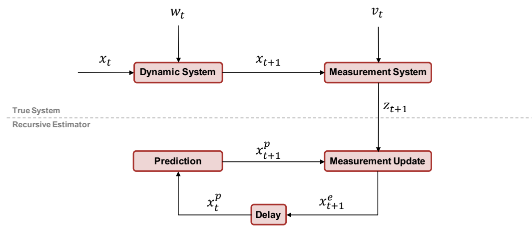

ETH zürich

Kalman Filter: Considered Model

- System model

system state, system noise

$$x_{t+1} = \boldsymbol{A} \cdot x_t + w_t$$

system matrix

- Measurement model

measurement function, measurement noise

$$z_t = \boldsymbol{H} \cdot x_t + v_t$$

measurement

ETH zürich

Kalman Filter: Prediction

estimate after prediction, estimate after previous update

$$x^p_{t+1} = \boldsymbol{A} \cdot x^e_t + E(w_t)$$

covariance after prediction, covariance after update

$$\boldsymbol{P}^p_{t+1} = \boldsymbol{A} \cdot \boldsymbol{P}^e_t \cdot \boldsymbol{A}^\top + \boldsymbol{Q}_t$$

system noise covariance
(in scalar cases sometimes σ_w^2)

ETH zürich

Kalman Filter: Update

$$x^e_t = x^p_t + \boldsymbol{K} \cdot \underbrace{(z_t - \boldsymbol{H} \cdot x^p_t)}_{\text{innovation}}$$

Kalman gain

$$\boldsymbol{P}^e_t = \boldsymbol{P}^p_t - \boldsymbol{K} \cdot \boldsymbol{S} \cdot \boldsymbol{K}^\top$$

covariance of z

$$\boldsymbol{S} = \boldsymbol{H} \cdot \boldsymbol{P}^p_t \cdot \boldsymbol{H}^\top + \boldsymbol{R}_t$$

measurement noise covariance
(in scalar cases sometimes σ_v^2)

$$\boldsymbol{K} = \boldsymbol{P}^p_t \cdot \boldsymbol{H}^\top \cdot \boldsymbol{S}^{-1}$$

ETH zürich

Kalman Filter: Simple Example

- Identity system model
  $x_{t+1} = x_t + w_t$,
  with $\sigma_w^2 = 0.01$.
- Noisy direct measurements
  $z_t = x_t + v_t$
  with different noise levels.

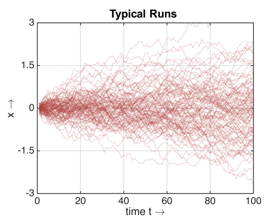

Kalman Filter: Simple Example (contd.)

$\sigma_v^2 = 0.3$

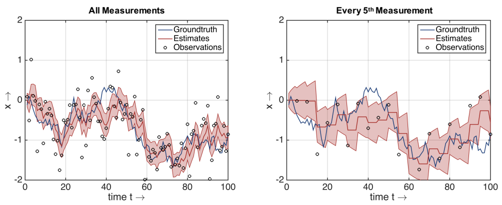

Kalman Filter: Simple Example (contd.)

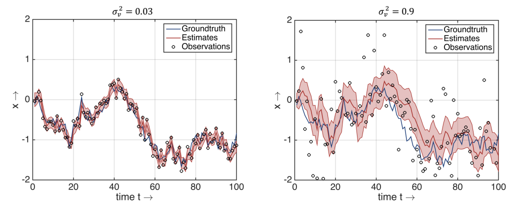

Overview

Nonlinear Case

- System Model

system state   system noise

$$x_{t+1} = a(x_t) + w_t$$

system function

- Measurement Model

measurement   measurement noise

$$z_t = h(x_t) + v_t$$

measurement function

Extended Kalman Filter

- Linearize system around current estimate.
- Linearize measurement model around prediction.
- Make use of Taylor series expansion.
- First-order approximation.

Extended Kalman Filter: Prediction

$$x_{t+1}^p = a(x_t^e) + E(w_t)$$

$$\boldsymbol{A}_t = \overbrace{\left(\frac{\partial a}{\partial x}\right)_{x=x_t^e}}^{\text{jacobian of system function at current estimate}}$$

covariance after prediction   covariance after update

$$\boldsymbol{P}_{t+1}^p = \boldsymbol{A}_t \cdot \boldsymbol{P}_t^e \cdot \boldsymbol{A}_t^\top + \boldsymbol{Q}_t$$

system noise covariance

Extended Kalman Filter: Update

$$x_t^e = x_t^p + \underbrace{\mathbf{K}}_{\text{Kalman gain}} \cdot \overbrace{\left(z_t - h(x_t^p)\right)}^{\text{residual}}$$

$$\boldsymbol{P}_t^e = \boldsymbol{P}_t^p - \boldsymbol{K} \cdot \underbrace{\boldsymbol{S}}_{\text{covariance of residual}} \cdot \boldsymbol{K}^\top$$

$$\boldsymbol{H}_t = \underbrace{\left(\frac{\partial h}{\partial x}\right)_{x = x_t^p}}_{\text{jacobian of measurement function}}$$

$$\boldsymbol{S} = \boldsymbol{H}_t \cdot \boldsymbol{P}_t^p \cdot \boldsymbol{H}_t^\top + \boldsymbol{R}_t$$

$$\boldsymbol{K} = \boldsymbol{P}_t^p \cdot \boldsymbol{H}_t^\top \cdot \boldsymbol{S}^{-1}$$

Overview

General Gaussian Filter based on Moment Matching

- Maintain Gaussian assumption for prior and posterior.
- Gaussian distribution described by mean and covariance.
- Key idea: propagate merely mean and covariance.

General Gaussian Filter: Prediction

$$x_{t+1}^p = \boldsymbol{E}(a(x_t^e) + w_t)$$

potentially burdensome

$$\boldsymbol{P}_{t+1}^p = \boldsymbol{E}\left((x_{t+1}^p - \boldsymbol{E}(x_{t+1}^p)) \cdot (x_{t+1}^p - \boldsymbol{E}(x_{t+1}^p))^\top\right) + \boldsymbol{Q}_t$$

General Gaussian Filter: Update

$$x_t^e = x_t^p + \boldsymbol{K}_t(z_t - \hat{z}_t)$$

$$\boldsymbol{P}_t^e = \boldsymbol{P}_t^p - \boldsymbol{K} \cdot \boldsymbol{S} \cdot \boldsymbol{K}^\top$$

$$\boldsymbol{K}_t = \boldsymbol{C} \cdot \boldsymbol{S}^{-1}$$

$$\boldsymbol{C} = \boldsymbol{E}\left(\left(x_t^p - \boldsymbol{E}(x_t^p)\right) \cdot \left(h(x_t^p) - \hat{z}_t\right)^\top\right)$$

$$\boldsymbol{S} = \boldsymbol{E}\left(\left(h(x_t^p) - \hat{z}_t\right) \cdot \left(h(x_t^p) - \hat{z}_t\right)^\top\right) + \boldsymbol{R}_t$$

$$\hat{z}_t = \boldsymbol{E}(h(x_t^p))$$

Integration Approaches

$\mathbf{E}(f(x))$

Adaptive Numerical Integration
- Use of adaptive grids.
- High accuracy can be guaranteed.
- Suffers from curse of dimensionality.
- Potentially high computational demand.

Monte-Carlo Integration
- Less prone to curse of dimensionality.
- Requires random sampling.
- Probabilistic accuracy guarantees.

Linearization
- Linearization around estimate.
- Propagation possible in closed form.
- Errors due to linearization and choice of linearization point.

Deterministic Sampling
- Deterministic (sample-based) approximation of continuous densities.
- Computationally tractable.
- Outperforms randomized approaches.

Overview

- Introduction
- Kalman Filter
- Extended Kalman Filter
- Moment Matching
- **Unscented Kalman Filter**
- Directional Approaches
- Conclusions

Density Approximation

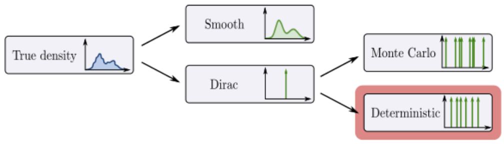

Unscented Kalman Filter: Unscented Transform

- Key Idea: Approximate Gaussian by a discrete distribution.
- Maintain first two moments.
- Outcome: No derivatives required in propagation.

Unscented Transform: Sigma Points

$$\chi_{t,0} = \mu$$

$$\chi_{t,i} = \mu + \left(\sqrt{(n+\lambda)\cdot\boldsymbol{\Sigma}}\right)_i \text{ for } i = 1, \dots, n$$

$$\chi_{t,i} = \mu - \left(\sqrt{(n+\lambda)\cdot\boldsymbol{\Sigma}}\right)_{i-n} \text{ for } i = n+1, \dots, 2n$$

Unscented Transform: Weights

$$w_0^m = \frac{\lambda}{n+\lambda},$$

$$w_0^c = w_0^m + (1 - \alpha^2 + \beta),$$

$$w_i^m = w_i^c = \frac{1}{2(n+\lambda)}$$

Tuning Parameters

- Scaling parameter

$$\lambda = \alpha^2(n+\kappa) - n.$$

- $\beta = 2$ optimal for Gaussians.
- α (typically small, e.g. 1e-3), κ (typically zero) are further tuning parameters.

Unscented Kalman Filter: Prediction

$$\chi^p_{t+1,i} = a(\chi^e_{t,i})$$

$$x^p_{t+1} = \sum_{i=1}^{2n+1} w_i^m \cdot \chi^p_{t+1,i} + E(w_t)$$

$$\boldsymbol{P}^p_{t+1} = \sum_{i=1}^{2n+1} w_i^m \cdot (\chi^p_{t+1,i} - x^p_{t+1}) \cdot (\chi^p_{t+1,i} - x^p_{t+1})^\top + \boldsymbol{Q}_t$$

Unscented Kalman Filter: Update

$$x^e_t = x^p_t - \boldsymbol{K}_t(z_t - \hat{z}_t)$$

$$\boldsymbol{P}^e_t = \boldsymbol{P}^p_t - \boldsymbol{K} \cdot \boldsymbol{S} \cdot \boldsymbol{K}^\top$$

$$\boldsymbol{K}_t = \boldsymbol{C} \cdot \boldsymbol{S}^{-1}$$

$$\boldsymbol{S} = \sum_{i=0}^{2n+1} w_i^m \cdot \left(h(\chi^p_{t,i}) - \hat{z}_t\right) \cdot \left(h(\chi^p_{t,i}) - \hat{z}_t\right)^\top + \boldsymbol{R}_t$$

$$\boldsymbol{C} = \sum_{i=0}^{2n+1} w_i^m \cdot (\chi^p_{t,i} - x^p_t) \cdot \left(h(\chi^p_{t,i}) - \hat{z}_t\right)^\top$$

$$\hat{z}_t = \sum_{i=0}^{2n+1} w_i^m \cdot h(\chi^p_{t,i})$$

Example: Polar to Cartesian Transform

- Scenario involving range and bearings measurements.
- **Range** r: Mean $1m$, Std. deviation $2cm$.
- **Bearing** θ: Mean $90°$, Std. deviation $15°$.
- Transformation into (x, y) plane using

$$\begin{pmatrix} x \\ y \end{pmatrix} = \begin{pmatrix} r\cos(\theta) \\ r\sin(\theta) \end{pmatrix}.$$

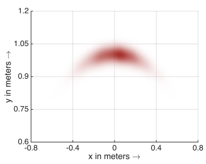

Further Sampling Schemes

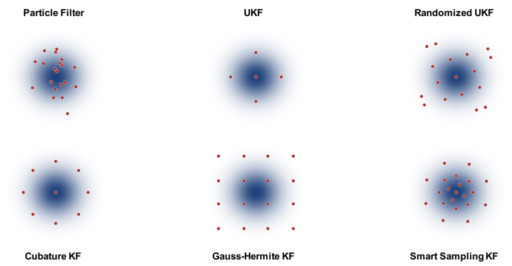

What can still go wrong?

- Multimodal densities particularly prone to errors from Gaussian approximation.
- Consider propagation of $z \sim N(0,1)$ through

$$a(x) = sign(x) \cdot \sqrt[5]{|x|}.$$

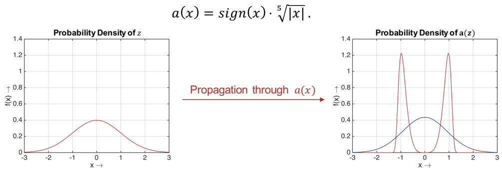

Overview

ETH zürich

Directional Statistics

- Directional statistics is a subfield of statistics that considers uncertainty on nonlinear manifolds.
- These manifolds involve circles, hyperspheres, or rigid-body motions.
- Exploitation of local linearity possible for small uncertainty
- Consideration of underlying geometry required for strong uncertainties (e.g. because of periodicity).

ETH zürich

Bingham Distribution

Definition

A probability distribution described by the PDF

$$f(\underline{x}) = \frac{1}{N(\mathbf{Z})} \exp\left(\underline{x}^\top \mathbf{M}\,\mathbf{Z}\,\mathbf{M}^\top \underline{x}\right)$$

with $\underline{x} \in S_{d-1} \subset \mathbb{R}^d$, orthogonal $\mathbf{M} \in \mathbb{R}^{d\times d}$ and diagonal $\mathbf{Z} \in \mathbb{R}^{d\times d}$ (with all entries negative) is called the Bingham distribution.

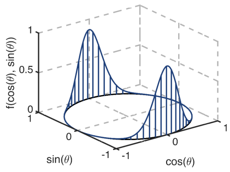

Normalization Constant

$$N(\mathbf{Z}) = \int_{S_{d-1}} \exp(\underline{x}^\top \mathbf{Z}\,\underline{x})\, \mathrm{d}\underline{x}$$

Second Moment

$$\mathbf{Cov}(\underline{x}) = \mathbf{M} \cdot \mathrm{diag}\left(\frac{\frac{\partial}{\partial z_1} N(\mathbf{Z})}{N(\mathbf{Z})}, \ldots, \frac{\frac{\partial}{\partial z_n} N(\mathbf{Z})}{N(\mathbf{Z})}\right) \cdot \mathbf{M}^\top$$

ETH zürich

Bingham Distribution (contd.)

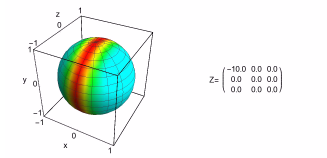

- Arises naturally by conditioning zero-mean Gaussian to unit length.
- 4d variant can be used for representing uncertain quaternions.
- Antipodal symmetry accounts for the fact that quaternions q and –q represent the same orientation.

ETH zürich

Considered Model

- System Model

system state system noise

$$x_{t+1} = x_t \oplus w_t$$

manifold-aware shift

- Measurement Model

measurement measurement noise

$$z_t = x_t \oplus v_t$$

ETH zürich

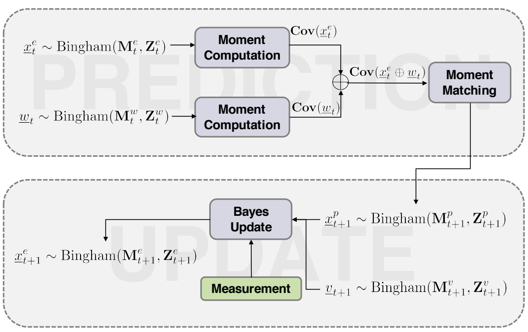

ETH zürich

Nonlinear Domains

- System Model

system state system noise

$$x_{t+1} = a(x_t) \oplus w_t$$

system function manifold-aware shift

- Measurement Model

measurement measurement noise

$$z_t = h(x_t) \oplus v_t$$

measurement function

ETH zürich

Deterministic Sampling

- Deterministic Sampling required for approximate propagation.
- Generation of UKF-like samples using (trigonometric) moment matching.

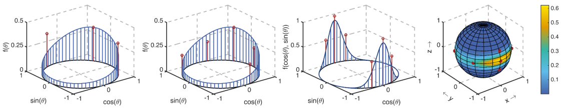

ETH zürich

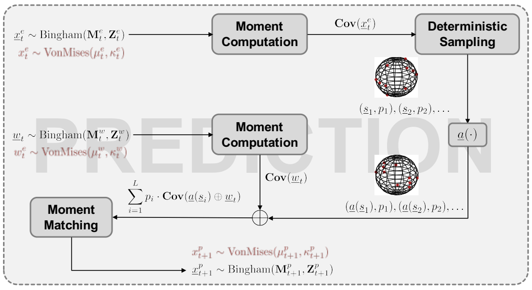

Overview

ETH zürich

How to choose a Filter?

- **Linear problem:** Kalman filter.
- **Weak nonlinearity:** EKF / UKF.
- **Stronger nonlinearities:** UKF (and other sample based Filters) / Particle Filters.
- **Nonlinear domain / weak noise:** Kalman type filters (EKF, UKF, …).
- **Nonlinear domain / strong noise:** directional statistics.

ETH zürich

Some Frameworks

- Nonlinear Estimation Toolbox
  http://nonlinearestimation.bitbucket.org/
- EKF based modular sensor fusion framework
  https://github.com/ethz-asl/ethzasl_msf/wiki/
- libDirectional
  https://github.com/libDirectional/libDirectional/

ETH zürich

Further Reading

- Andrew Jazwinski, *Stochastic Processes and Filtering Theory*, Dover, 1970.
- Kanti Mardia and Peter Jupp, *Directional Statistics*, Wiley, 2000.
- Simo Särkkä, *Bayesian Filtering and Smoothing*, Cambridge University Press, 2013.
- Dan Simon, *Optimal State Estimation*, Wiley, 2006.

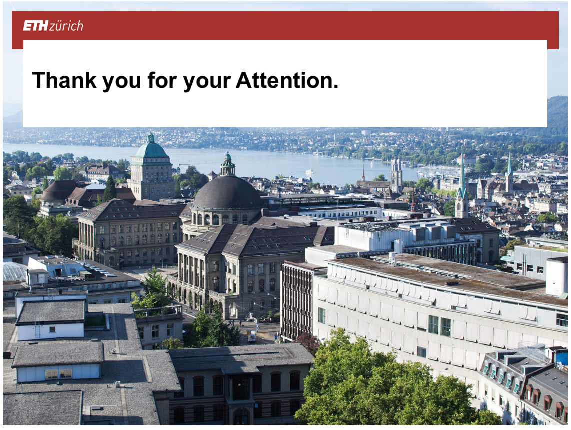
ETH zürich
Thank you for your Attention.

Vision for Autonomous Flight of Light-weight Micro Air Vehicles

Guido de Croon

Light-weight MAVs

DelFly II, 16g

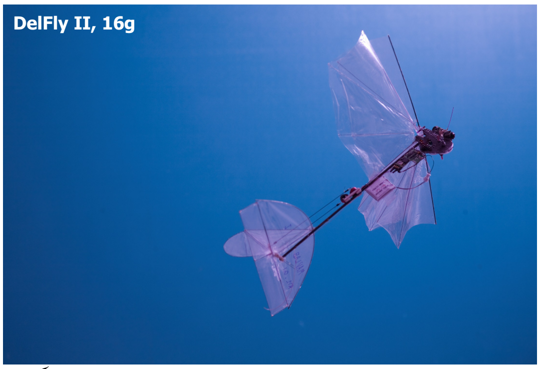

Walkera Ladybird, 35g

Why so light-weight / small?

- Navigation in narrow spaces
- Inherently safe
- Possibly cheap and expandible – swarms!
- Scientific, physical, and technological challenges

Challenges

- Faster dynamics
- Different aerodynamic regime
- Little payload / energy: fewer and worse resources
  - Sensors
  - Processing
  - Actuators

Fewer and worse resources

Example: **gyros**

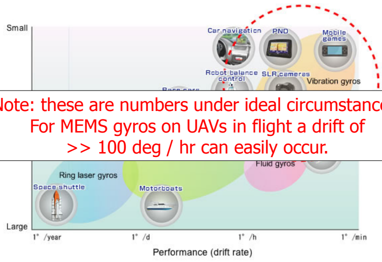

Note: these are numbers under ideal circumstances.
For MEMS gyros on UAVs in flight a drift of
>> 100 deg / hr can easily occur.

Fewer and worse resources

Example: **Processing power**

	Processor	Memory (RAM)	Weight	Power
Typical laptop	4-core 1.8 GHz + graphics card GPU	6 GB	1.6 kg	65 W
Odroid-U3	4-core 1.7 GHz	2 GB	48 g	10 W
OMAP 3630 (on AR drone)	1-core 1 GHz	1 GB	> 10 g	0.720 W
STM32F04 (on DelFly)	1-core 168 MHz	192 kB	> 4 g	0.200 W

Please note:

These are coarse estimates – actual numbers depend on the specific type and use

King of all sensors: the camera ☺

A camera:

- Is a passive sensor, requiring relatively little energy
- Can be miniaturized to tiny scales
- Can potentially provide rich information on the environment up to large distances

Problems of using a camera

Problems:

- What information should be extracted for successful navigation?
- How to extract this information?
- How to extract this information **efficiently**?

Inspiration from nature?

Fly, avoid obstacles, navigate, find food and shelter, interact socially with other fruitflies, learn, …

All for ~100,000 neurons!

Dragonfly

UAV

Optical flow

Gibson (1940-50s) – Optical flow

Ecological approach to psychology:
Perception is all about the affordance of action.

Optical flow:

The retinal flow of imaged world points.

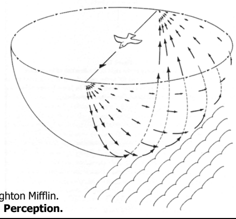

Gibson, J.J. (1950). The Perception of the Visual World. Houghton Mifflin.
Gibson, J.J. (1986). The Ecological Approach To Visual Perception.

Optical flow

Optical flow

In the 1940s Gibson performed experiments with pilots, studying how they know where they are moving to.

How do you think we do it?

Focus of Expansion

Expanding optical flow at approach

The flow “originates” from the focus of expansion (FoE) – the point the camera is moving towards.

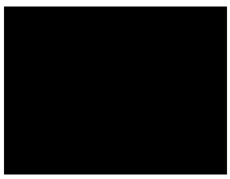

Translation and rotation

When does the rover translate? Does it rotate?

Parallax

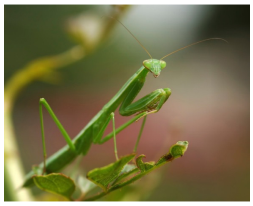

Parallax

Parallax

Time-to-contact

Rate of expansion gives us an idea of the time-to-contact – used for braking by persons.

Lee, D., **A theory of visual control of braking based on information about time-to-collision**, *Perception*, Vol. 5, 1967, pp. 437–459.

How to extract such information from images?

Pinhole camera model

Longuet-Higgins and Prazdny (1980)

Camera coordinate system:

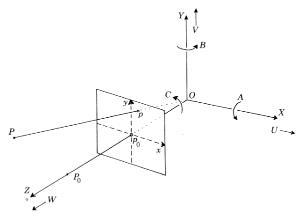

$$(x,\,y) = (X/Z,\; Y/Z)$$
$$(u,\,v) = (\dot{x},\,\dot{y})$$

$$\left.\begin{aligned}\dot{X} &= -U - BZ + CY,\\ \dot{Y} &= -V - CX + AZ,\\ \dot{Z} &= -W - AY + BX.\end{aligned}\right\}$$

Optical flow formula

Optical flow (u,v) expressed in relative position of a point (X,Y,Z) and camera velocities (U,V,W) and rotation rates (A,B,C):

$$u = \dot{X}/Z - X\dot{Z}/Z^2 = (-U/Z - B + Cy) - x(-W/Z - Ay + Bx)$$
$$v = \dot{Y}/Z - Y\dot{Z}/Z^2 = (-V/Z - Cx + A) - y(-W/Z - Ay + Bx)$$

Flow has a rotational and translational component

$$u = u^{\mathrm{T}} + u^{\mathrm{R}}, \quad v = v^{\mathrm{T}} + v^{\mathrm{R}},$$
$$u^{\mathrm{T}} = (-U + xW)/Z, \quad v^{\mathrm{T}} = (-V + yW)/Z,$$
$$u^{\mathrm{R}} = -B + Cy + Axy - Bx^2, \quad v^{\mathrm{R}} = -Cx + A + Ay^2 - Bxy.$$

- Using a gyro, the optical flow can be *derotated*, which removes u^R, v^R, facilitating vision processing.

Flow has a rotational and translational component

$$u = u^{\mathrm{T}} + u^{\mathrm{R}}, \quad v = v^{\mathrm{T}} + v^{\mathrm{R}},$$
$$u^{\mathrm{T}} = (-U + xW)/Z, \quad v^{\mathrm{T}} = (-V + yW)/Z,$$

- What is the flow at (x,y)=(0,0)?
- At what (x,y) is $(u^T, v^T) = (0,0)$?

- First substitute $x_{uT=0}$ into the formula of u^T. Express the "relative velocity", W/Z, in terms of u^T, x, and $x_{uT=0}$.

How to retrieve information from the optical flow?

$$u = (-U/Z - B + Cy) - x(-W/Z - Ay + Bx)$$
$$v = (-V/Z - Cx + A) - y(-W/Z - Ay + Bx)$$

How to retrieve information from the optical flow?

$$u = (-U/Z - B + Cy) - x(-W/Z - Ay + Bx)$$
$$v = (-V/Z - Cx + A) - y(-W/Z - Ay + Bx)$$

- 7 unknowns (A,B,C – U,V,W – Z)
- Z can be different per point

How many optical flow vectors do we need to resolve for the unknown variables?

How to retrieve information from the optical flow?

$$u = (-U/Z - B + Cy) - x(-W/Z - Ay + Bx)$$
$$v = (-V/Z - Cx + A) - y(-W/Z - Ay + Bx)$$

- 7 unknowns (A,B,C – U,V,W – Z)
- Z can be different per point

How many optical flow vectors do we need to resolve for the unknown variables?

Nistér, David. **An efficient solution to the five-point relative pose problem.** *Pattern Analysis and Machine Intelligence, IEEE Transactions on* 26.6 (2004): 756-770.

3D-reconstruction with multiple view geometry

Determine: the translation, rotation, and the world point coordinates (up to a scale)…

Hartley, Richard, and Andrew Zisserman. **Multiple view geometry in computer vision.** Cambridge university press, 2003.

Is 3D-reconstruction the goal of animal / robot vision?

Gibson vs. Marr

Gibson vs. Marr

Computing optical flow

Traditional cameras

Standard pipeline sparse optical flow:

1. Corner detector (FAST[1], Harris[2], …)
2. Lucas-Kanade feature tracking[3]

1. Harris, C., & Stephens, M. (1988, August). **A combined corner and edge detector.** In *Alvey vision conference* (Vol. 15, p. 50).
2. Rosten, E., Porter, R., & Drummond, T. (2010). **Faster and better: A machine learning approach to corner detection.** *Pattern Analysis and Machine Intelligence, IEEE Transactions on, 32*(1), 105-119.
3. Lucas, B. and Kanade, T. **An iterative image registration technique with an application to stereo vision.** In proceedings of Imaging understanding workshop, pp. 121–130. 1981.

Insects

Flying insects have facet eyes with ommatidia.

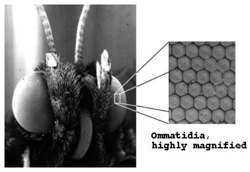

Insects

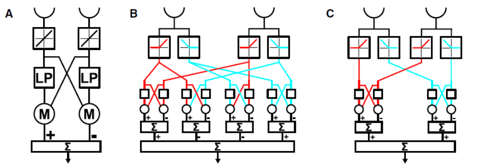

Reichardt model

Franceschini model

Eichner, H., Joesch, M., Schnell, B., Reiff, D. F., & Borst, A. (2011). **Internal structure of the fly elementary motion detector.** *Neuron, 70*(6), 1155-1164.

Bio-inspired sensors

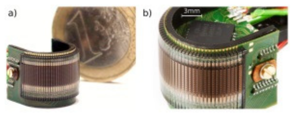

Floreano et al. 2013

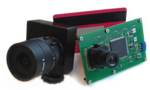

DVS Inilabs

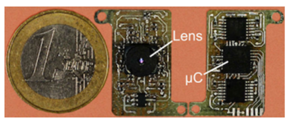

Roubieu et al. 2011

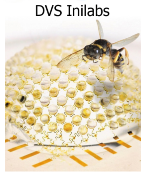

Song et al. 2013

Landing Control

Bee landing

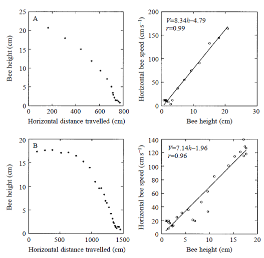

M.V. Srinivasan, S.W. Zhang, M. Lehrer, and S. Collett, **Honeybee navigation en route to the goal: visual flight control and odometry.** The Journal of Experimental Biology 199, 237–244 (1996).

Constant divergence landing

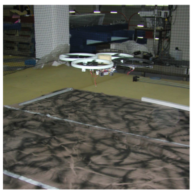

B. Hérissé, T. Hamel, R. Mahony, and F.-X. Russotto. **Landing a VTOL Unmanned Aerial Vehicle on a moving platform using optical flow.** IEEE Transactions on Robotics, 28(1):77–89, 2012.

Constantly / exponentially decreasing TTC

Enforce different landing dynamics (e.g., faster):

$$\dot{\tau} = -c^2$$

$$\dot{\tau} = -c^2 \tau$$

https://www.youtube.com/watch?v=mKgqe0k_Hy8

D. Izzo and G. de Croon. **Landing with time-to-contact and ventral optic flow estimates.** *Journal of Guidance, Control, and Dynamics* 35.4 (2012): 1362-1367.

4-dimensional guidance with Tau-pilot

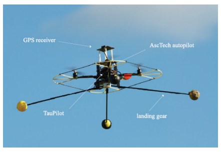

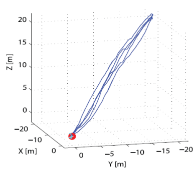

Kendoul, Farid. **Four-dimensional guidance and control of movement using time-to-contact: Application to automated docking and landing of unmanned rotorcraft systems.** *The International Journal of Robotics Research* 33.2 (2014): 237-267.

Honeybees land with constant divergence

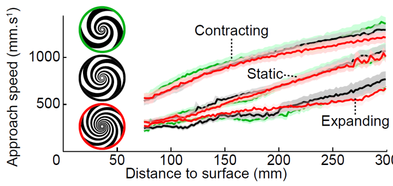

E. Baird, N. Boeddeker, M.R. Ibbotson, and M.V. Srinivasan. **A universal strategy for visually guided landing.** *PNAS: Biological Sciences - Neuroscience*, 2013.

Limitations optical flow

- Relies on sufficient texture
- For obstacle avoidance, flow close to the FoE is problematic: small errors result in large time-to-contact estimation errors.

Beyond optical flow

Visual appearance cues

Humans not only use optical flow and stereo vision to see distances, but also:

- Occlusion
- Texture gradient
- Image position where an object touches the ground plane
- Distance fog
- Sizes of known objects
- ...

Imitation learning

Learning from a human pilot: map a feature vector with optical flow and appearance features to a control input.

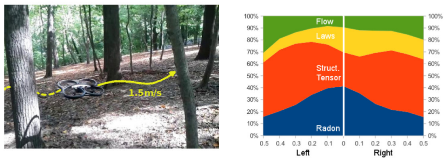

Ross, S., Melik-Barkhudarov, N., Shankar, K. S., Wendel, A., Dey, D., Bagnell, J. A., & Hebert, M. (2013, May). Learning monocular reactive uav control in cluttered natural environments. In Robotics and Automation (ICRA), 2013 IEEE International Conference on (pp. 1765-1772). IEEE.

Self-supervised learning

Drone uses optical flow as a scaffold to learn about the appearance of its environment.

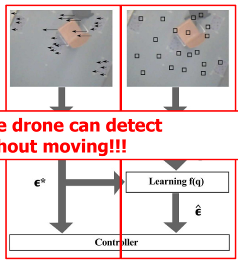

After learning, the drone can detect obstacles without moving!!!

H.W. Ho, C. De Wagter, B. Remes, and G.C.H.E. de Croon, Optical flow for self-supervised learning of obstacle appearance, IROS 2015.

Self-supervised learning

TU Delft Delft University of Technology

MAVLab

Case study: **DelFly Explorer**

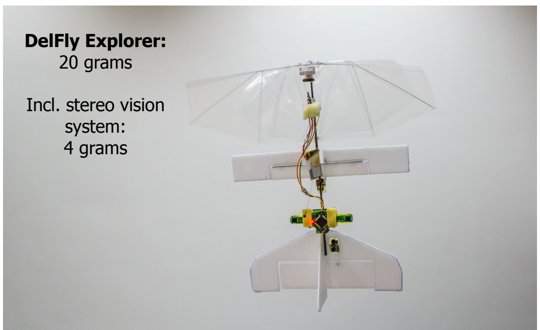

(2014), De Wagter, C., Tijmons, S., Remes, B.D.W., and de Croon, G.C.H.E., "Autonomous Flight of a 20-gram Flapping Wing MAV with a 4-gram Onboard Stereo Vision System", at the 2014 IEEE International Conference on Robotics and Automation (ICRA 2014)

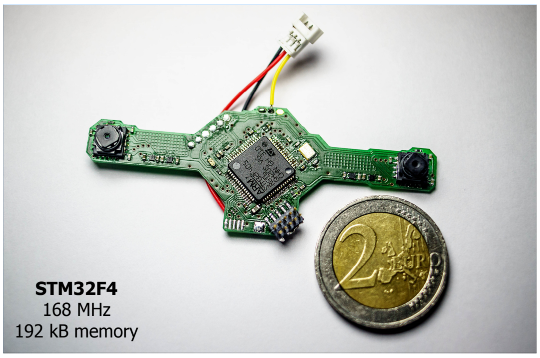

Stereo vision processing

Huge number of stereo vision methods in the literature:

- Accuracy vs. computational efficiency
- Global vs. local processing

Two efficient and accurate methods:

- Semi Global Matching[1]
- Geiger stereo matching[2]

1. Hirschmüller, H. (2005, June). Accurate and efficient stereo processing by semi-global matching and mutual information. In *Computer Vision and Pattern Recognition, 2005. CVPR 2005. IEEE Computer Society Conference on* (Vol. 2, pp. 807-814). IEEE.
2. Geiger, A., Roser, M., & Urtasun, R. (2011). Efficient large-scale stereo matching. In *Computer Vision–ACCV 2010* (pp. 25-38). Springer Berlin Heidelberg.

Stereo vision on DelFly Explorer

LongSeq:

- Line-by-line processing
- Search for longest sequence of pixels with the same disparity
- Efficient (~11Hz for 128 x 96 image)

Effects of sub-sampling

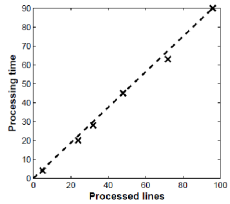

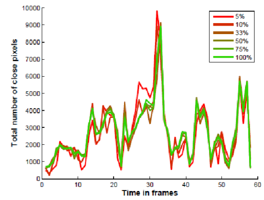

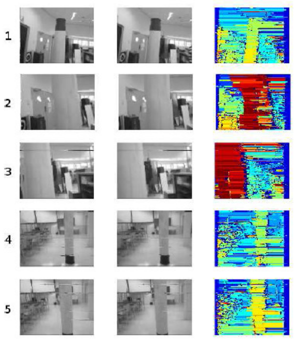

Obstacle avoidance algorithms

Challenges:

- Forward speed (~0.5 m/s) and maximum turn rate → nonholonomic vehicle.
- Limited field of view (~60º)
- Indoor, narrow, closed-off areas (instead of a sparse obstacle field as in outdoor forests)
- Little processing…

Reactive obstacle avoidance - failure cases

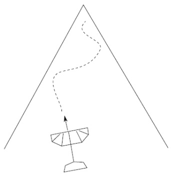

Left / right turning

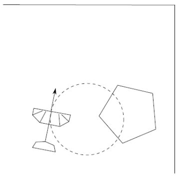

Full turning

Droplet strategy

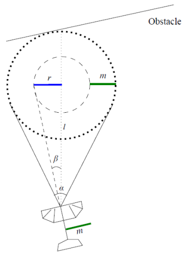

(2013), Tijmons, S., de Croon, G.C.H.E., Remes, B.D.W., De Wagter, C., Ruijsink, R., van Kampen, E., and Chu, Q.P., "Off-board processing of Stereo Vision images for Obstacle Avoidance on a Flapping Wing MAV", Pegasus AIAA conference, Prague.

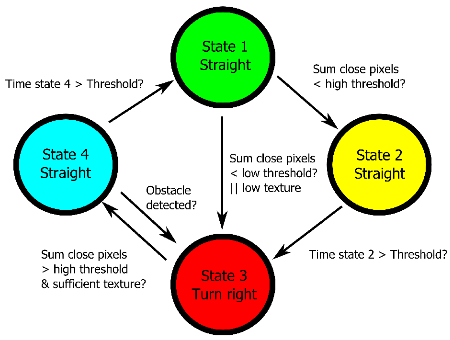

TU Delft Delft University of Technology

Next step: Evolving controllers

TU Delft Delft University of Technology

MAVLab

(in press) Behaviour Trees for Evolutionary Robotics, Kirk Y.W. Scheper, Sjoerd Tijmons, Coen C. de Visser, Guido C.H.E. de Croon, accepted in Artificial Life, MIT Press

Take-home messages / questions

- Tiny drones require extremely efficient Artificial Intelligence for autonomous flight
- Is 3D-reconstruction necessary for navigation?
- Insects (and drones) can land by directly using optical flow cues.
- There is more to life than optical flow: robots can learn about the appearance of their environment themselves.

Additional slides

Objectives of this lecture

Students …

1. Can explain the consequences of light-weight drones on the algorithms used for autonomous flight.
2. Can apply a pinhole camera model to extract optical flow variables useful for control: focus of expansion, divergence, time-to-contact, ventral flow, …
3. Can describe different methods of computing optical flow.
4. Can explain in which animal behaviors optical flow has been found to play an essential role, and why optical flow is of interest to MAVs.
5. Can explain the importance of additional, visual appearance features for control.

Sky segmentation

Outdoors, objects that are higher than a camera stick out of the horizon. Segmenting the camera image into "sky" and "obstacle" allows obstacle-free flight: the MAV can either deviate or fly over the obstacles, making them disappear under the horizon.

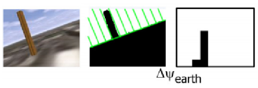

McGee, T. G., Sengupta, R., & Hedrick, K. (2005, April). Obstacle detection for small autonomous aircraft using sky segmentation. In Robotics and Automation, 2005. ICRA 2005. Proceedings of the 2005 IEEE International Conference on (pp. 4679-4684). IEEE.
de Croon, G. C. H. E., De Wagter, C., Remes, B. D. W., & Ruijsink, R. (2011, March). Sky Segmentation Approach to obstacle avoidance. In *Aerospace Conference, 2011 IEEE* (pp. 1-16). IEEE.

Appearance variation cue

As one approaches an objects, more and more other objects go out of view. Typically, the texture of a single object has less variation than the texture of many different objects.

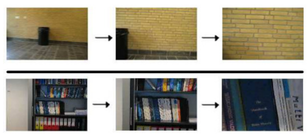

De Croon, G. C. H. E., De Weerdt, E., De Wagter, C., Remes, B. D. W., & Ruijsink, R. (2012). The appearance variation cue for obstacle avoidance. *Robotics, IEEE Transactions on, 28*(2), 529-534.

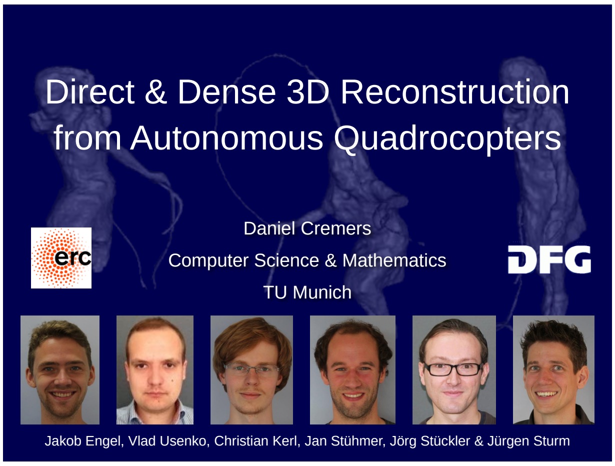
Direct & Dense 3D Reconstruction from Autonomous Quadrocopters
erc
Daniel Cremers
Computer Science & Mathematics
TU Munich
DFG
Jakob Engel, Vlad Usenko, Christian Kerl, Jan Stühmer, Jörg Stückler & Jürgen Sturm

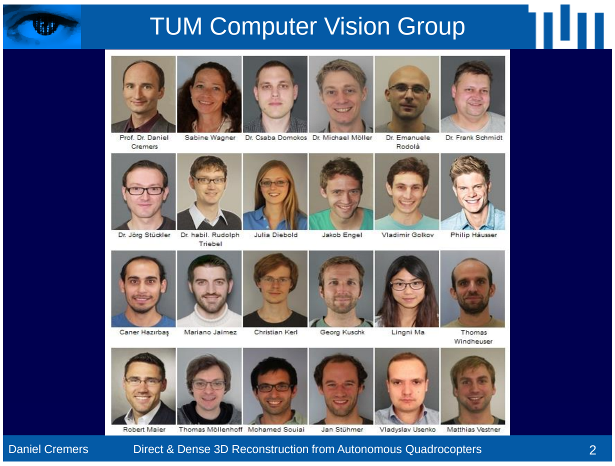
TUM Computer Vision Group
Prof. Dr. Daniel Cremers
Sabine Wagner
Dr. Csaba Domokos
Dr. Michael Möller
Dr. Emanuele Rodolà
Dr. Frank Schmidt
Dr. Jörg Stückler
Dr. habil. Rudolph Triebel
Julia Diebold
Jakob Engel
Vladimir Golkov
Philip Häusser
Caner Hazırbaş
Mariano Jaimez
Christian Kerl
Georg Kuschk
Lingni Ma
Thomas Windheuser
Robert Maier
Thomas Möllenhoff
Mohamed Souiai
Jan Stühmer
Vladyslav Usenko
Matthias Vestner
Daniel Cremers
Direct & Dense 3D Reconstruction from Autonomous Quadrocopters
2

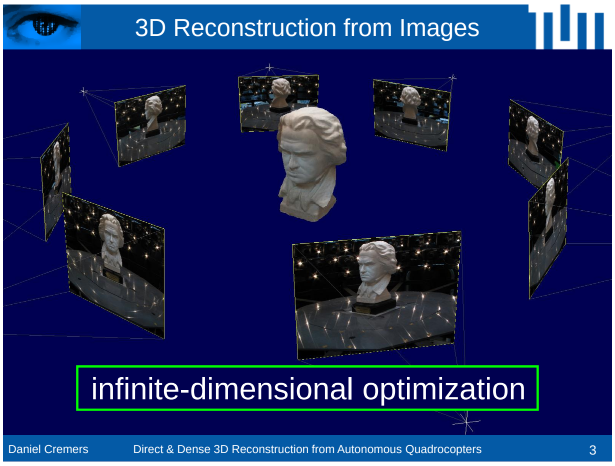
3D Reconstruction from Images
infinite-dimensional optimization
Daniel Cremers
Direct & Dense 3D Reconstruction from Autonomous Quadrocopters
3

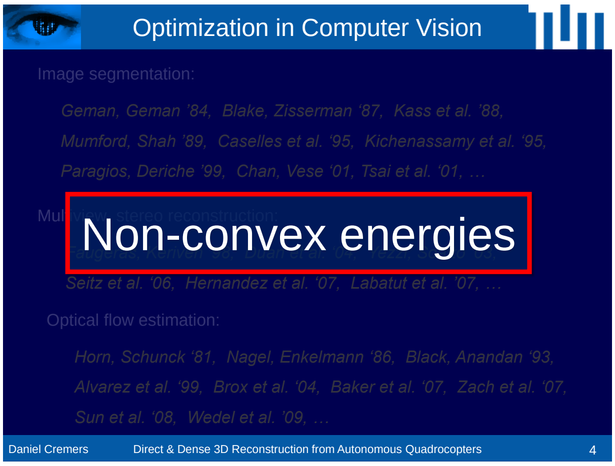
Optimization in Computer Vision
Image segmentation:
Geman, Geman '84, Blake, Zisserman '87, Kass et al. '88,
Mumford, Shah '89, Caselles et al. '95, Kichenassamy et al. '95,
Paragios, Deriche '99, Chan, Vese '01, Tsai et al. '01, …
Multiview stereo reconstruction:
Non-convex energies
Seitz et al. '06, Hernandez et al. '07, Labatut et al. '07, …
Optical flow estimation:
Horn, Schunck '81, Nagel, Enkelmann '86, Black, Anandan '93,
Alvarez et al. '99, Brox et al. '04, Baker et al. '07, Zach et al. '07,
Sun et al. '08, Wedel et al. '09, …
Daniel Cremers
Direct & Dense 3D Reconstruction from Autonomous Quadrocopters
4

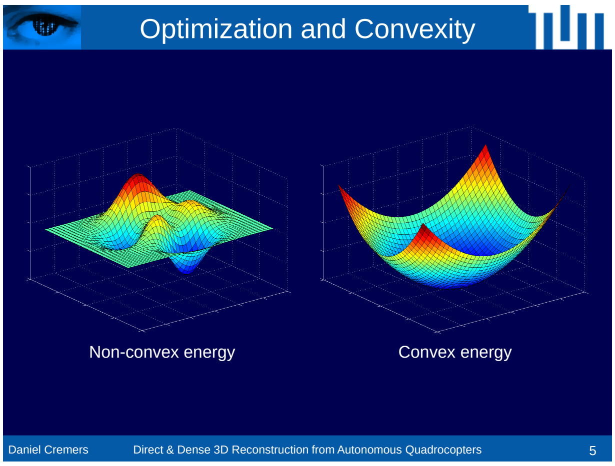
Optimization and Convexity
Non-convex energy
Convex energy
Daniel Cremers
Direct & Dense 3D Reconstruction from Autonomous Quadrocopters
5

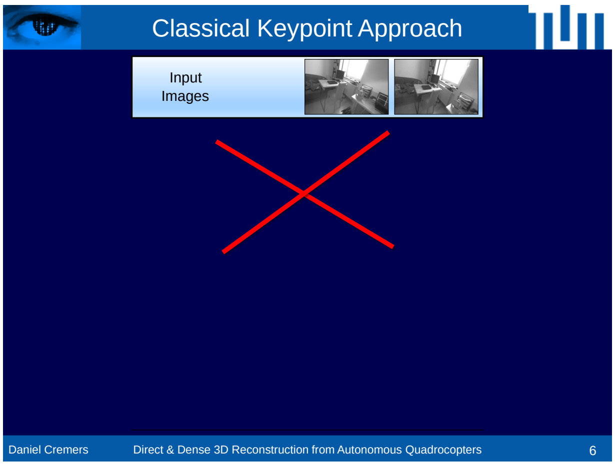
Classical Keypoint Approach
Input
Images
Daniel Cremers
Direct & Dense 3D Reconstruction from Autonomous Quadrocopters
6

Overview

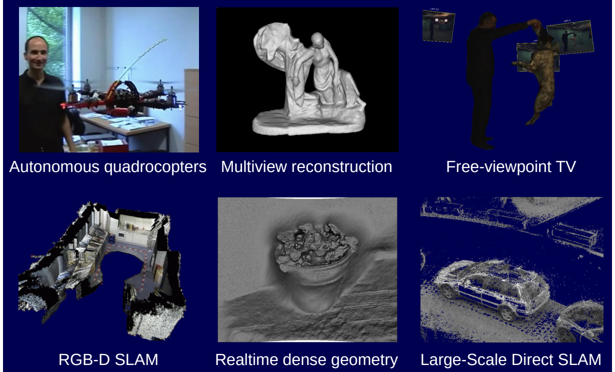

Overview

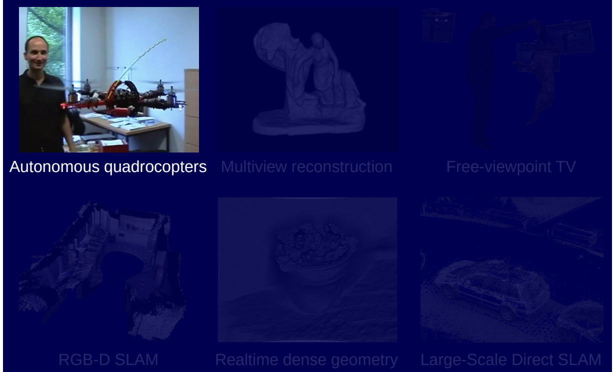

Autonomous Quadrocopters

Quadrocopters juggling
Mueller, Lupashin, D'Andrea IROS '11

Swarms of quadcopters
Kushleyev, Mellinger, Kumar RSS '12

Drawbacks:
- Controlled environment
- Marker points
- External sensors / mocap systems

Realworld Environments

Quadrocopters & Nanocopters

Can we use visual SLAM for autonomous quadrocopter navigation?

Can we reconstruct the world from autonomous quadcopters?

Gesture-Control of a Nanocopter

Dunkley, Engel, Sturm, Cremers, IROS 2014 Workshop on Nanocopters

…add a Camera…

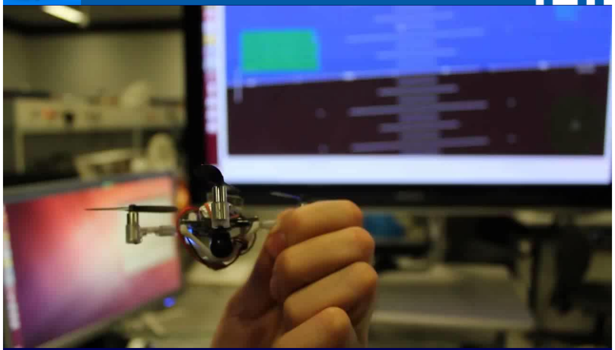

Dunkley, Engel, Sturm, Cremers, IROS 2014 Workshop on Nanocopters

…and Create a Selfie

Dunkley, Engel, Sturm, Cremers, IROS 2014 Workshop on Nanocopters

Overview

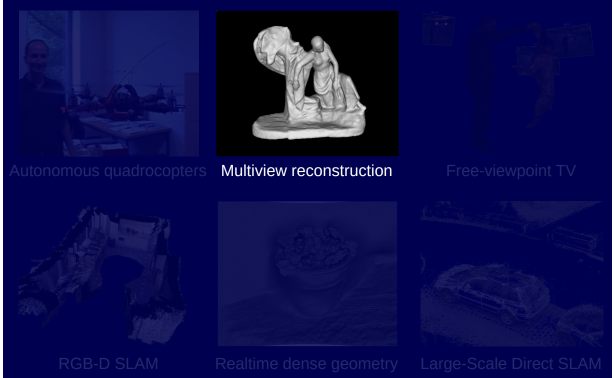

Solutions via Energy Minimization

Photoconsistency function:

$$\rho : \mathbb{R}^3 \rightarrow [0, 1]$$

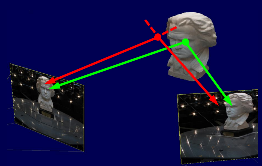

Determine a surface S of optimal photoconsistency by minimizing

$$E(S) = \int_S \rho \, dA$$

Kolev, Klodt, Brox, Cremers, Int. J. of Computer Vision '09:
Theorem: Globally optimal surfaces can be computed via convex relaxation.

Evolution to Global Optimum

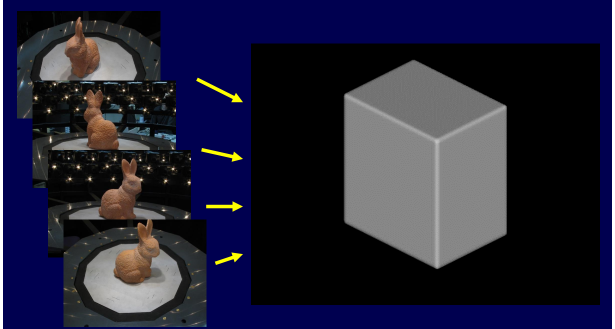

Kolev, Klodt, Brox, Cremers, IJCV 2009

Super-Resolution Texture Map

Given all images $\mathcal{I}_i : \Omega_i \rightarrow \mathbb{R}^3$, determine the surface color $T : S \rightarrow \mathbb{R}^3$

$$\min_T \sum_{i=1}^{n} \int_{\Omega_i} \Big(\underbrace{b *}_{\text{blur \& downsample}} (T \circ \underbrace{\beta_i}_{\text{back-projection}}) - \mathcal{I}_i \Big)^2 dx + \lambda \int_S \|\nabla_S T\| ds$$

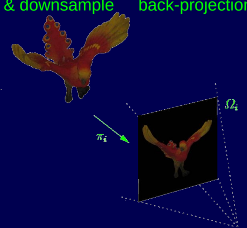

Goldlücke, Cremers, ICCV '09, DAGM '09, IJCV '13*

* Best Paper Award

Super-Resolution Texture Map

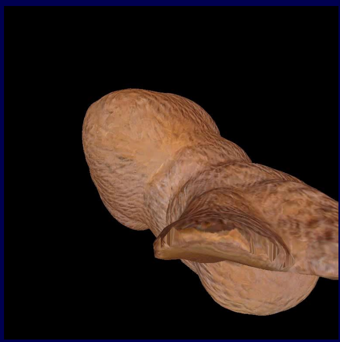

Goldlücke, Cremers, ICCV '09, DAGM '09, IJCV '13* * Best Paper Award

Super-Resolution Texture Map

Closeup of input image

Super-resolution texture

Goldlücke, Cremers, ICCV '09, DAGM '09, IJCV '13* * Best Paper Award

Overview

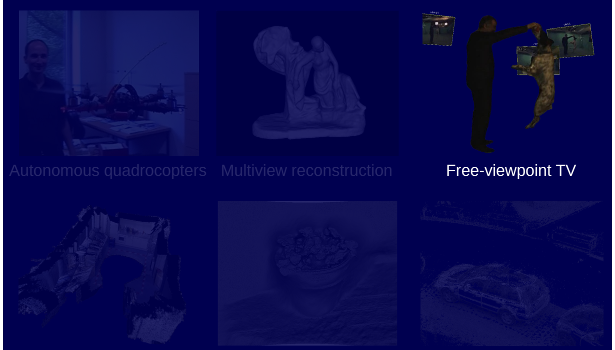

Silhouette-Consistent Reconstruction

Kolev, Cremers, ECCV '08, PAMI '11:
Theorem: Provably silhouette-consistent reconstructions can be computed by convex optimization over convex domains.

Silhouette-Consistent Reconstruction

$$\min_S \int_S \rho \, dA \quad \text{s.t. } \pi_i(S) = S_i \quad \forall i = 1, \dots, n$$

$$u = 1_{\text{int}(S)} \downarrow$$

$$\min_u \int_V \rho(x) \, |\nabla u| \, dx$$

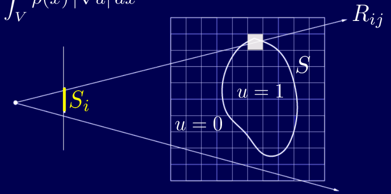

Kolev, Cremers, ECCV '08, PAMI 2011

Silhouette-Consistent Reconstruction

$$\min_S \int_S \rho \, dA \quad \text{s.t. } \pi_i(S) = S_i \quad \forall i = 1, \dots, n$$

$$u = 1_{\text{int}(S)} \downarrow$$

$$\min_u \int_V \rho(x) \, |\nabla u| \, dx \; = \min_{u \in \Sigma} \sup_{|\xi| \le \rho} \int u \, \text{div} \xi \, dx$$

$$\text{s.t.} \quad \Sigma = \begin{cases} \cancel{u : V \to \{0,1\}} \quad u : V \to [0,1] \\ \int_{R_{ij}} u(x) \, dx \ge 1 \quad \text{if } j \in S_i \quad \forall i, j \\ \int_{R_{ij}} u(x) \, dx = 0 \quad \text{if } j \notin S_i \quad \forall i, j \end{cases}$$

Proposition: The set Σ of silhouette-consistent solutions is convex.

Kolev, Cremers, ECCV '08, PAMI 2011

An Efficient Saddle Point Solver

Given the saddle point problem

$$\min_{u \in \Sigma} \sup_{\xi \in K} \langle Au, \xi \rangle + \langle g, u \rangle - \langle h, \xi \rangle$$

with close convex sets Σ and K and linear operator A of norm L.

Proposition: The primal-dual algorithm

$$\begin{cases} \xi^{n+1} = \Pi_K\left(\xi^n + \sigma(A\bar{u}^n - h)\right) \\ u^{n+1} = \Pi_\Sigma\left(u^n - \tau(A^*\xi^{n+1} + g)\right) \\ \bar{u}^{n+1} = 2u^{n+1} - u^n \end{cases}$$

converges with rate $O(1/n)$ to a saddle point for $\sigma\, \tau\, L^2 \leq 1$.

Pock, Cremers, Bischof, Chambolle, ICCV '09, Chambolle, Pock '11

Reconstructing the Niobids Statues

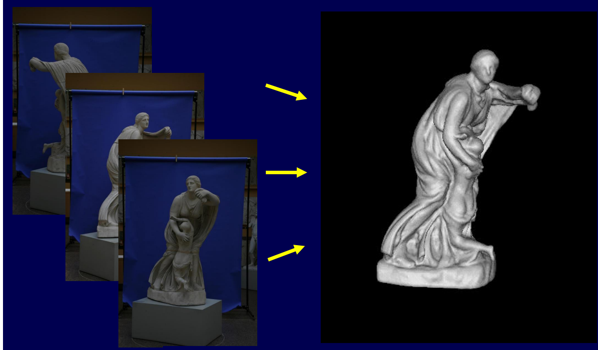

Kolev, Cremers, ECCV '08, PAMI '11

Reconstructing Dynamic Scenes

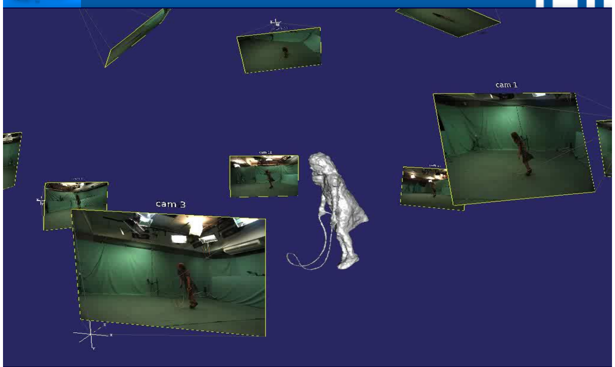

Oswald, Stühmer, Cremers, ECCV '14

Action Reconstruction

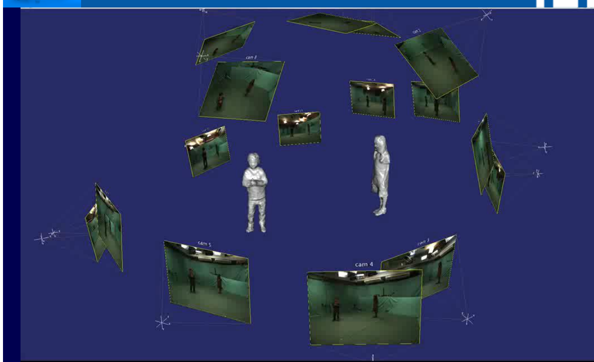

Oswald, Cremers, ICCV '13 4DMoD Workshop

Overview

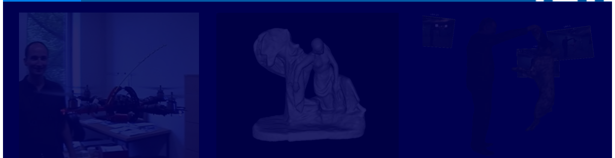

Autonomous quadrocopters | Multiview reconstruction | Free-viewpoint TV

RGB-D SLAM | Realtime dense geometry | Large-Scale Direct SLAM

RGB-D SLAM Benchmark

- 39 sequences (19 with ground truth)
- one zip-archive per sequence containing:
  - color & depth images (png),
  - accelerometer data,
  - trajectory file

http://vision.in.tum.de/datasets/rgbd-dataset

Sturm, Engelhard, Burgard, Cremers IROS '12

RGB-D SLAM Benchmark

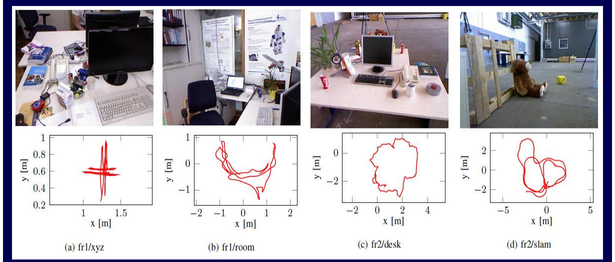

http://vision.in.tum.de/datasets/rgbd-dataset

Sturm, Engelhard, Burgard, Cremers IROS '12

Realtime Dense Camera Calibration

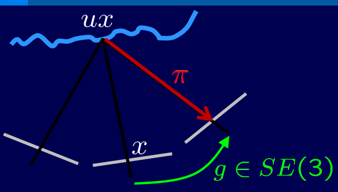

Lie algebra representation of rigid body motion:

$$g_\xi = \exp\left(\hat{\xi}\right), \quad \xi \in \mathbb{R}^6$$

Photo-consistency:

$$\min_{\xi \in \mathbb{R}^6} \int_\Omega \left| I_0(x) - I_i\Big(\pi\big(g_\xi(u \cdot x)\big)\Big)\right|^2 dx$$

Steinbruecker, Sturm, Cremers '11, Kerl et al. ICRA '13

Realtime Dense Camera Calibration

Photo-consistency:

$$E(\xi) = \int_\Omega \left| I_0(x) - I_i\Big(\pi\big(g_\xi(u \cdot x)\big)\Big)\right|^2 dx$$

Taylor expansion:

$$E(\xi) \approx \int_\Omega \left| I_0(x) - I_i - \nabla I^\top \left(\frac{d\pi}{dg_\xi}\right)\left(\frac{dg_\xi}{d\xi}\right)\xi\right|^2 dx$$

Optimal solution:

$$\frac{dE(\xi)}{d\xi} = A\xi + b = 0 \quad \longrightarrow \quad \xi = -A^{-1}b$$

Solve in coarse-to fine manner.

Steinbruecker, Sturm, Cremers '11, Kerl et al. ICRA '13

Realtime Dense Camera Calibration

http://cvpr.in.tum.de/datasets/rgbd-dataset

Third Person Perspective

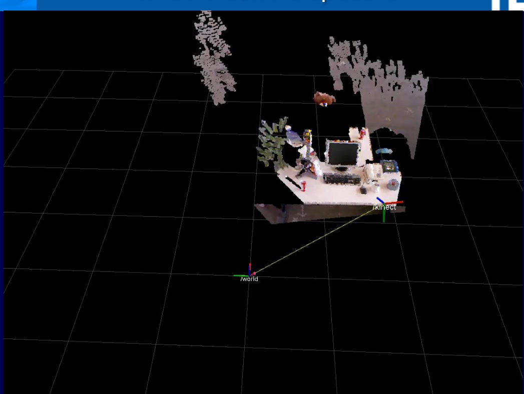

Quantitative Comparison

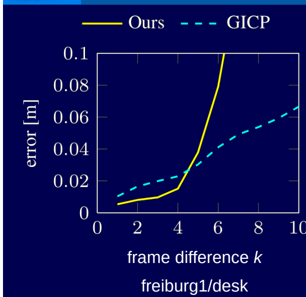

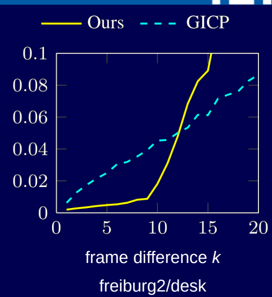

Pose accuracy for increasing baseline

Steinbruecker, Sturm, Cremers '11, Kerl et al. ICRA '13

Realtime 3D Modeling

Sturm, Bylow, Kahl, Cremers, GCPR '13

Download demo @ http://www.fablitec.com

Realtime 3D Modeling

Download demo @ http://www.fablitec.com

Realtime 3D Modeling

Download demo @ http://www.fablitec.com

Realtime 3D Modeling

Download demo @ http://www.fablitec.com

Realtime 3D Modeling

Download demo @ http://www.fablitec.com

Reconstruction on the Fly

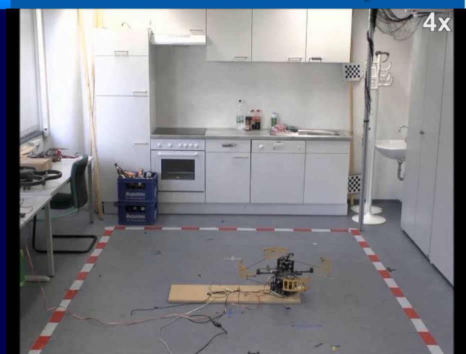

Bylow, Sturm, Kerl, Kahl, Cremers RSS '13

Large Scale: Loop Closure

Kerl, Sturm, Cremers ICRA '13

Large Scale: Octrees

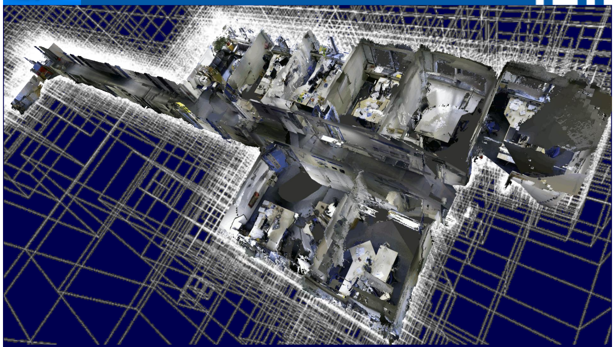

Steinbrücker, Kerl, Sturm, Cremers ICCV '13

Realtime Large-Scale Reconstruction

Steinbrücker, Kerl, Sturm, Cremers ICCV '13, ICRA '14

Overview

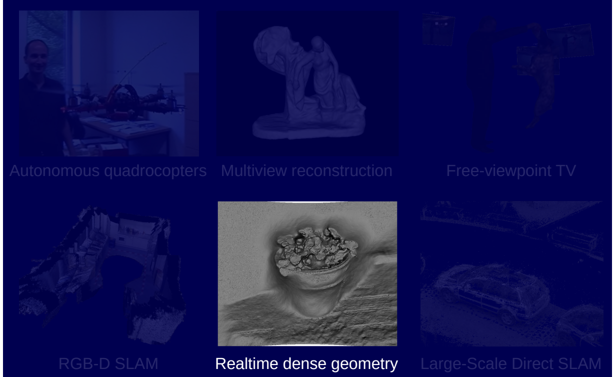

Multiview Reconstruction

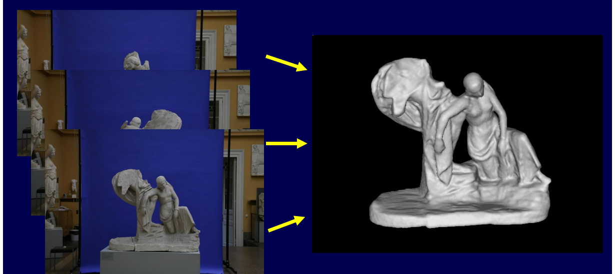

Can we do realtime dense reconstruction
from a handheld camera?

From Variational Optical Flow…

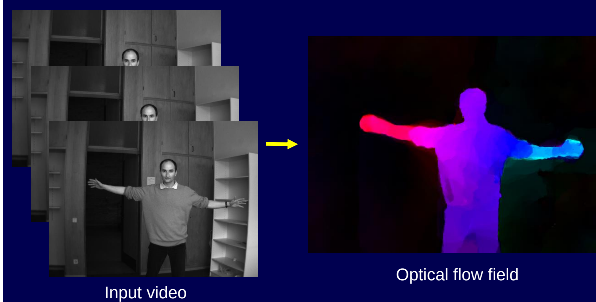

Wedel, Pock, Bischof, Cremers, ICCV '09

From Variational Optical Flow…

Input video

Optical flow field*

* 60 fps at 640 x 480 resolution

Wedel, Pock, Bischof, Cremers, ICCV '09

…to Realtime Dense Reconstruction

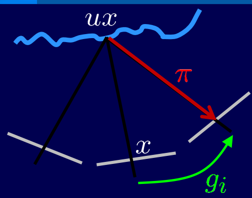

Brightness constancy:

$$I_0(x) \overset{!}{=} I_i\Big(\pi\big(g_i(ux)\big)\Big)$$

$$\min_{u,v} \sum_i \int_\Omega \Big|I_0(x) - I_i\Big(\pi\big(g_i(u \cdot x)\big)\Big)\Big|\, dx + \cancel{\int_\Omega |\nabla u(x)|\, dx}$$

$$+ \frac{1}{\theta} \int_\Omega (u - v)^2\, dx + \int_\Omega |\nabla v(x)|\, dx$$

Stuehmer, Gumhold, Cremers, DAGM '10

Realtime Dense Reconstruction

Stuehmer, Gumhold, Cremers, DAGM '10

Realtime Dense Reconstruction

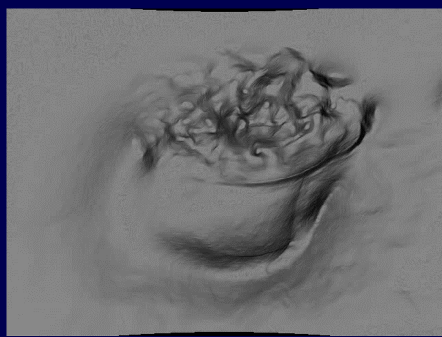

Stuehmer, Gumhold, Cremers, DAGM '10

Realtime Dense Reconstruction

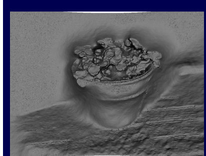

1.8 fps

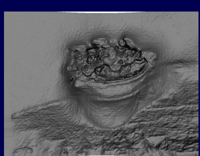

11.3 fps

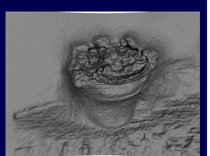

24 fps

Stuehmer, Gumhold, Cremers, DAGM '10

Realtime Dense Reconstruction

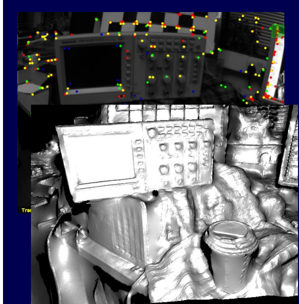

Newcombe et al., ICCV '11

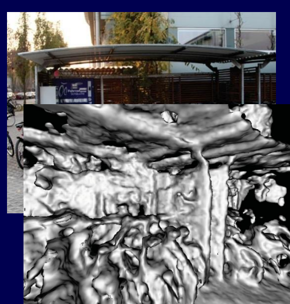

Wendel et al., CVPR '12

3D Modeling from a Quadrocopter

Mapping on Demand: Dense 3D Reconstruction

Frank Steinbrücker, Jürgen Sturm,
Jörg Stückler, Daniel Cremers

October 2014

Computer Vision and Pattern Recognition Group
Department of Computer Science
Technical University of Munich

DFG Project "Mapping on Demand"

Overview

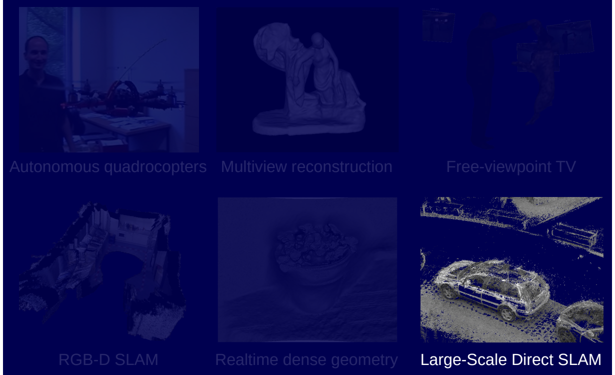

Real-time Visual SLAM

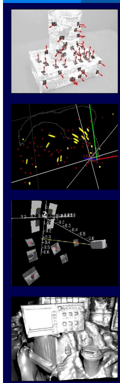

Structure from Motion Causally Integrated Over Time.
Chiuso, Favaro, Jin, Soatto; PAMI '02.

Visual Odometry.
Nistér, Naroditsky, Bergen; CVPR '04.

Scalable monocular SLAM.
Eade, Drummond; CVPR '06.

Parallel Tracking and Mapping for Small AR Workspaces. *Klein, Murray*; ISMAR '07.

MonoSLAM: Real-time single camera SLAM.
Davison, Reid, Molton, Stasse; PAMI '07.

Scale Drift-Aware Large Scale Monocular SLAM.
Strasdat, Montiel, Davison; RSS '10.

DTAM: Dense Tracking and Mapping in Real-Time.
Newcombe, Lovegrove, Davison; ICCV '11.

REMODE: Probabilistic, Monocular Dense Reconstruction in Real Time. *Pizzoli, Forster, Scaramuzza*; ICRA '14.

PTAM (*Klein, Murray ISMAR '07*)

Parallel Tracking and Mapping for Small AR Workspaces

Extra video results made for ISMAR 2007 conference

Georg Klein and David Murray
Active Vision Laboratory
University of Oxford

The Parrot AR.Drone

available online @ 260€

no hardware / onboard software modifications

connected to ground station via WLAN

Onboard sensors:

- front camera (320 x 240 @ 18fps)
- inertial measurement unit
- ultrasound altimeter
- onboard, optical-flow-based velocity estimation

Realtime structure and motion / visual SLAM:

Chiuso et al., ECCV '00, Favaro, Jin, Soatto, ICCV '01, Nister, ICCV '03, Davison, ICCV '03, Klein, Murray, ISMAR '07,…

Sensor Fusion

Open source mono-SLAM system PTAM *(Klein & Murray '07)*

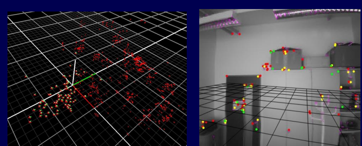

Drawbacks: Unreliable, no scale information

Our contributions:

- camera-based autonomous navigation
- enhanced reliability by incorporating IMU data
- ML scale estimate using ultrasound & velocity

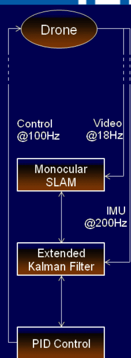

Engel, Sturm, Cremers, IROS 2012

Autonomous Flying & Hovering

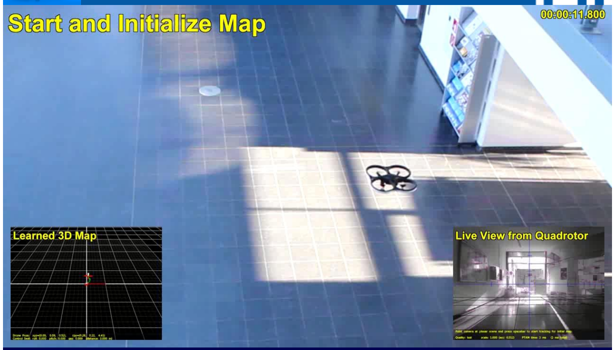

Engel, Sturm, Cremers, IROS 2012

Improvement by Sensor Fusion

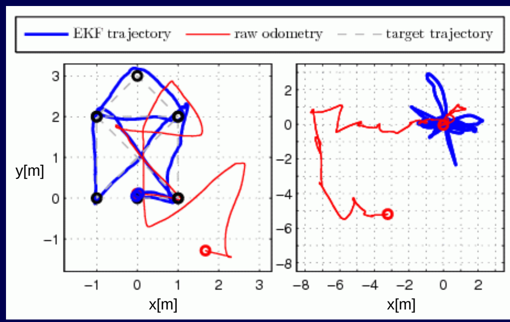

Engel, Sturm, Cremers, IROS 2012

Autonomous Nanocopter Flight

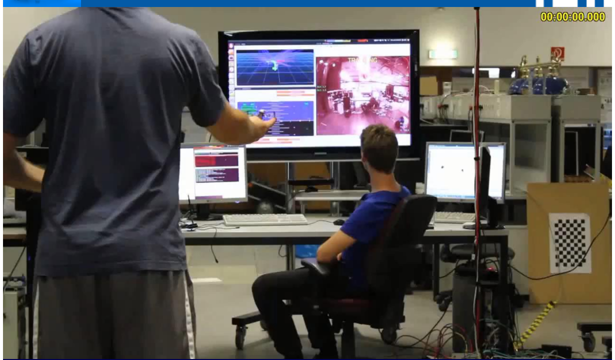

Dunkley, Engel, Sturm, Cremers, IROS 2014 Workshop on Nanocopters

Visual-Inertial Odometry on iPhone

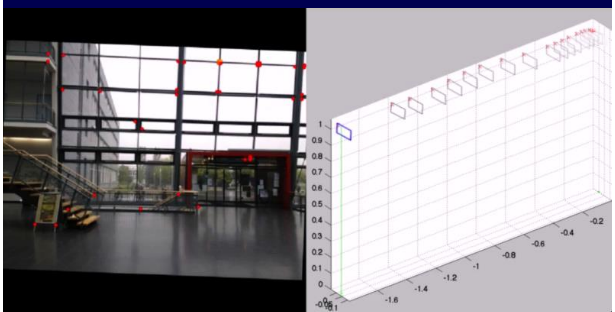

Li, Mourikis, IJRR 2014

Implementation: Michael Shelley (TUM)

Visual-Inertial Odometry on iPhone

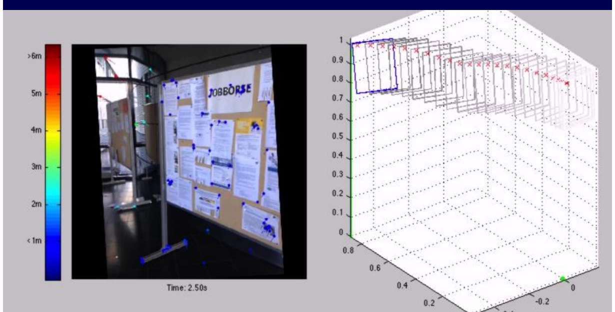

Li, Mourikis, IJRR 2014

Implementation: Michael Shelley (TUM)

Toward Direct Visual SLAM

Keypoint-Based

Input Images

Extract & Match Features (SIFT / SURF / BRIEF /...)

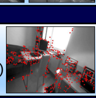

abstract images to feature observations

Track: min. reprojection error (point distances)

Map: est. feature-parameters (3D points / normals)

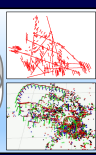

Direct (LSD-SLAM)

Input Images

keep full image

Track: min. photometric error (intensity difference)

Map: est. per-pixel depth (semi-dense depth map)

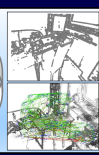

LSD SLAM: Large-Scale Direct SLAM

Engel, Sturm, Cremers, ICCV '13, Engel, Schöps, Cremers, ECCV '14

Implementation on a Smartphone

Schöps, Engel, Cremers, ISMAR 2014 (Best Student Paper)

LSD SLAM: Large-Scale Direct SLAM

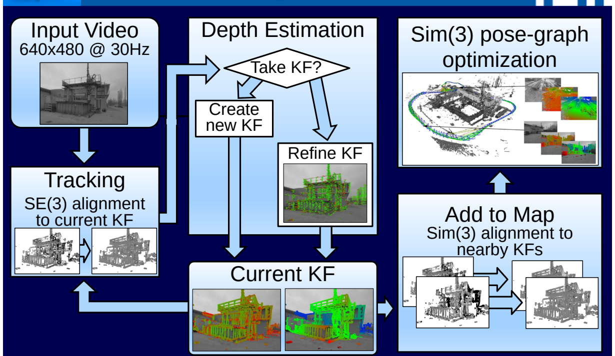

Engel, Sturm, Cremers, ICCV '13, Engel, Schöps, Cremers, ECCV '14

LSD SLAM: Large-Scale Direct SLAM

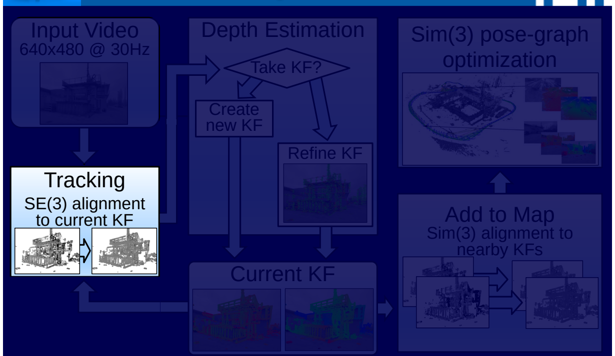

Engel, Sturm, Cremers, ICCV '13, Engel, Schöps, Cremers, ECCV '14

Direct Tracking on Keyframes

$$\min_{\xi\in\mathbb{R}^6}\int_\Omega \left| I_{KF}(x) - I\Big(\pi\big(\underbrace{g_\xi(u\, x)}\big)\Big)\right| dx$$

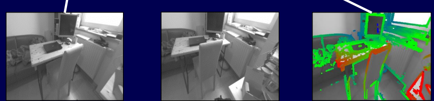

Minimize using coarse-to-fine linearization:

single core timings:
320x240: 5-10ms
640x480: 20-30ms

Keypoint versus Direct SLAM

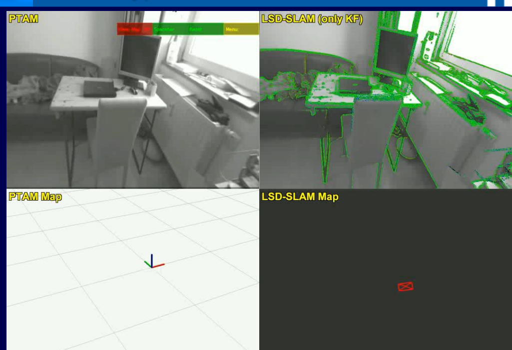

Engel, Schöps, Cremers, ECCV 2014

LSD SLAM: Large-Scale Direct SLAM

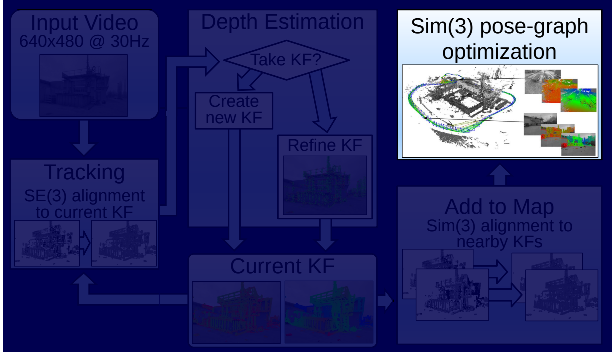

Engel, Sturm, Cremers, ICCV '13, Engel, Schöps, Cremers, ECCV '14

Pose Graph Optimization on Sim(3)

Enhance poses with an additional scaling: $g_\xi \in Sim(3)$

$$Sim(3) = \left\{ \begin{pmatrix} sR & T \\ 0 & 1 \end{pmatrix} \text{ with } R \in SO(3),\ T \in \mathbb{R}^3,\ s \in \mathbb{R}_+ \right\}.$$

Compute a globally consistent trajectory by minimizing

$$\min_{\xi_1,\dots,\xi_T} \sum_{i\sim j} \left(\hat{\xi}_{ij} \circ \xi_i^{-1} \circ \xi_j\right)^\top \Sigma_{ij}^{-1} \left(\hat{\xi}_{ij} \circ \xi_i^{-1} \circ \xi_j\right)$$

tracked relative pose optimized pose inverse covariance

Camera Pose Graph Optimization

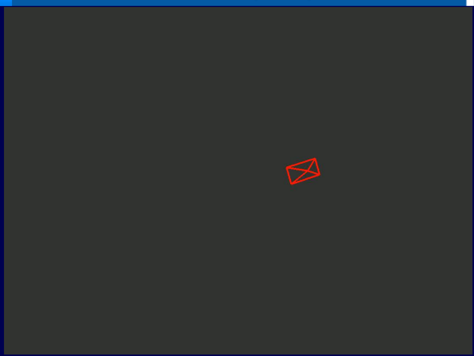

Engel, Schöps, Cremers, ECCV '14

LSD SLAM: Large-Scale Direct SLAM

Engel, Sturm, Cremers, ICCV '13, Engel, Schöps, Cremers, ECCV '14

LSD SLAM: Large-Scale Direct SLAM

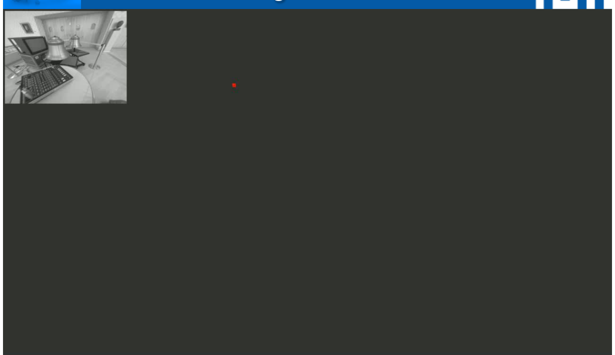

Engel, Sturm, Cremers, ICCV '13, Engel, Schöps, Cremers, ECCV '14

Large-Scale Direct Monocular SLAM

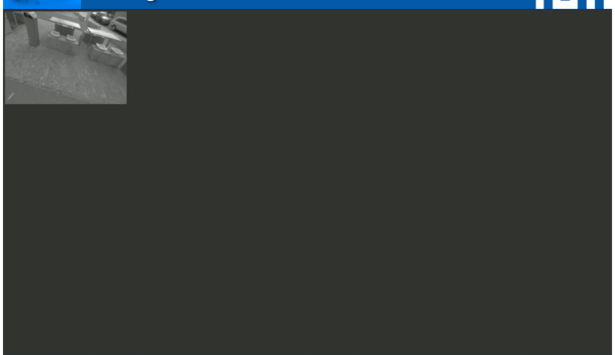

Engel, Sturm, Cremers, ICCV '13, Engel, Schöps, Cremers, ECCV '14

Autonomous Quadcopter

Camera-Based Navigation of a Low-Cost MAV using LSD-SLAM

Lukas von Stumberg, Jakob Engel, Jörg Stückler, Daniel Cremers

Computer Vision Group
Department of Computer Science
Technical University of Munich

Von Stumberg, Engel, Stückler, Usenko, Cremers '15

Autonomous Quadcopter

3D-Mapping on a Low-Cost MAV using LSD-SLAM

Lukas von Stumberg, Jakob Engel, Jörg Stückler, Vladyslav Usenko, Daniel Cremers

Computer Vision Group
Department of Computer Science
Technical University of Munich

Von Stumberg, Engel, Stückler, Usenko, Cremers '15

Realtime Stereo LSD SLAM

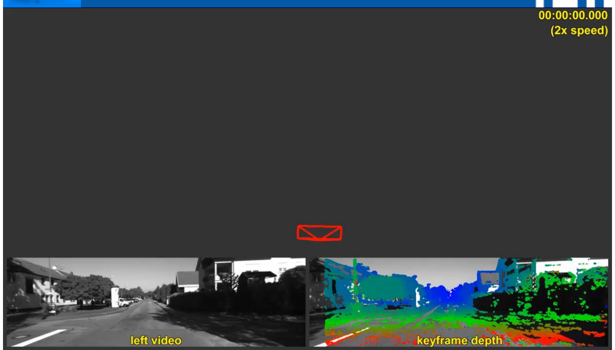

Engel, Stückler, Cremers, IROS '15

Stereo LSD SLAM with IMU

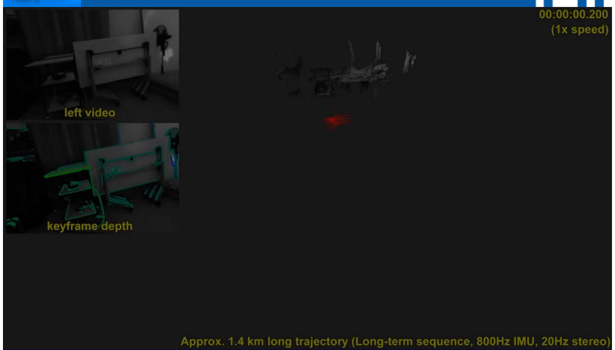

Usenko, Engel, Stückler, Cremers '15

Summary

autonomous quadcopters

dense reconstruction

RGB-D SLAM…

…for autonomous MAVs

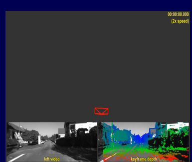

LSD SLAM…

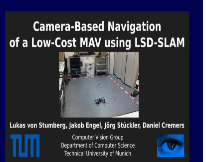

…for autonomous MAVs

Aerial Robotic Manipulation: Control, perception and planning functionalities

Anibal Ollero
Professor and head of GRVC University of Seville (Spain)
aollero@us.es

Scientific Advisor of the Center for Advanced Aerospace Technologies (Seville, Spain)
aollero@catec.aero

Coordinator of the Aerial Robotics Topic Group of Eurobotics
Co-Chair IEEE TC on Aerial Robotics and Unmanned Aerial Vehicles

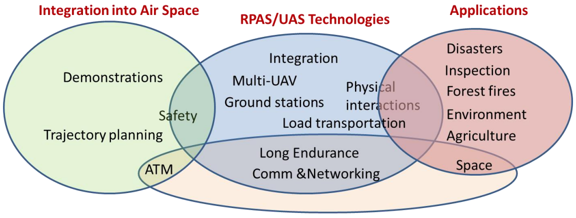

Testing Aerospace Technologies



RPAS fleet and experimentation facilities

2014 UAS and Aerial Robotics Projects at USE and CATEC

- 90 researchers and technicians working in RPAS and aerial robotics
- 23 running projects (35 contracts) in 2014
  - 8 European FP7 projects
    - Coordination of 3 projects: ARCAS (2 contracts), EC-SAFEMOBIL (2 contracts), MUAC-IREN (2 contracts)
    - Partner in 5 projects: PLANET (2 contracts), FIELDCOPTER, ARIADNA, DEMORPAS, EUROATHLON
  - 15 Spanish Projects
    - 1 Project National Programme: CLEAR (2 subprojects)
    - 1 Regional Programme: UAVLIDETECT
    - SAVIER Project funded by AIRBUS DS (2 contracts)
    - 2 INNPRONTA (6 contracts with companies): ADAM, PERIGEO
    - 2 CENIT (4 contracts with companies): SINTONIA, PROMETEO
    - 2 INNPACTO: IGNIS and ADALSCOM
    - 2 INNTERCONECTA (4 contracts with companies): CITIUS, ARIDLAP
    - 2 additional contracts with companies on VTOL systems and simulation for training (ARIDLAP)

FADA-CATEC Experimentation facilities

- Indoor
  - Testbed 16x15x6 m
  - VICON System
  - Able to fly more than 10 vehicles at the same time

- ATLAS RPAS Experimentation facility
  - Segregated aerial space: 35 x 30 Km , Altitude: up to 5000 ft
  - Main runway: 800m x 18m
  - Auxiliary sand runway: 400m x 15m
  - Control center for mission operations
  - Independent Hangars for different customers
  - Logistic and Technical support


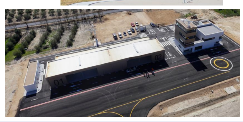

Technologies

- **Increasing safety**: FP7 EC-SAFEMOBIL
- Multi-UAV **coordination and cooperation**: FP7 EC-SAFEMOBIL, FP7 ARCAS, ADAM
- UAV **physically interacting** with the environment: FP7 ARCAS
- **Long endurance**: FP7 MUAC-IREN, CLEAR, SAVIER
- UAV **communication and Networking**: ADALSCOM, IGNIS PROSES, other contracts with companies
- Development of **Ground Stations**: SAVIER, contracts with companies
- Integration with **ground and marine vehicles**: ADAM, PROMETEO
- Integration with **ground infrastructure**: FP7 PLANET

Outline

- Introduction: Aerial Robots Physically interacting with the environment
- Aerial robotic manipulators
- Control in aerial robotic manipulation
- Perception in aerial robotic manipulation
- Planning aerial robotic manipulation
- AEROARMS H2020 project
- Conclusions

Physical interactions

- Introduction

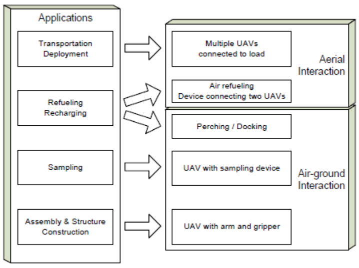

Kondak, Ollero et all, Chapter of UAS Springer Handbook

Physical interactions

- Load transportation

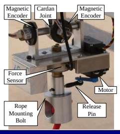

AWARE FP6 project 2006-2009

Physical interactions

Air-air refuelling

- Interactions: boom or drogue
- Active drogue: lateral and vertical position control

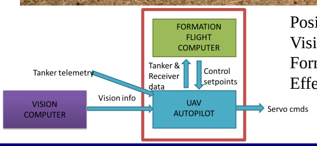

Position estimation: GPS+ vision+ IMU
Vision system: Visual markers
Formation flight controller
Effect of the taker stream

SAVIER funded by AIRBUS DS

Physical interactions: Sampling

UGAV Project: Universidad de Sevilla

Physical interactions: Sampling and UGV Deployment

FP7 PLANET Project

EC-SAFEMOBIL (FP7 ICT, 2011-2015)

http://www.ec-safemobil-project.eu

New estimation and cooperative control methodologies and their practical application to unmanned systems. Safety & reliability while optimising performance.

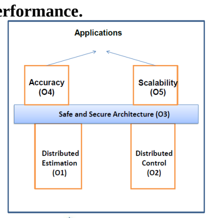

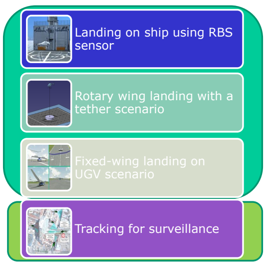

Physical interactions: Tethered helicopter

- Landing with cable: FP 7 EC-SAFEMOBIL Project

Control of helicopter with tether:
- Model of the aerial tethered system
- Analysis of the influence in system dynamics
  - Robustness against external perturbations in translational dynamics.
  - Undesired translational influence on rotation due to tether induced moment.
- Guidelines for control design
  - Saturation of lift-force
  - Feed-forward action for counteracting tether tension induced moment
- No GPS is needed
- Applications: Landing and recharging

Tether tension: Higher as possible to maximize stabilizing properties in translation
Bounded since induced moment should be always less than maximum moment exerted by main rotor control action (saturation of cyclic pitch)
=> Maximum value for tether tension should not exceed 20% of lifting force at hover (for a typical small-size helicopter

"Tether-guided landing of unmanned helicopters without GPS sensors", L.A. Sandino, D. Santamaría, M. Bejar, A. Viguria, K. Kondak and A. Ollero. International Conference on Robotics and Automation (ICRA 2014). Hong Kong, China, 31 May to 5 June 2014.

AERIAL ROBOTIC MANIPULATION

Unmanned Aerial Systems

Mobile Robotic Manipulation

Aerial Robotic Manipulation

Aerial Robotics Cooperative Assembly System (ARCAS)

Coordinator: A. Ollero

Large-scale integrating project (IP) Project No. 287617 • FP7-ICT-2011-7

ARCAS

Aerial Robotics Cooperative Assembly System FP7 ARCAS (2011-2015)

Flying + Manipulation + Perception + Multi-robot Cooperation

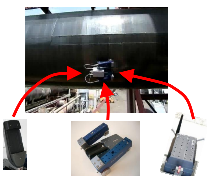

Space Applications

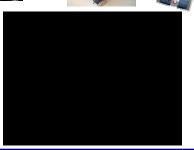

Aerial Robotics Applications

Objective

- Research, development and experimental validation of the first cooperative flying robots system for assembly and manipulation.

Structure assembly

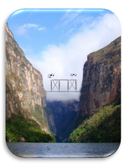

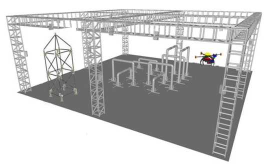

Aerial Robotics Cooperative Assembly System
FP7 ARCAS (2011-2015)

Structure assembly mission

- Several aerial robots should cooperate for structure assembly
- Several robots flying at the same time
  - Looking for parts
  - Approaching and grasping parts
  - Transporting parts
    - Special case: Cooperation in the transportation
  - Assembling parts

Aerial Robotics Cooperative Assembly System
FP7 ARCAS (2011-2015)

Aerial Manipulation

General Solutions (Redundancy) instead of particular solutions: Aerial platforms with 6/7 DOF robotic arms

Control problems

Control of the aerial platform and the robotic arms
Close proximity to objects
Coordinated control of two aerial manipulators

Perception

Mapping the environment
Detection of areas for structure construction and landing
Localization: parts and robots
Tracking

Planning

Assembly planning
Task planning
Motion planning
Collision detection and avoidance

Aerial robots in ARCAS

First world-wide multi-rotor with 6 joints Very Light arm

First world-wide multi-rotor with 7 joint arm

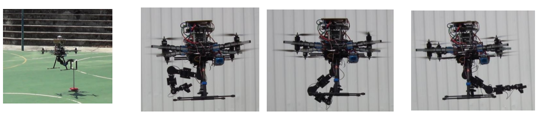

Aerial Robotics Cooperative Assembly System
(ARCAS) FP7-ICT-2011-7

First cooperative free-flying robot system for assembly and structure construction

Aerial robots in ARCAS

First world-wide helicopters with industrial 7DoF arms

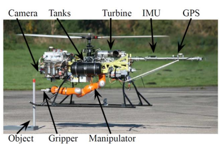

Flettner helicopter

AERIAL ROBOT CONTROL

Helicopters with 7DoF arms

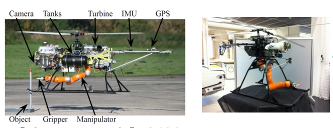

Analysis of interactions between helicopter and manipulator
Dynamic model inversion

Impedance control
Image based control

Multi-rotors with 2/6/7 DoF arms

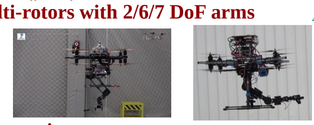

Integral backsteping
Adaptive control
Passivity
Force/moment estimator

Space environment

Cooperative Control of Servicer Satellite and Manipulator
Client trajectory following

Outdoor Multirotor: 7 dof Manipulator control

- **Modification of the Closed Loop Inverse Kinematic (CLIK) Algorithm**: for a given end-effector position and orientation
- **Robust behavior close to singular configurations**: modified pseudoinverse (DLS pinv) with variable damping factor based on gaussian-weighted functions of the manipulability measure.

$$J_g^{\dagger} \Rightarrow J_g^{*} = J_g^T\left(J_g J_g^T + \kappa^2 I_7\right)^{-1} \quad \text{with} \quad \kappa := \kappa_0 e^{-\frac{1}{2}\left(\frac{\sqrt{\det(J_g J_g^T)}}{\epsilon}\right)^2}$$

- **Saturation in the Null Space (SNS)** to take into account:
  - joint angles limits,
  - maximum joint rates and accelerations,
  - cartesian constraints to avoid collisions with landing gear and rotor blades
  - unified framework for all joint motion constraints

"Integral Action in First-Order Closed-Loop Inverse Kinematics. Application to Aerial Manipulators", M.I. Sánchez, J.A. Acosta and A. Ollero. ICRA 2015. Seattle, USA, May 2015.

Aircraft with arm: Control approach

Underactuated system, subject to perturbations (air movement): difficult to maintain arm TCP (tool center point) at desired position for manipulation
Dynamic model of the aircraft with n-link arm

- **Model**: standard aircraft model + articulated body (displacement of c.o.g.)
- Aircraft controller: takes into account displacement of c.o.g. and variation of moments of inertia.
- Arm controller: takes state as input, compensate to stabilize TCP.
  Aircraft state + arm model

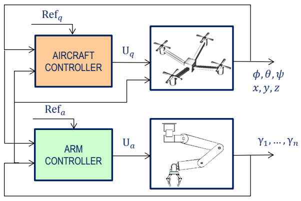

"Control of an aerial robot with multi-link arm for assembly tasks", A. E. Jimenez-Cano, J. Martin, G. Heredia, R. Cano and A. Ollero. 2013 IEEE International Conference on Robotics and Automation (ICRA 2013). Karlsruhe, Germany, 2013.

Attitude Control

Variable Parameter Integral Backspepping (VPIB) controller with full coupled dynamics instead of simplified model

$$B(\xi)\ddot{\xi} + C(\xi,\dot{\xi}) + g(\xi) = u + u_{ext} \qquad \xi = [x\ y\ z\ \theta\ \varphi\ \psi\ \gamma_1\ \gamma_2\ \gamma_3\ \gamma_4\ \gamma_5\ \gamma_6\ \gamma_7]$$

$$U_\theta = K(\gamma_i)\left[(1-k_1^2+\lambda_1)e_\theta + (k_1+k_2)e_{\dot{\theta}} - k_1\lambda_1\chi_\theta\right] - D_1(\xi,\ddot{\xi})\xi - C_1(\xi,\dot{\xi}) - G_1(\xi)$$

$$U_\theta = K(\gamma_i)\left[K_P e_\theta + K_I\chi_\theta + K_D e_{\dot{\theta}}\right] - D_1(\xi,\ddot{\xi})\xi - C_1(\xi,\dot{\xi}) - G_1(\xi)$$

- $e_\theta = \theta_d - \theta$ angular tracking error and $e_{\dot{\theta}} = k_1 e_\theta + \lambda_1\chi_\theta + \dot{\theta}_d - \dot{\theta}$ as the rate tracking error. $\chi_1 = \int_0^t e_1(\tau)d_\tau$

Same for roll and yaw

$$U_\phi = K_\phi(\gamma_i)\left[K_{\phi_P}e_\phi + K_{\phi_I}\chi_\phi + K_{\phi_D}e_{\dot{\phi}}\right] - D_2(\xi,\ddot{\xi})\xi - C_2(\xi,\dot{\xi}) - G_2(\xi)$$

$$U_\psi = K_\psi(\gamma_i)\left[K_{\psi_P}e_\psi + K_{\psi_I}\chi_\psi + K_{\psi_D}e_{\dot{\psi}}\right] - D_3(\xi,\ddot{\xi})\xi - C_3(\xi,\dot{\xi}) - G_3(\xi)$$

Control of a Multirotor Outdoor Aerial Manipulator", G. Heredia, A. Jimenez-Cano, M.I. Sanchez, D. Llorente, V. Vega, J. Braga, J.A. Acosta and A. Ollero. IROS 2014. Chicago, USA, 14-18 September 2014.

Attitude Control (Experiments)

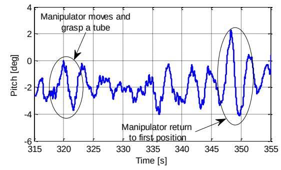

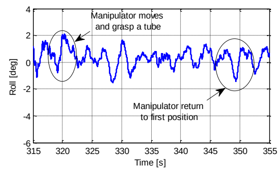

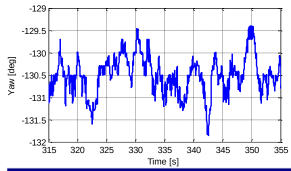

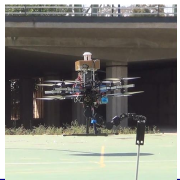

Position control

- Horizontal: Generates the attitude references ϕ_d and θ_d (tracked by the attitude controller) in response to a deviation from the y_d or x_d references
- Control law derived using Integral Backstepping techniques:

$$\begin{bmatrix}U_x\\U_y\end{bmatrix} = \begin{bmatrix}\frac{1}{g}\left[(1-k_x^2+\lambda_x)e_x + (k_x+k_{\dot{x}})e_{\dot{x}} - k_x\lambda_x\chi_x\right]\\ \frac{1}{g}\left[(1-k_y^2+\lambda_y)e_y + (k_y+k_{\dot{y}})e_{\dot{y}} - k_y\lambda_y\chi_y\right]\end{bmatrix}$$

- Adapted to generate the attitude references ϕ_d and θ_d:

$$\begin{bmatrix}\theta_d\\\phi_d\end{bmatrix} = R_z\begin{bmatrix}U_x\\U_y\end{bmatrix} \qquad [R_z] = \begin{bmatrix}\cos(\psi) & \sin(\psi)\\ -\sin(\psi) & \cos(\psi)\end{bmatrix}$$

- Altitude controller:

$$U_z = \frac{m}{\cos(\phi)\cos(\theta)}\left[g - (1-k_z^2+\lambda_z)e_z + (k_z+k_{\dot{z}})e_{\dot{z}} - k_z\lambda_z\chi_z\right]$$

$$e_{\dot{z}} = k_z e_z + \lambda_z\chi_z + \dot{z}$$

Position Control. Experiments (I)

Fig. a

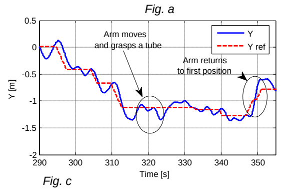

Fig. b

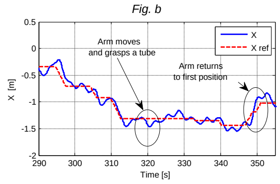

Fig. c

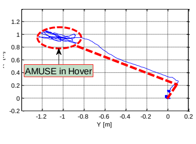

Altitude control

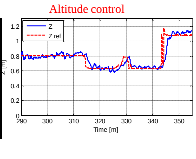

AERIAL ROBOT MANIPULATION CONTROL

- Passivity-Based Control
  - **Fully actuated systems**: many results (PD/PD/PID/Computed Torque, Adaptive & Robust Control, Output feedback).
  - **Underactuated systems**: Results for Fully actuated robots are no longer applicable.
- Theoretical extension needed: Possibility of recovering Passivity, but Partial Differential Equations (PDEs) need to be solved.
- *Energy-Shaping* Methodology: Interconnection and Damping Assignment Passivity-Based Control, IDA-PBC (Hamiltonian)
- Solving PDEs is required to compute control action

$$\boxed{H_d(q,p) = \frac{1}{2}p^\top M_d^{-1}(q)p + V_d(q)} \qquad \boxed{\hat{F}(q,p) = G^\dagger(\nabla_q H - M_d M^{-1}\nabla_q H_d + J_2 M_d^{-1}p)}$$

- Boundedness and Stability are assured
- Analytical solutions of IDA-PBC in the plane

$$\begin{aligned} V_d(\bar{q}) &= -gkm_B\frac{I_{22}}{m_{13}}\ln(\cos\bar{q}_3) \\ &+ \Phi\left(\bar{q}_2 - \frac{I_{22}}{m_{13}}\ln(\cos\bar{q}_3), \bar{q}_3 - \frac{m_{13}}{I_{22}}\bar{q}_1, \bar{q}_4\right) \end{aligned}$$

$$M_d(\bar{q}) = k\cdot\begin{bmatrix} m_B & 0 & m_{13}/k & 0 \\ 0 & m_B & 0 & 0 \\ m_{13}/k & 0 & I_{22}/k, & 0 \\ 0 & 0 & 0 & m_Q L_{CG}(\bar{q}_3,\bar{q}_4)^2 \end{bmatrix}$$

AERIAL ROBOT MANIPULATION CONTROL

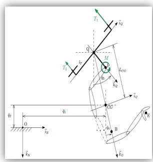

2D AERIAL MANIPULATOR CONTROL BLOCK SCHEME

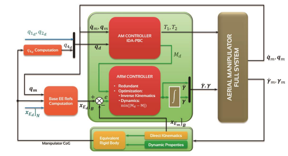

Experimental characterization of aerodynamic effects

- Test stand for motor/rotor characterization: measure thrust, rotor speed and pwm input, controlled from a console with a data acquisition GUI.
  - Tests with different distance/ inclination angle to surfaces.
  - Single or coaxial rotors.
  - Allows dynamic tests.

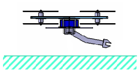

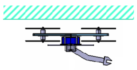

Ground effect **Ceiling effect**

Wall effect

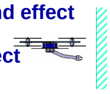

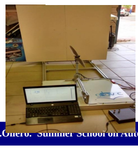

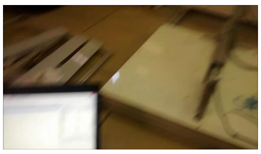

Experimental Results

- Example test (ground effect).

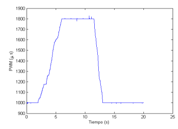

Input (pwm)

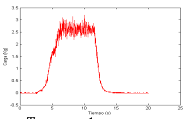

Thrust (Kg)

$$\frac{T_{\{IGE\}}}{T_{\{OGE\}}} = \frac{1}{k_G} \qquad k_G = 1 - \frac{1}{16}\left(\frac{R}{z}\right)^2$$

- ARCAS octocopter with 20 cm rotor radius and at distances of 9, 12, 19.5, 25, 40 and 95 cm (OGE).
- Compared to experimental results for helicopters (*Cheeseman & Bennet*)

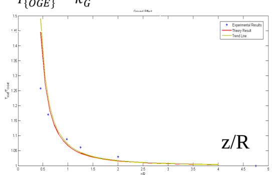

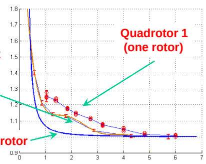

Multirotors: only some rotors under aerodynamic surface effects

- Aerial manipulation: multicopter has to fly near environment to manipulate objects: only some rotors under surface effects.
- **Partial ground effect**: "**safe**" (for multirotor) **destabilizing moment**.
- Destabilizes multirotor, but takes it away from ground.
- Oscillations may lead to arm collision.
- **Partial ceiling effect**: "**unsafe**" (for multirotor) **destabilizing moment**.
- Destabilizes multirotor, AND takes it to hit ceiling.
- Oscillations may lead to arm collision.

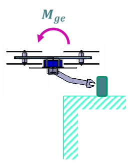

Partial ground effect

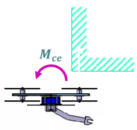

Partial ceiling effect

AERIAL ROBOT MANIPULATION CONTROL

Coordinated Control: General configuration

The task formulation is developed for multi-robot systems composed by two types of robots:

- N_T ***Transporting Robots*** (TRs), i.e. robots grasping an object and move it according to a planned trajectory
- N_A *Auxiliary Robots* (ARs), i.e. robots whose motion needs to be coordinated with that of the object grasped by TRs

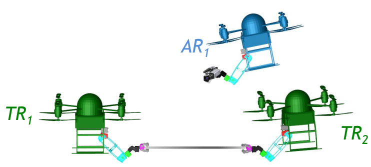

Environment perception in ARCAS

- **Pose estimation from low resolution images:** classifier trained with high resolution images (3D map) to compute the robot pose from low resolution images taken from the robot (robust to motion blur, image degradation, and occlusions) and low computational cost.
- **Fast 3D model generation:** stereo pair, hardware for fast processing (FPGA) and Semi Global Matching.
- **Object detection and recognition** by means of n-line Random Ferns, Rotationally-invariant: 3D data with 5 Hz.
- **Detection of planar areas** (landing or building the structure) without training based on 3D maps (built with visual odometry with refined Map/Pose and dense mapping) and local plane fitting.
- **Reliable tracking of 3D objects.** 3D Pose Estimation and Tracking, Uncalibrated Image-Based Visual Servo, Image-based UAV onboard velocity estimation (close for solution using visual and inertial data), use of visual markers to detect and identify structure elements.

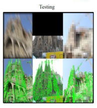

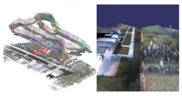

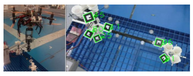

Range-only SLAM in structure assembly - Issues

- Low-informative measurements: only range
  - Range between pair of sensors: $\boldsymbol{\rho_i}$
  - Sensor ID
- 3D Parametrization: lack of bearing information
  - **2 multi-modal variables**: Azimuth θ and elevation φ angle.
  - Initial distribution (only 1 range measurement): **uniform spherical distribution**

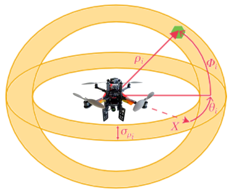

A.Ollero. Summer School on Autonomous Micro Aerial Vehicles. Schloss Birlinghoven (Germany), August 28, 2015

Range-only SLAM in structure assembly – First Approach

- Delayed centralized EKF: $\mathbf{x}_t = [\mathbf{x}_r\, \mathbf{f}_1\, \mathbf{f}_2\, \mathbf{f}_3\, \mathbf{f}_4 \ldots \mathbf{f}_k]$
  - Robot 3D pose $\mathbf{x}_r$
  - Map landmark $\mathbf{f}_i$.
  - Keeps the correlation between robot and features.
- Ladmarks are initialized using a Particle Filter

Input: P_{t-1} and r_t
Output: P_t

for $n = 1$ *to* N **do**
  Compute $r_t^{[n]} = ||\boldsymbol{p}_t^{[n]} - \boldsymbol{x}_{r,t}||$
  Determine $\mu(r_t^{[n]})$ and $\sigma(r_t^{[n]})$
  Update weight of particle n as $\omega_t^{[n]} = \omega_{t-1}^{[n]} p(r_t|\boldsymbol{p}_t^{[n]}) = \omega_{t-1}^{[n]} \mathcal{N}(r_t; \mu(r_t^{[n]}), \sigma(r_t^{[n]}))$
end
Normalize weights $\omega_t^{[n]}$
Compute N_{eff}
if $N_{eff} < N_{th}$ **then**
  Resample with replacement N particles from P_t.
end

Algorithm 1: Particle filter for mapping range-only sensors

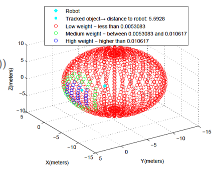

A.Ollero. Summer School on Autonomous Micro Aerial Vehicles. Schloss Birlinghoven (Germany), August 28, 2015

Range-only SLAM in structure assembly – ARCAS approach

- Centralized EKF: $\mathbf{x}_t = [\mathbf{x}_r\, \mathbf{f}_1\, \mathbf{f}_2\, \mathbf{f}_3\, \mathbf{f}_4 \ldots \mathbf{f}_k]$
  - Robot 3D pose $\mathbf{x}_r$
  - Map features $\mathbf{f}_i$
  - Keeps the correlation between robot and features.
- How the initial spherical uniform distribution of a feature can be included into a Gaussian filter with only one range measurement?
  - Use of spherical parametrization: 2 multi-modal variables
  - Two independent Gaussian mixtures
    - Azimuth angle: $f_{\theta_i}(x) = \mathcal{U}(0, 2\pi) \approx \sum_{j_\theta=1}^{n_\theta} \omega_{\theta_{ij_\theta}} \mathcal{N}(\theta_{ij_\theta}, \sigma_{\theta_{ij_\theta}})$
    - Elevation angle: $f_{\phi_i}(x) = \mathcal{U}(-\frac{\pi}{2}, \frac{\pi}{2}) \approx \sum_{j_\phi=1}^{n_\phi} \omega_{\phi_{ij_\phi}} \mathcal{N}(\phi_{ij_\phi}, \sigma_{\phi_{ij_\phi}})$
  - The combination of both GMM models the complete spherical distribution.

$$f_i = [x_i, y_i, z_i, \rho_i, \theta_{i1}, \ldots, \theta_{in_\theta}, \phi_{i1}, \ldots, \phi_{in_\phi}]^T$$

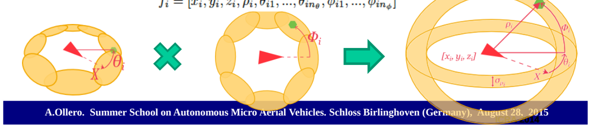

A.Ollero. Summer School on Autonomous Micro Aerial Vehicles. Schloss Birlinghoven (Germany), August 28, 2015

Range-only SLAM in structure assembly – ARCAS approach

Reduced parametrization

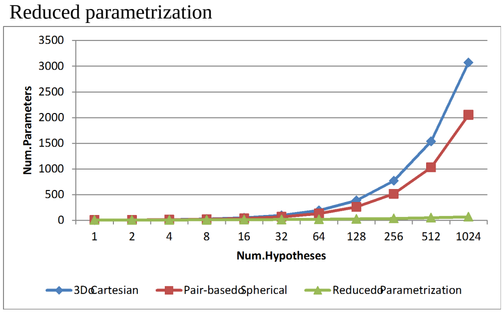

Improving robustness: Outlier rejection filter

A.Ollero. Summer School on Autonomous Micro Aerial Vehicles. Schloss Birlinghoven (Germany), August 28, 2015

Range-only SLAM results

Range

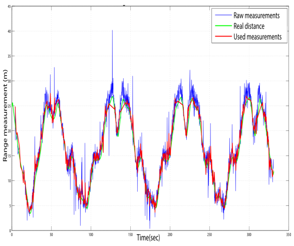

Absolute error

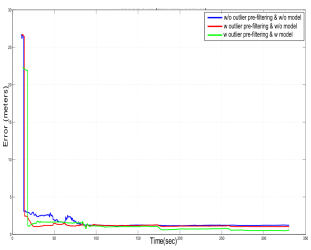

A.Ollero. Summer School on Autonomous Micro Aerial Vehicles. Schloss Birlinghoven (Germany), August 28, 2015

Range-only SLAM conclusions

- Efficient Multi-hypotheses 3D RO-SLAM method.
  - Use of 2 Gaussian Mixture Models to model bearing information (2 multimodal variables).
  - Reduced required computational resources: Memory and CPU time.
  - Use of reduced spherical parametrization and optimal correction scheme.
  - Centralized EKF keeps correlation between radio emitters embedded in structural elements.
- Localization RMS absolute error: < 1m and mapping error: ≈ 0,5m
- Outlier rejection filter makes convergence faster and reduces mapping errors.
- Model propagation estimation reduces mapping errors when there is a fixed offset and scale in range measurements due to multi-path or other effects.

Real-time pose estimation with contour registration (UPC)

Object detection is a very important task in ARCAS because the pose will provide useful information for assembly operations.

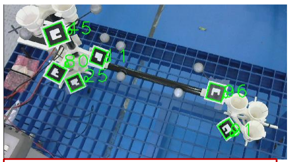

- Marker contours selection to reduce marker confusion
- Definition of two main marker sets:
  - Big marker for global localization of the manipulation zones.
  - Small marker for bar detection.

- On-board real time pose estimation for UAV using deformable visual contours (multi-marks)
- Rotation-invariance for multi-mark
- Fast processing (30 FPS)
- Accuracy: 0.5-1.5cm (short range tracking); 2.0-4.0cm (localization)
- Improved robustness to 180º orientation ambiguity.
- Improved inter-marker detections
- Evaluation: ARCAS testbeds, outdoor scenarios

Real-time pose estimation with contour registration

Experiments for Grasping Operations

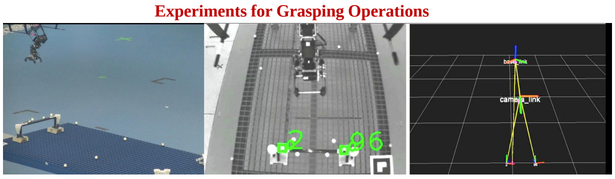

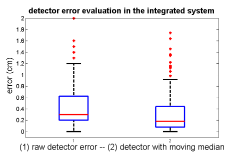

Detection error range: 0.2 to 1.2 cm

Cooperative perception

- Objective: Combining information from multiple aerial robots to improve the estimations obtained by single robots
  - **Data fusion:** Data fusion of robot perceptions and local sensors for improved multirobot localization.
  - **Cooperative perception:** Distributed methods that scale well with the number of robots will be studied.
  - **Active perception:** Techniques to generate motions of the aerial robots as they observe the scene to improve the perception.

Previous result: Data fusion of RO-SLAM + Visual detection

- Structural elements estimation:
  - Rough estimation from RO-SLAM : Only range sensors.
  - Fusion of visual detections with RO-SLAM estimations in short distances:
    - Visual estimations integrated in centralized EKF from RO-SLAM developed for WSN map refinement.

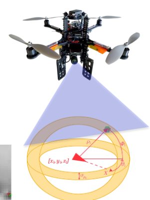

$$x^V_{f_i} = x_i + \rho_i cos(\theta_i) cos(\phi_i) - x_r$$
$$y^V_{f_i} = y_i + \rho_i sin(\theta_i) cos(\phi_i) - y_r$$
$$z^V_{f_i} = z_i + \rho_i sin(\phi_i) - z_r \ ,$$

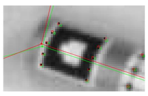

"Localization and mapping for aerial manipulation based on range-only measurements and visual markers", F.R. Fabresse, F. Caballero, I. Maza and A. Ollero. International Conference on Robotics and Automation (ICRA 2014). Hong Kong, China, 2014.

Multi-robot RO-SLAM

- Approach:
  - Use of Bhattacharyya distance to match external hypotheses with local ones.
  - Exclude external and local hypotheses which don't match.
  - Integrate matched hypotheses in local filter: weight more local hypothesis over external ones.

Local belief of node i

Matched hypotheses

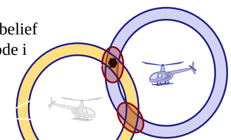

External belief of node i

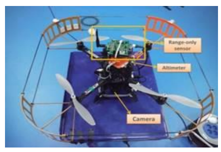

"Decentralized Simultaneous Localization and Mapping for Multiple Aerial Vehicles Using Range-Only Sensors", F.R. Fabresse, F. Caballero and A. Ollero. ICRA 2015. Seattle, USA, 26-30 May 2015.

Multi-robot RO-SLAM: Experimental results

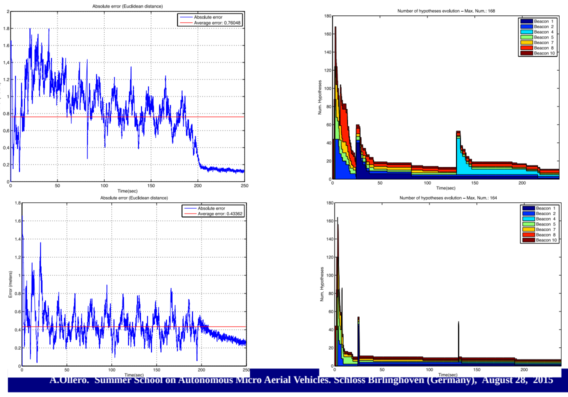

Planning in ARCAS

Structure Assembly

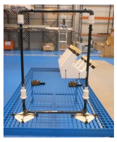

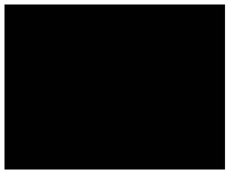

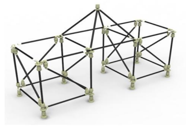

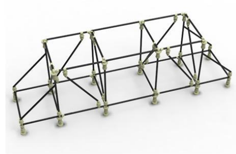

Planning in ARCAS

Assembly sequence planning

Construction of a non-directional blocking graph, get sequence plans from assembly-by-disassembly technique, select best sequence by a metric value

Structure to assemble → Assembly sequence planner → Assembly plans

Structure dynamics included

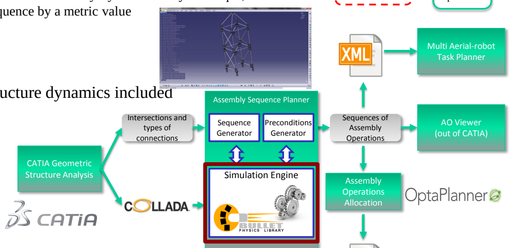

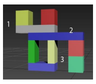

Bullets Physics library:
gravity and friction
Mass balance (1)
Redundant supports (2)
Parallel subassemblies (3)

"Assembly Planning for the Construction of Structures with Multiple UAS Equipped with Robotic Arms", J. Muñoz-Morera, I. Maza, C. Fernández-Aguera, F. Caballero and A. Ollero. International Conference on Unmanned Aircraft Systems (ICUAS 2015). pp 567-576. Denver, USA, 9-12 June, 2015.

Assembly sequence planning

Structure to assemble → Assembly sequence planner → Assembly plans

- Architecture overview
  - Simulation engine
    - Avoids combinatorial explosion
      - Algorithm running in $O(n^2)$
    - Examples

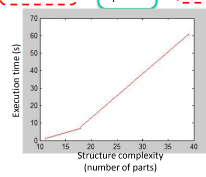

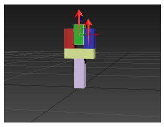

Fig. 1: Inadecuate ordering in disassembly can lead to unstable substructures

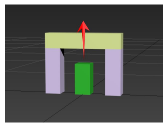

Fig 2: A disassembly obstruction between parts without direct contact

Task planning

UAV Assembly Planning Domain

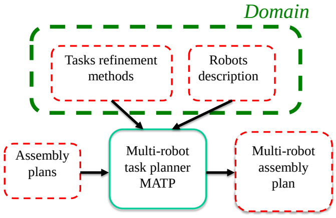

A partially ordered set of transport, monitoring and assembly actions for a set of UAVs

Task planning (LAAS-CNRS)

- MATP : Multi Aerial-robot Task Planner
- HTN planner based on previous work (HATP):
  - Multi-stream : one stream of actions per agent.
  - Cost and duration functions can be associated to actions (basic tasks)
- Interfaced with assembly planner represents structures with dependency trees

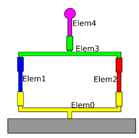

Dependency tree:
Elem4 depends on Elem3
Elem3 depends on Elem1 and Elem2
Elem1 and Elem2 depends on Elem0

Task planning (LAAS-CNRS)

Link symbolic and geometric. Intricate task and motion:

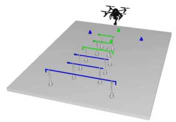

Unsuccessful plan

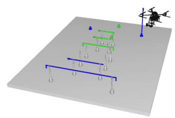

Successful plan

Link symbolic and geometric
UAVs in parallel, link with assembly planner (through a parser), grammar defined to represent assembly plan

Motion planning – *Link symbolic-geometric (LAAS-CNRS)*

A task is decomposed into several motion planning requests
Example: the task ***Pick:***

Finding intermediate configurations:
- Grasping (Q4)
- Extraction (Q5)
- Approach (Q3)
- Pre-approach (Q2)

Computing the motions:
- Grasping (Q3→Q4)
- Extraction (Q4→Q5)
- Approach (Q2→ Q3)
- Navigation (Q1→Q2)

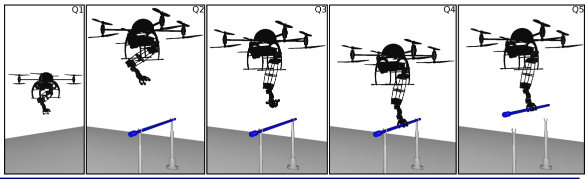

Planning in ARCAS

Motion planning. (LAAS-CNRS)

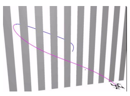

Industrial inspection problem: computes good-quality paths and a good order to move between points, Multi-T-RRT with clearance-based cost

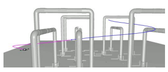

New sampling strategy and global planning methods to decrease CPU time: Directed bi-RRT, Directed PRM

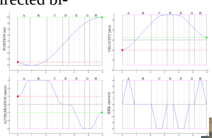

Local planner using 4th-order splines: Trapezoidal jerk profile

Motion planning for coordinated manipulation (with cables)

Plan refinement using mixed initiatives (UPC)

New method to allow the operator to refine the trajectory and then learn the new environment forces for future path planning. Steps:

1- The operator flies the trajectory and can modify any time the pose of the aerial robot and its velocities.
2- The new trajectories are used to learn the effects of the environment over the trajectory (the attractive and repulsive forces) as well as the human way of operation.
3- Obtain the forces (accelerations) coming from the environment.
4- Modify the planning cost function including the influence of the environment.

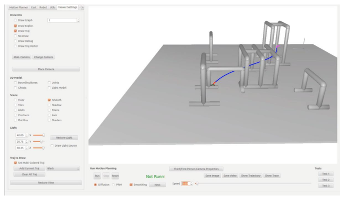

Plan refinement using mixed initiatives (UPC)

New approach:

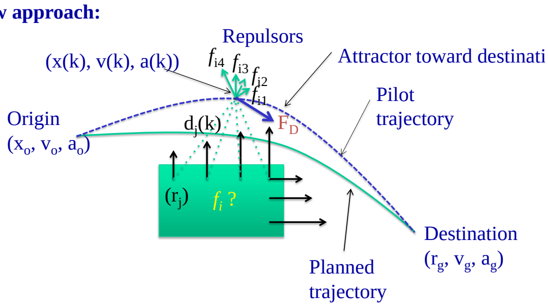

Safe coordinated trajectories generation and execution with collision detection and avoidance

Motion plans → Trajectory coordination → Input for controllers

- Anytime approach based on Particle Swarm Optimization (PSO)
  – Velocity profile of the aerial robots adjusted to avoid collisions minimizing J

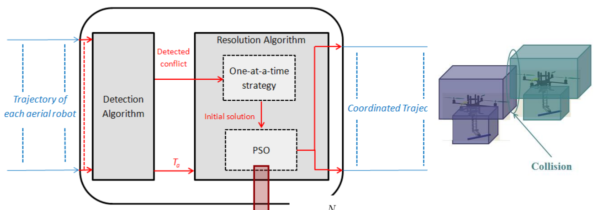

L_i total length, Δv_i change of speed, ω_i collision penalty

$$J = \sum_{i=1}^{N} (L_i + k\Delta v_i^2) + \omega_c$$

Safe coordinated trajectories generation and execution with collision detection and avoidance

Motion plans → Trajectory coordination → Input for controllers

- Anytime approach based on Particle Swarm Optimization (PSO)
  - Tested with quadcopters at FADA-CATEC testbed
  - Example: Initial trajectories

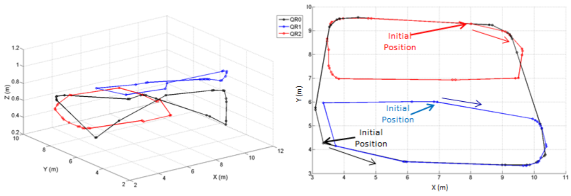

Task 6.3: Safe coordinated trajectories generation and execution with collision detection and avoidance

Motion plans → Trajectory coordination → Input for controllers

- Anytime approach based on Particle Swarm Optimization (PSO)
  - Tested with quadcopters at FADA-CATEC testbed
  - Example: Initial trajectories

"Collision-free trajectory planning based on Maneuver Selection-Particle Swarm Optimization", D. Alejo, J.A. Cobano, G. Heredia and A. Ollero. Proceedings of the IEEE International Conference on Unmanned Aircraft Systems (ICUAS 2015). Denver, USA, 9-12 June, 2015.

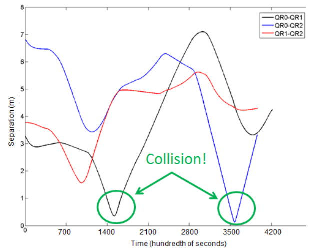

Task 6.3: Safe coordinated trajectories generation and execution with collision detection and avoidance

Motion plans → Trajectory coordination → Input for controllers

- Anytime approach based on Particle Swarm Optimization (PSO)
  - Tested with quadcopters at FADA-CATEC testbed
  - Example: Computed solution

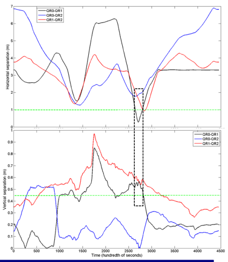

Safe coordinated trajectories generation and execution with collision detection and avoidance

Motion plans → Trajectory coordination → Input for controllers

- Optimal Reciprocal Collision Avoidance (ORCA)
  - Time horizon τ for the detection and avoidance
  - Works in the velocity space (first order algorithm)
    - Kinematic constraints modeled
    - Velocity vector changes (module and direction) triggered when the safety volumes overlap in the velocity space
    - Minimize the difference with the planned cruise speeds
  - Avoidance effort shared among the involved vehicles in each potential collision
  - Distributed
    - The calculations are carried out independently for each robot
    - State of the system (position, velocity) known by each agent

Safe coordinated trajectories generation and execution with collision detection and avoidance

Motion plans → Trajectory coordination → Input for controllers

Multi-vehicle system state Computing safe velocities

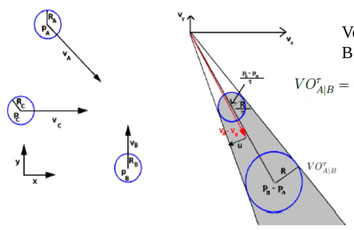

Velocity obstacle for A induced by B within time τ

$$VO^{\tau}_{A|B} = \{v \mid \exists t \in [0,\tau] :: tv \in D(p_B - p_A, r_A + r_B)\}$$

Safe coordinated trajectories generation and execution with collision detection and avoidance

Motion plans → Trajectory coordination → Input for controllers

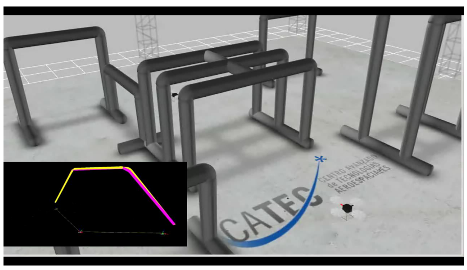

Safe coordinated trajectories generation and execution with collision detection and avoidance

Motion plans → Trajectory coordination → Input for controllers

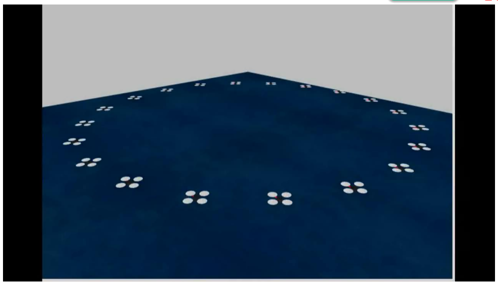

"Collision-free 4D trajectory planning in Unmanned Aerial Vehicles for assembly and structure construction", D. Alejo, J.A. Cobano, G. Heredia and A.Ollero. Journal of Intelligent and Robotic Systems. Vol. 73. Núm. 1-4, pp 783-795. January 2014.

Safe coordinated trajectories generation and execution with collision detection and avoidance

Motion plans → Trajectory coordination → Input for controllers

- Contributions to ORCA
  - Bug-fixes on the original RVO2-3D library
  - 3D obstacles included
    - Static obstacles are considered (meshes import - assimp library)
    - Automatically decomposed into quasi-convex obstacles
    - Online changes allowed
    - PQP library (proximity query package) collision detection

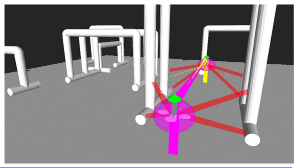

Safe coordinated trajectories generation and execution with collision detection and avoidance

Motion plans → Trajectory coordination → Input for controllers

- Contributions to ORCA
  - ROS module generated
  - Dynamic constraints included
    - Configurable maximum allowed acceleration
  - Three safety regions (ellipsoid) defined
    - Warning: the reaction smoothly increases as the conflict zone is closer
    - Conflict: In this zone, the reaction is maximum and the speed of the UAVs decreases
    - Emergency: The mission of each involved UAV is paused

"Optimal Reciprocal Collision Avoidance with Mobile and Static Obstacles for Multi-UAV Systems", D. Alejo, J.A. Cobano, G. Heredia and A. Ollero. 2014 International Conference on Unmanned Aircraft Systems (ICUAS 2014). Orlando, USA, 27-30 May 2014.

Experiments

- ARCAS Summary Year 1 and Year 2
  http://www.arcas-project.eu/multimedia
- ARCAS Second year video
  http://www.arcas-project.eu/multimedia
- ARCAS Third year video
  https://www.youtube.com/watch?v=-rIEBWrtHkc&feature=player_embedded

ARCAS in Euronews (youtube)
https://www.youtube.com/watch?v=Xrpi5mA6gDA&list=PLyMUk47rPuqoGtsuuBB1BQ0QfeVZryT40&index=1

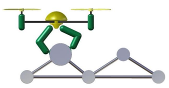

H2020

AErial RObotic system integrating multiple ARMS and advanced manipulation capabilities for inspection and maintenance (AEROARMS)

Coordinator: A. Ollero

Inspection and Maintenance of oil and gas industries

Infrared inspection of leakages

Maintenance procedures

Robotic applications to inspection and maintenance

Problems:

Locomotion system: Access to the sites to be inspected or maintained

Scaffolding needed for deploying and maintenance of the robots

AEROARM project (2015-2019)

AErial RObotic system integrating multiple ARMS and advanced manipulation capabilities for inspection and maintenance (AEROARMS)

- Multi-rotor platform anchored to perform drilling tasks

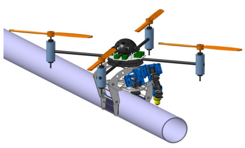

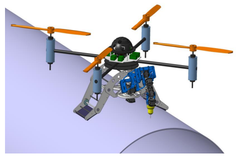

AEROARM project (2015-2019)

AErial RObotic system integrating multiple ARMS and advanced manipulation capabilities for inspection and maintenance (AEROARMS)

- Aerial robot with two arms operating in free flying for the placing of light weight elements such as a tape on the surface of a pipe or a apply sealant in the pipe junction.

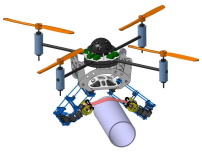

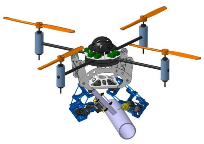

AEROARM project (2015-2019)

AErial RObotic system integrating multiple ARMS and advanced manipulation capabilities for inspection and maintenance (AEROARMS)

Validations in industrial environments

- **Application 1**: Installation and maintenance of permanent Non Destructive Tests (NDT) sensors on remote components such as pipe works, fire flares or structural components.. The application involves the preparation of structures to install the sensors (drilling a hole into insulation, removing paint etc.), the installation of the sensors and the finishing of the structure.
- **Application 2:** Deploying and maintaining a mobile robotic system permanently installed on a remote structure. Assuming the presence of a newly designed mobile robot allowing easy exchange and maintenance of components (e.g., batteries etc.), the application consists of the use of the aerial robot to maintain the robot permanently installed in the structure without costly and dangerous human operations.

AEROARM project (2015-2019)

Applications of aerial robotics for inspection and maintenance

Applications

- Infrared and visual non-contact inspection
- Contact inspection
  - Eddy current
  - Ultrasonic
- Installation of sensors in inaccessible locations
- Deployment and maintenance of robots in inaccessible locations
- Other maintenance activities

Conclusions

- First steps in general aerial robotic manipulation
- Integration of control, perception and planning
- First world-wide demonstrations: aerial robots general manipulation with multi-joint arms
- Future work includes
  - Cooperative manipulation
  - Increase reliability and safety
  - Consideration of regulation constraints
  - Application in industrial environments
  - Multi-arms aerial robots (AEROARMS)
  - Oil and gas applications (AEROARMS)
  - Bridge inspection (AEROBI)
  - Wind mill maintenance (AEROMAIN)

- Join the Aerial Robotics Topic Group of euRobotics
  - Workshops at ERF
  - Road Map and Strategic Agenda: Robotics Calls
- Join the IEEE Aerial Robotics and Unmanned Aerial vehicle
  - ICUAS and RED-UAS Conferences

    RED-UAS 2015 23-25 November 2015,

    Cancun (Mexico). Deadline Open
  - Workshops at ICRA and IROS Conferences

aollero@us.es